Deterministic Attitude and Pose Filtering, an Embedded Lie Groups Approach

Mohammad Zamani

A thesis submitted for the degree of
Doctor of Philosophy
The Australian National University

May 2013

Draft Copy – 20 May 2013

This thesis is the result of my own original work and my collaborations with others during the period of my PhD degree at the Australian National University. The following is the list of journals and conference publications I have produced in collaboration with colleagues while I was enrolled in the PhD program at the Australian National University. Most of the materials presented in this thesis are closely related to these publications.

Journal Papers

- Zamani M, Trumpf J, Mahony R, Minimum-Energy Filtering for Attitude Estimation, to appear. IEEE Transactions on Automatic Control, accepted for publication, November 2012.
- Zamani M, Trumpf J, and Mahony R. Near-optimal deterministic filtering on the rotation group. IEEE Transactions on Automatic Control, 56(6):1411-1414, 2011.

Conference Papers

- M. Zamani, M.-D. Hua, J. Trumpf, and R. Mahony. Minimum-energy filtering on the unit circle using velocity measurements with bias and vectorial state measurements. In Proceedings of the 2012 Australian Control Conference (AUCC), pages 283-288, 2012.
- M. Zamani, J. Trumpf, and R. Mahony. Minimum-energy pose filtering on the special euclidean group. In Proceedings of the 20th International Symposium on Mathematical Theory of Networks and Systems (MTNS), 2012. Paper no. 189.

- M. Zamani, J. Trumpf, and R. Mahony, A Second Order Minimum-Energy Filter on the Special Orthogonal Group. In Proceedings of the American Control Conference (ACC), pages 1895-1900, 2012.
- M. Zamani, J. Trumpf, and R. Mahony, Minimum-Energy Filtering on the Unit Circle. In Proceedings of the Australian Control Conference (AUCC), pages 236-241, 2011.
- M.-D. Hua, M. Zamani, J. Trumpf, R. Mahony, and T. Hamel. Observer design on the Special Euclidean group SE(3). In Proceedings of the 50th IEEE Conference on Decision and Control (CDC), pages 8169-8175, 2011.
- Zamani M, Trumpf J, Mahony R, Near-optimal deterministic attitude filtering. In Proceedings of the 49th IEEE Conference on Decision and Control (CDC), pages 6511-6516, 2010.

Mohammad Zamani
20 May 2013

To my parents, Jalal and Sima

Acknowledgments

I would like to thank my supervisors, Jochen Trumpf and Robert Mahony for their great work and dedication. In particular, I am grateful to Jochen for being an excellent mentor, teacher and supervisor for me. I am also indebted to Robert from whom I have learnt a lot and from whom I have benefited great support and help towards my academic growth.

I also want to thank Tarek Hamel, Minh-Duc Hua, Pascal Morin, Alessandro Saccon and Iman Shames for their collaboration and our valuable discussions. I appreciate the efforts and support of the students and the staff of the Research School of Engineering who provided me with a pleasant working environment at the Australian National University.

I want to thank my parents whose love and support has always guided me forward. My sister Behnaz has inspired me with her sweetness and energy. I am thankful to Ronak for her kind attention and care during my degree. I also want to thank my many friends who have all been important parts of my life and who have lifted my spirit during difficult times. In no particular order they include Ashkan, Iman, Nima, Amir, Saeed Z, Saeed E, Pouyan, Hadi, Ario and many others whom although I haven't mentioned with name, I have great appreciation for.

This work has been jointly supported by the Australian National University and the Australian Research Council discovery grants DP0987411 and DP120100316.

Chapter 1

Abstract

Attitude estimation is a core problem in many robotic systems that perform automated or semi automated navigation. The configuration space of the attitude motion is naturally modelled on the Lie group of special orthogonal matrices $\mathrm{SO}(3)$. Many current attitude estimation methods are based on non-matrix parameterization of attitude. Non-matrix parameterization schemes sometimes lead to modelling issues such as the singularities in the parameterization space, non-uniqueness of the attitude estimates and the undesired conversion errors such as the projection or normalization errors. Moreover, often attitude filters are designed by linearizing or approximating the nonlinear attitude kinematics followed by applying the Kalman filtering based methods that are primarily only suitable for linear Gaussian systems.

In this thesis, the attitude estimation problem is considered directly on $\mathrm{SO}(3)$ along with nonlinear vectorial measurement models. Minimum-energy filtering is adapted to respect the geometry of the problem and in order to solve the problem avoiding linearization or Gaussian assumptions. This approach allows for obtaining a geometric approximate minimum-energy (GAME) filter whose performance is tested by means of Monte Carlo simulations. Many of the major attitude filtering methods in the literature are surveyed and included in the simulation study. The GAME filter outperforms all of the state of the art attitude filters studied, including the multiplicative extended Kalman filter (MEKF), the unscented quaternion estimator (USQUE), the right-invariant extended Kalman filter (RIEKF) and the nonlinear constant gain attitude observer, in the asymptotic estimation error. Furthermore, the proposed GAME filter is shown to be near-optimal by deriving a bound on the optimality error of the filter that is proven to be small in simulations. Moreover, similar GAME filters are derived for pose filtering on the special Euclidean group $\mathrm{SE}(3)$, attitude and bias filtering on the unit circle and attitude and bias filtering on the special orthogonal group. The approximation order of the proposed method can potentially be extended to arbitrary higher orders. For instance, for the case angle estimation on the unit circle an eighth-order approximate minimum-energy filter is provided.

Contents

Chapter 2

Introduction

This thesis concerns the problem of estimating the attitude state of a rigid-body moving in the 3D space. Attitude estimation is an important subtask of many automated or semi-automated robotic vehicles. The control process of such vehicle relies on the knowledge of the attitude state of the system that is provided via an attitude estimation algorithm. Such information is for example required to be used in a feedback control loop to attain a certain automated navigational task. When dealing with fast attitude dynamics such as in unmanned aerial vehicle (UAV) manoeuvres, any degradation of the attitude estimate can quickly cause the overall system to go unstable. Therefore, a robust, accurate and preferably 'optimal' attitude filtering algorithm is required to minimize the attitude estimation error and to ensure that the system's overall performance remains within the desirable bounds. The kinematics model of the rigid-body motion is naturally modelled on the Lie group of special orthogonal matrices $\mathrm{SO}(3)$. However, this problem is traditionally tackled using the conventional vector space methods. In this thesis the Lie group structure of the system is exploited to improve the estimation quality.

The main focus of the thesis is to provide theoretical results on geometric deterministic minimum-energy (optimal) filtering treatment of this problem. Note that although the problem considered is purely theoretical it is strongly motivated by many applications in automated control systems and robotics. The following sections are to further explain the problem considered and the results of this thesis.

2.1 Problem Considered

Attitude and pose filtering are two challenging problems that are widely studied in the systems and control literature. Attitude encodes the rotation (a 3 by 3 orthogonal matrix whose determinant equals 1) that indicates the orientation of the body-fixed frame attached to a moving object relative to a reference frame. In fact, a rotation acts as a linear transformation of the set of axes of a coordinate frame (represented by a matrix of three orthogonal unit vectors) yielding the set of axes of the rotated coordinate frame. Pose encodes the rotation as well as the linear translation of the body-fixed frame relative to the reference frame.

In this thesis, multiple filtering problems are considered including attitude filter-

ing in two dimensions, attitude filtering (in the 3D space) and pose filtering. In all of these problems the state space model is chosen as the nonlinear kinematics modelled on Lie groups, the special orthogonal group in two dimensions $\mathrm{SO}(2)$ (or the unit circle S^1), the special orthogonal group $\mathrm{SO}(3)$ and the special Euclidean group $\mathrm{SE}(3)$. The attitude kinematics on $\mathrm{SO}(3)$ however is selected to explain the main ideas of this thesis and full algebraic derivations are provided for this particular system.

This work considers a deterministic optimal filtering approach (also known as minimum-energy filtering) to produce the attitude estimates using vectorial measurements. Vectorial measurements obtained from sensors are often contaminated with measurement errors and time-varying bias terms that need to be rejected through the filtering algorithm to produce a smooth and accurate attitude estimate. In the deterministic optimal filtering approach, the error signals are modelled as deterministic unknown functions of time. The filtering objective is to provide a state estimate by minimizing a cost function on the collective energy of the unknown signals of the system. These unknowns include the initial state conditions along with the unknown measurement errors.

2.2 Applications

Attitude estimation is a critical component of many automated control systems in aerial vehicles. The very fast dynamics of attitude in flight manoeuvres requires a very reliable attitude estimate so that the overall control task be successfully executed. Historically, this issue was tackled by using high quality measurement units. These high-end gadgets are either expensive or very large in size restricting their application. In some cases these sensors are only available to military research that further limits their adoption. Recent technological developments in micro electromechanical systems (MEMS)s have driven the emergence of a range of inertial measurement units that are small, inexpensive and light-weight. However, the challenge is with the larger errors and the existence of time-varying bias in the measurements obtained. Following this line of reasoning further, better attitude estimation algorithms are required to compensate for the less expensive sensors used in small automated flight systems . Other potential control and robotics applications include but are not limited to the unmanned aerial vehicles (UAVs), mini UAVs, quadrotors, spacecrafts and satellites.

It is also interesting to consider applications in power systems where the three phase components of an element of the grid needs to be estimated with similar measurements. Another potentially interesting case is in communications where the attitude of a rotating radar needs to be estimated using similar measurements. Quantum spin systems involve systems that evolve on Lie groups other than the ones consider in this thesis. Nevertheless, the theory developed in this thesis could potentially motivate similar results in that area.

2.3 Desired Attributes of an Attitude or Pose Filter

This section contains some desirable attributes that are expected from an attitude or pose filter. Having these qualities in mind will further elucidate the various aspects of the attitude filtering problem. The principles outlined in this list provide qualitative criteria against which the various filters proposed in this thesis can be compared with the state of the art filters in the literature.

Rigorous Modelling
An attitude filter should be based on a well conditioned attitude representation and accurate system model. In particular, other than the estimation errors there should be minimal errors introduced in the process of interpreting the attitude estimates or modelling the system response.

Although attitude is naturally modelled as a rotation matrix, conventional filtering methods have considered vectorial parameterizations of rotations to represent attitude in order to exploit the natural vector formulation of the majority of filter design algorithms. These parameterization are either Euclidean such as the Euler angles or non-Euclidean such as the unit quaternions. Using these parameterizations allows an engineer to use familiar designing methodologies such as extended Kalman filtering and simplifies the algebra. However, these parameterizations have critical weaknesses such as singularities in the attitude representation, non-uniqueness of the representation and the numerical errors introduced in the process of translating estimates back to rotations. In particular, the Euclidean parameterizations are not well defined for certain rotations and continuous control algorithms cannot globally operate on these systems.

Sometimes the result of an algebraic operation on a parameterized rotation needs to be projected such that it yields a meaningful rotation. The projection process itself can introduce secondary errors in the algorithms. For example, straightforward integration of the kinematics model of attitude when represented in vectors is an obvious operation that can involve projection errors. The kinematics of the attitude represented with a rotation matrix is naturally modelled on the Lie group $\mathrm{SO}(3)$. Using the exponential map to integrate the kinematics equation preserves the structure of the attitude rotation matrix and avoids any projection error. Another well-known issue with unit quaternions is the non-uniqueness of quaternions, in other words the fact that any rotation is associated with two different unit quaternions. This causes issues such as the well-known unwinding phenomenon in control algorithms [11]. Using rotations instead of parameterizations is beneficial to avoid the abovementioned issues. Of course, this way of modelling leads to more a complicated algebra. However, Lie groups and their associated algebraic methods are well studied in other literatures and recently there has been more theory [3, 39] available to facilitate their application in systems and control. For an excellent and thorough review of rotations and their parameterizations in rigid-body motion control see [11].

Robustness

An attitude filter should be robust with respect to any initialization errors and measurement errors with large deviations. In particular regarding initialization errors, an attitude filter should converge to the desired solution for almost any initial condition. If for some reason the characteristics of the errors in the measurements change, an ideal method should adaptively continue generating estimates close to the true solution.

Implementability
There are various aspects to the implementability of an attitude filter. Many attitude filtering applications are subject to fast deviations of attitude with respect to time and must run on small scale embedded computer architectures. Consequently, a suitable filtering algorithm should be computationally inexpensive in order to deal with the high data rates and limited computational resources. Recursiveness often makes an algorithm computationally efficient and also allows for real-time and on-line implementability. Recursive methods do not require all the past measurements but rather only the latest measurements in order to update the solution obtained in the previous iteration, in an optimal fashion. Another important factor in the implementability of a filtering algorithm is the practicality of the tuning process. Tuning should not be an lengthy offline process but rather a filtering method should be easily tunable according to the expected level of initialization and measurement errors in a particular situation.

Quantifiable Performance
Trying to quantify and measure how well attitude filters are performing is a daunting task. Sometimes attitude filters are based on different philosophies or are constructed upon different optimization problems with different cost functionals. Even if the standard cost functionals are considered, there is no true optimal attitude filter yet known in the literature and consequently even the available methods that are based on optimality principles involve an approximation that usually has little or no connection to the underlying optimality criteria making a characterization of the resulting loss in performance almost impossible. Therefore, it is very interesting to be able to determine how well a filtering algorithm works. In other words, an attitude filter should in some sense have a justifiable performance measure that is preferably experimentally quantifiable. There is significant value to undertake a simulation study that provides quantitative evidence of the relative performance of various filter design methodologies.

2.4 Attitude Filtering Methods

Many attitude estimation algorithms have been proposed in the literature. The earliest methods are based on the famous Kalman filter [30], an optimal stochastic filtering approach for linear systems. In this method the measurement errors are regarded as white noise and a filter is derived using the noisy measurements by minimizing the

expected value of the square norm difference between the estimated and the true state. For nonlinear systems, due to the lack of finite dimensional parameterizations of general stochastic processes, it is in general impossible to find a finite dimensional optimal stochastic filter [23]. Linearized system equations are usually considered for nonlinear systems to derive the extended Kalman filter (EKF) [6]. According to a relatively recent survey by Crassidis *et. al* [18], EKF is the most adopted method in space flight attitude estimation applications. While, early implementations of EKF were mainly based on singular attitude parameterizations, later trends use non-singular representations (mostly unit quaternions) to achieve better results. A particularly novel approach by Choukroun *et. al* [13] modifies the unit quaternions kinematics and measurements models to obtain an equivalent linear set of equations with measurement errors depending on the quaternion state. A modified Kalman filter is derived for the resulting linear equations and is shown to outperform the EKF. However, a brute force normalization is required to preserve the unit norm property of the resulting quaternion estimate.

The multiplicative extended Kalman filter [24] is the state of the art EKF-based attitude filter that is widely used in spacecraft applications. The idea behind the MEKF is to consider the true attitude state as the product of a reference quaternion and an error quaternion that represents the difference between the reference and the true attitudes. The error quaternion is parameterized by a three dimensional representation of attitude and is estimated using an EKF. The MEKF estimates the true attitude by multiplying the estimated error quaternion (converted back to a unit quaternion) and the reference quaternion. In order to avoid the redundancy of having to estimate both the reference quaternion and the error quaternion, the reference quaternion is chosen in a way that the error quaternion is the identity quaternion. Therefore, the MEKF directly calculates the reference quaternion as a unit quaternion estimate of the true attitude by implicitly running an EKF in the vector space of its angular velocity input.

Motivated by robotics applications, Bonnabel *et. al* [8, 10] proposed the invariant extented Kalman filters (IEKFs) that were based on unit quaternion attitude kinematics and were derived by modifying the EKF equations to be invariant with respect to the group operation in the group of unit quaternions. The left-invariant extended Kalman filter (LIEKF) coincides with the MEKF for a basic attitude filtering problem. The right-invariant EKF [8, 10] or the generalized MEKF (GMEKF) [27] considers measurement errors to be modelled in the reference frame different to the usual body-fixed frame modelling of errors. The gains of the RIEKF/GMEKF stabilize on a wider range of trajectories and are expected to result in better convergence properties of the filter than the MEKF.

Considering the EKF-based methods against the desired attributes of an attitude filter mentioned before, the biggest downfall of these methods is that they are based on first order linearization of the system equations and hence are not robust to large second-order error components. These filters are fairly simple to implement and require little computational power. However, precise tuning of the filter parameters is necessary to attain the best possible performance depending on the experiment. Un-

fortunately, there is no clear performance measure to show how the approximations employed will affect the optimality condition of EKF filters except in some special cases [7].

The unscented Kalman filter (UF) [34] takes a different approach by using the Kalman filtering equations to propagates a carefully chosen set of sigma points to approximate the probability distribution. In this manner it is expected that it can better model the nonlinear propagation of the probability distribution of state expectation as opposed to the EKF that uses a linearization of the nonlinear equations. This method has the potential to achieves a better estimation error lower than the error of the EKF and avoid calculating the Jacobian. Furthermore, UF-based methods have the potential of using higher order moments to approximate the unknown probability distribution. The unscented quaternion estimator (USQUE [15]) is a relatively new adaptation of the UF to attitude filtering that uses unit quaternions to represent the attitude. The unit norm condition of quaternions is claimed to be preserved in the USQUE method where a three-component attitude error is used to derive an unscented filter and the resulting estimated error is converted back to unit quaternions and multiplied with the previously estimated quaternion to produce the attitude estimate. The hope is that the singularities would not occur since a singular parameterization of attitude is only used for the quaternion error that is supposed to be small. The USQUE is shown to outperform the EKF in simulations though with the cost of more computations and complicated tuning process. In a very recent paper [38], by simulations it was shown that the USQUE achieves slightly higher or similar estimation error compared to the MEKF although with a faster convergence rate.

The UF-based methods score similar to EKF-based methods with regards to the desired attributes of an attitude filter. Again there is no clear measure to know how close to optimal a UF-based filter is performing. However, in contrast to the EKF-based methods the UF-based methods have the potential to achieve lower error bounds by using higher order approximations to a general probability distribution. The parameters introduced in the sigma point calculations can potentially complicate the implementation and tuning process.

The stochastic methods introduced so far are based on a Gaussian assumption on the error signals of the attitude filtering problem. Particle filtering includes a wide range of filters that do not have the Gaussian assumption. Rather, Monte-Carlo simulations are performed in order to approximate the general nonlinear distribution using weighted particles. Particle filters have proven to have better error characteristics compared to the EKF however with the cost of significantly increasing the computations. An straightforward implementation of a particle filter is not suitable for small scale embedded architectures due to computational load. In a recent work [12], a unit quaternion boot-strap particle filter was shown to achieve comparable performance to the USQUE with higher computational cost. Particle filters also do not come with clear performance measures to indicate how optimal their solution is.

The MEKF, LIEKF, RIEKF, the USQUE and similar methods that are based on unit quaternions do not have the issue of singularity in their attitude parameteriza-

tion. Unit quaternions have the disadvantage of not being a unique representation for rotations, although using quaternion vectors reduces the computational power compared to using orthogonal rotation matrices. However, any filter that is derived in terms of rotation matrices can be implemented using unit quaternions (but not vice versa).

Aside from the stochastic filtering methods that are mentioned above, attitude estimation algorithms are also proposed based on deterministic modelling schemes. In a deterministic approach the errors of the system are treated as unknown signals of time with no *a priori* stochastic assumptions on them. The filter is usually obtained by minimizing a cost on the size of the errors. Therefore, normally a square norm integrability assumption is needed on the error signals. For linear systems, deterministic filtering leads to the exact same Kalman filter's equations as has been shown in many references, cf. [1, 16, 17]. For nonlinear systems, Mortensen [31] introduced a systematic approach to deriving filtering algorithms based on the properties of the value function of the optimal filtering problem. This approach known as minimum energy filtering, was further explored by Hijab [28]. In this approach the optimal filtering problem is broken down into an optimal control part, assuming a constant initial state, followed by a further optimization over the initial state value. Mortensen's approach [31] proposes an inductive Taylor's expansion of the optimal value function to compute the trajectory of the optimal filter estimate. Convergence of minimum-energy filters was studied by Krener [21] who proved that under some conditions including the uniform observability of the system, a minimum-energy estimate converges exponentially fast to the true state.

In a nonlinear application Aguiar *et al.* [4] applied Mortensen's minimum-energy filtering approach to systems with perspective outputs by embedding the nonlinear geometry in an overarching Euclidean space. Under suitable assumptions, the filter is shown to be asymptotically convergent. The resulting estimates however, need to be projected back to the group $\mathrm{SE}(3)$ which arguably affects the optimality of the filter in an untraceable fashion. Coote *et al.* [29] proposed a near-optimal deterministic filter on the unit circle using a geometric state representation on S^1. This method was then generalized by Zamani *et al.* [42] to attitude filtering on the Lie group $\mathrm{SO}(3)$ using full state measurements. The distance to optimality of these methods are mathematically shown with an upper bound on the difference between the cost these filters achieve and an optimal cost.

Other deterministic methods include attitude determination methods and H-infinity filtering methods. Attitude determination started with what is known as the Wahba's problem [40] in the 1965s. An attitude determination algorithm does not require integrating the attitude kinematics and yields the attitude estimate by optimizing a cost on partial attitude measurement errors. Filtering versions of attitude determination methods on the other hand use the kinematics or dynamics models of attitude to propagate the estimates followed by a measurement update using the attitude determination algorithm. Early attitude determination methods relied on non-$\mathrm{SO}(3)$ parameterizations of attitude while more recently there are methods directly based on $\mathrm{SO}(3)$ [36, 37]. The last two mentioned methods are based on the

dynamics of attitude modelled on the tangent bundle $TSO(3)$ and rely on an implicit QR decomposition in order to provide an optimal attitude and angular velocity estimate by minimizing the attitude and velocity measurements errors. The downside with the attitude determination methods is that they are not robust to state initialization errors that is sometimes compensated for by introducing secondary estimation processes that takes away the simplicity of the original method.

There are also deterministic attitude filters that are based on H-infinity control theory that are designed to minimize the worst case errors rather than minimizing the average error (cf. [26]) . The point with the H-infinity methods is that they are independent of any *a priori* information on the size of initialization and measurement errors. However, lack of incorporating any such information when available leads to reduced performance of these filters compared to the EKF-like methods [18].

Another important class of attitude estimation methods that are not based on optimization methods are drawn from the nonlinear observers family [9, 19, 20, 22, 32, 33, 35]. Nonlinear attitude observers are usually based on nonsingular representations of attitude including unit quaternions and rotation matrices. The distinct feature of these methods is their mathematically guaranteed stability and convergence properties. The limiting fact with these methods is the constant gain of these observers as opposed to filters that have adaptively changing gains, usually obtained using a Riccati equation. In fact, the gains of the nonlinear observers need to be pretuned precisely according to the attitude motion trajectory and hence are less robust to initialization errors.

2.5 Thesis Contributions

In this thesis a novel attitude filtering solution is proposed based on Mortensen's deterministic minimum-energy filtering approach. The following are the main contributions of the thesis. Some of these contributions have already been published in the form of papers.

- In this work the problem of rigid body attitude estimation is tackled by modelling the kinematics of rotations directly on the Lie group $\mathrm{SO}(3)$ along with using nonlinear vectorial models of the angular velocity and attitude sensor measurements, see Chapter 4.
- Tools from differential geometry are utilized to generalize Mortensen's minimum-energy filtering to the space of rotations on $\mathrm{SO}(3)$.
- A comprehensive simulation study is provided to study some of the main attitude filters. In Chapter 7 some of the prominent attitude filters are surveyed. In particular, the main ideas behind each method are summarized and implementation details of each are provided. The GAME filter is then compared against these attitude filters in different situations including scenarios simulating a UAV experiment as well as another scenario simulating a spacecraft experiment. Monte Carlo simulation experiments show that the proposed GAME

filter outperforms all of the competing attitude filters in asymptotic estimation error. Analysis also shows that the GAME filter has the best balanced transient and asymptotic performance in all the situations tested.

- The proposed GAME filter is mathematically analyzed using a least square argument similar to the author's previous work [42]. This is the subject of Chapter 5 where it is shown that the GAME filter is near-optimal. It is proven that the difference between the cost incurred by the proposed GAME filter and a minimum-energy cost is less than or equal to a bound that is decreasing with the estimation error. This bound is numerically quantifiable and is useful for monitoring the GAME filter's performance. In simulations in Chapter 5 it has been shown that this bound is small relative to the optimal cost demonstrating the near-optimality of the GAME filter.

- The filtering approach in this work can systematically yield nonlinear filters with arbitrary order of approximation to an ideal minimum-energy filter. For the case of filtering on the unit circle S^1, an eighth-order approximate minimum-energy filter is provided in Chapter 6. Previous work on this system [29] had only demonstrated a second-order approximate minimum-energy filter that was developed without a general design methodology. For the case of attitude filtering on $\mathrm{SO}(3)$ a second-order approximate minimum-energy filter on $\mathrm{SO}(3)$ (called the GAME filter) using vectorial measurements is proposed in Chapter 4. Previous filtering work on $\mathrm{SO}(3)$ by Zamani *et al.* [42] relied on guessing the correct geometric form of the filter equations based on a least squares analysis of the cost functional. However, only the case with full state measurements was tackled using that method.

- The systematic nature of the approach taken in this thesis facilitates deriving similar filters on other Lie groups. For instance, in Chapter 6 geometric minimum-energy based filters are given for angle kinematics on the unit circle S^1, angle kinematics on $\mathrm{SO}(2)$ with bias in angular velocity measurements, rotation kinematics on $\mathrm{SO}(3)$ with biased angular velocity measurements, and pose kinematics on $\mathrm{SE}(3)$. The latter filter is obtained by geometrically adapting Mortensen's minimum-energy filtering to the problem of rigid-body pose filtering on the group $\mathrm{SE}(3)$ with vectorial measurements.

In summary the proposed attitude filter, called the GAME filter complies with the desired attributes of an attitude filter that were mentioned before. In particular, the GAME filter and its derivation are based on rigorous modelling and truly respect the natural configuration space of the attitude motion being posed on the Lie group $\mathrm{SO}(3)$. The minimum-energy filtering method makes the GAME filter robust with respect to initialization and measurement errors. Another advantage of the proposed geometric minimum-energy filtering approach is that a meaningful cost function is used to derive the filter. The cost function can be modified to incorporate *a priori* knowledge on the expected size of initialization and measurement errors. These a

priori information translate vividly into the proposed filtering equations and thus no extra tuning effort is needed for the proposed algorithms. On the other hand the equations of the GAME filter are slightly more complicated than the main competing method, the MEKF. As a matter of fact the GAME filter, when it is cast in unit quaternions form for the ease of implementability, has the same observer equation as the MEKF with a couple of additional terms in the Riccati equations. Nevertheless, as it is mentioned in Chapter 7, the extra terms have minimal increase of computational load in the GAME filter and overall the implementability of the GAME filter is fairly straightforward. The last but not the least desired attribute of the proposed GAME filter is due to it's quantifiable performance. This is due to the numerically quantifiable optimality gap of the GAME filter that is introduced in Chapter 5 and also due to the meaningful cost function introduced in Chapter 4 that yields the GAME filter.

Chapter 3

Notation

This Chapter contains a brief review of the notation and the identities that are used throughout this thesis .

3.1 Notation

The rotation group is denoted by $\mathrm{SO}(3)$.

$$\mathrm{SO}(3) = \{X \in \mathbb{R}^{3\times 3} \mid X^\top X = I, \det(X) = 1\},$$

where I is the 3 by 3 identity matrix. The associated Lie algebra $\mathfrak{so}(3)$ is the set of skew-symmetric matrices,

$$\mathfrak{so}(3) = \{A \in \mathbb{R}^{3\times 3} \mid A = -A^\top\}.$$

For $\Omega = [a, b, c]^\top \in \mathbb{R}^3$, the lower index operator $(.)_\times : \mathbb{R}^3 \longrightarrow \mathfrak{so}(3)$ yields the skew-symmetric matrix

$$\Omega_\times = \begin{bmatrix} 0 & -c & b \\ c & 0 & -a \\ -b & a & 0 \end{bmatrix}.$$

Inversely, the operator $\mathrm{vex} : \mathfrak{so}(3) \longrightarrow \mathbb{R}^3$ extracts the skew coordinates, $\mathrm{vex}(\Omega_\times) = \Omega$. The cost $\|.\|_R : \mathbb{R}^{3\times 3} \longrightarrow \mathbb{R}_0^+$ is given by

$$\|M\|_R \coloneqq \sqrt{\frac{1}{2}\,\mathrm{trace}(M^\top R M)},$$

where $R \in \mathbb{R}^{3\times 3}$ is symmetric positive definite. Note that $\|M\|_R$ coincides with the Frobenius norm of $R^{1/2}M$. The symmetric projector $\mathbb{P}_s$ is defined by

$$\mathbb{P}_s(M) \coloneqq 1/2(M + M^\top). \tag{3.1}$$

The skew-symmetric projector $\mathbb{P}_a$ is defined by

$$\mathbb{P}_a(M) \coloneqq 1/2(M - M^\top). \tag{3.2}$$

It is easily verified that the vector product of the two vectors $\gamma, \psi \in \mathbb{R}^3$ satisfies

$$(\psi \times \gamma) = \operatorname{vex}(2\mathbb{P}_a(\psi\gamma^\top)) = 2\operatorname{vex}(\mathbb{P}_a(\psi_\times\gamma_\times)). \tag{3.3}$$

Let $L_X : \mathrm{SO}(3) \longrightarrow \mathrm{SO}(3)$, $L_X S = XS$, be the left translation and let $TL_X : T\,\mathrm{SO}(3) \longrightarrow T\,\mathrm{SO}(3)$ denote the associated tangent map for $\Gamma \in \mathfrak{so}(3)$ and $X, S \in \mathrm{SO}(3)$. Let $\mathcal{D}_1 F(X,Y) \circ \mathrm{TL}_X\,\Gamma$ denotes the derivative of the function F with respect to the first argument $X \in \mathrm{SO}(3)$ in the tangent direction $\mathrm{TL}_X\,\Gamma = X\Gamma \in T_X\,\mathrm{SO}(3)$. Recall that the relationship between a directional derivative $\mathcal{D}$ and a gradient ∇ with respect to a Riemannian metric $\langle .,. \rangle_X : T_X\,\mathrm{SO}(3) \times T_X\,\mathrm{SO}(3) \longrightarrow \mathbb{R}$ is as follows.

$$\mathcal{D}_1 F(X,Y) \circ \mathrm{TL}_X\,\Gamma = \langle \nabla_1 F(X,Y), \mathrm{TL}_X\,\Gamma \rangle_X = \langle \mathrm{TL}_X^*\,\nabla_1 F(X,Y), \Gamma \rangle_I. \tag{3.4}$$

The asterisk denotes the adjoint with respect to the given Riemannian metric. We use the standard left-invariant Riemannian metric on $\mathrm{SO}(3)$. That is, for $\Gamma, \Omega \in \mathfrak{so}(3)$ and $X \in \mathrm{SO}(3)$

$$\langle \mathrm{TL}_X\,\Gamma, \mathrm{TL}_X\,\Omega \rangle_X = \langle \Gamma, \Omega \rangle_I := \frac{1}{2}\operatorname{trace}(\Gamma^\top\Omega). \tag{3.5}$$

One has

$$\langle \mathrm{TL}_X\,\Gamma, \mathrm{TL}_X\,\Omega \rangle_X = \langle \operatorname{vex}(\Gamma), \operatorname{vex}(\Omega) \rangle = \operatorname{vex}(\Gamma)^\top \operatorname{vex}(\Omega). \tag{3.6}$$

For the sake of simplicity, in the reminder of the chapter we will omit the subscript notation from the Riemannian metrics.

3.2 Identities

Consider a symmetric matrix $Z \in \mathbb{R}^{3\times 3}$ and the vectors $a, b, c \in \mathbb{R}^3$. The following identity is used to vectorize a skew-symmetric projection of a product between a symmetric and an skew-symmetric matrix.

$$\operatorname{vex}(Za_\times + a_\times Z) = (\operatorname{trace}(Z)I - Z)a. \tag{3.7}$$

The following identity is used to vectorize a product between two skew-symmetric matrices.

$$\operatorname{vex}(a_\times b_\times) = a_\times b = -a_\times b. \tag{3.8}$$

Chapter 4

Minimum-Energy Filtering on the Lie group $\mathrm{SO}(3)$

This chapter begins with a formal formulation of the proposed deterministic minimum-energy filtering problem. The problem formulation involves the kinematics of attitude modelled on the special orthogonal group $\mathrm{SO}(3)$ along with vectorial sensor measurements.

The solution to this problem is sought for along the lines of Hamilton-Jacobi-Bellman theory [5]. A cost functional is defined that depends on the unknown state and the unknown measurement error signals. A value function is defined for the cost function similarly to optimal filtering and optimal control theory.

A detailed derivation of minimum-energy filtering is provided using Mortensen's method [31], adapted to the Lie group structure of our problem. It will be shown that the optimal solution is potentially infinite dimensional as it requires the second-order derivative as well as all the higher order derivatives of the value function to be computed on-line. Every order derivative of the value function depends on the lower order derivatives as well as a one step higher order derivative of the value function.

An approximate solution is computed by neglecting the third order derivative of the value function and by proposing a matrix representation of the Hessian of the value function that respects the underlying geometric structure of the system. The resulting filter, namely the geometric approximate minimum-energy (GAME) filter is a second-order nonlinear attitude filter that is posed directly on $\mathrm{SO}(3)$.

The remainder of the chapter is organized as follows. Section 4.1 contains the details of the attitude filtering problem and the equations governing the attitude kinematics, measurements and cost functional. In Section 4.2 a detailed derivation of the filtering solutions i provided. Finally Section 4.3 provides a summary of the results and the main theorem of the this chapter.

4.1 Attitude Filtering Using Vectorial Measurements

Consider the aircraft shown in Figure 4.1, as an example of a rigid-body moving in the $3D$ space. Two coordinate frames are shown in this figure. The inertial frame or the reference frame is a known frame that is fixed at some reference point and is

denoted by $\{\mathcal{I}\}$. The body-fixed frame is a moving coordinate frame that is fixed to the aircraft and is denoted by $\{\mathcal{B}\}$. The attitude matrix X transforms the coordinates of the inertial frame to the the coordinates of the body-fixed frame. Recall the attitude

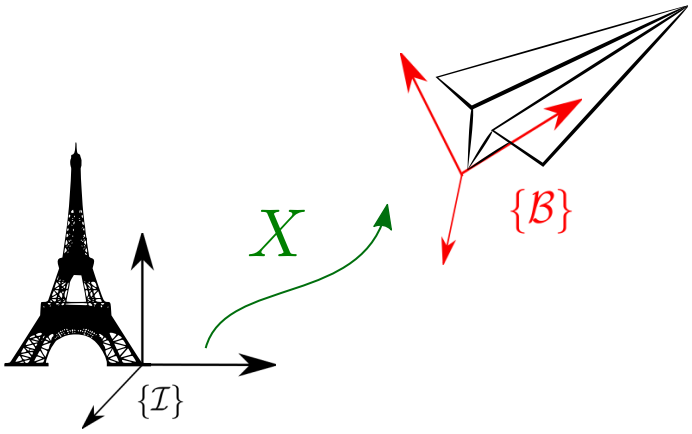

Figure 4.1: Rigid-body motion frames.

kinematics given by

$$\dot{X} = X\Omega_\times,\ X(0) = X_0. \tag{4.1}$$

The matrix X is an SO(3)-valued state signal with the unknown initial value X_0 and $\Omega \in \mathbb{R}^3$ represents the angular velocity of the moving body expressed in the body-fixed frame.

A rate-gyro sensor measures the angular velocity through the following equation

$$u = \Omega + Bv. \tag{4.2}$$

The signals $u \in \mathbb{R}^3$ and $v \in \mathbb{R}^3$ denote the body-fixed frame measured angular velocity and the input measurement error, respectively. The coefficient matrix $B \in \mathbb{R}^{3\times 3}$ allows for different weightings for the components of the unknown input measurement error v. We assume that B is full rank and hence that $Q := BB^\top$ is positive definite.

Consider the vectors $\mathring{y}_i \in \mathbb{R}^3$ as known vector directions in the reference frame. Measuring these vectors in the body-fixed frame provides partial information about the attitude X. Typically, magnetometer, visual sensors, sun sensor and star tracker are deployed for this purpose. The following model yields the measurements of theses sensors.

$$y_i = X^\top \mathring{y}_i + D_i w_i,\ i = 1, \cdots, n \tag{4.3}$$

The measurements $y_i \in \mathbb{R}^3$ are measurements of the $\mathring{y}_i$ in the body-fixed frame and the signals $w_i \in \mathbb{R}^3$ are the unknown output measurement errors. The coefficient matrix $D_i \in \mathbb{R}^{3\times 3}$ allows for different weightings of the components of the output measurement error w_i. The usual assumption is that the matrix D_i is full rank and $R_i := D_i D_i^\top$ is positive definite.

Consider the cost

$$J(t;\ X_0,\ v|_{[0,\,t]},\ \{w_i|_{[0,\,t]}\}) = \frac{1}{2}\,\text{trace}\left[(I - X_0)K_{X_0}(I - X_0)^\top\right] + \frac{1}{2}\int_0^\top \left(v^\top v + \sum_i w_i^\top w_i\right) d\tau, \tag{4.4}$$

in which $K_{X_0} \in \mathbb{R}^{3\times 3}$ is symmetric positive definite. The cost (4.4) can be thought of as a measure of the aggregate energy stored in the unknown initialization and measurement signals of (4.1), (4.2) and (4.3).

The principle of minimum-energy filtering is as follows. At each time t, given the measurements $\{y_i|_{[0,\,t]}\}$ and $u|_{[0,\,t]}$, the goal is to obtain an estimate $\hat{X}(t)$ of the true state $X(t)$ by minimizing the cost (4.4). In order to obtain $\hat{X}(t)$, one seeks a combination of the unknowns $(X_0,\ v|_{[0,\,t]},\ \{w_i|_{[0,\,t]}\})$ that is compatible with the measurements $\{y_i|_{[0,\,t]}\}$ and $u|_{[0,\,t]}$ in fulfilling the system equations (4.1). Note that in general, infinitely many combinations of these unknowns are compatible with the measurements. By minimizing the cost (4.4) a triplet $(X_0^*,\ v^*|_{[0,\,t]},\ \{w_i^*|_{[0,\,t]}\})$ is chosen that contains minimum collective energy.

The minimizing unknowns $(X_0^*,\ v^*|_{[0,\,t]},\ \{w_i^*|_{[0,\,t]}\})$ replaced in the system equation (4.1) yield the optimal state trajectory $X^*_{[0,\,t]}$. The subscript $[0,\ t]$ indicates that the optimization takes place on the interval $[0,\ t]$. We pick the final optimal state $X^*_{[0,\,t]}(t)$ as our minimum-energy estimate at time t, $\hat{X}(t) \coloneqq X^*_{[0,\,t]}(t)$.

A naive approach to the minimum energy filtering problem leads to an infinite dimensional optimization problem at each time interval $[0,\ t]$. To obtain a practical algorithm a recursive filter is desired that at each time t yields the minimum-energy estimate as its state value.

Note that the cost (4.4) depends on the unknowns X_0, $v|_{[0,\,t]}$ and $\{w_i|_{[0,\,t]}\}$, but given X_0, $v|_{[0,\,t]}$, the known $\{\mathring{y}_i\}$, and the measurements $u|_{[0,\,t]}$ and $\{y_i|_{[0,\,t]}\}$, the $w_i|_{[0,\,t]}$ are uniquely determined by (4.3). Hence, the cost (4.4) is equivalent to

$$J(t;\ X_0,\ v|_{[0,\,t]}) = \frac{1}{2}\,\text{trace}\left[(I - X_0)K_{X_0}(I - X_0)^\top\right] + \frac{1}{2}\int_0^\top \left(v^\top v + \sum_i (X^\top \mathring{y}_i - y_i)^\top R_i^{-1}(X^\top \mathring{y}_i - y_i)\right) d\tau, \tag{4.5}$$

which depends only on the signals X_0 and $v|_{[0,\,t]}$. Minimizing (4.5) over these four arguments is simplified by first assuming that X_0 is known and minimizing over $v|_{[0,\,t]}$, then later optimizing over X_0. The problem of minimizing (4.5) subject to (4.1) can be seen as an optimal control problem where the signal $v|_{[0,\,t]}$ is considered as a control input.

As in the maximum-principle [5] a pre-Hamiltonian is defined as

$$\begin{aligned}\mathcal{H}^-(X,\mu,v,t) \coloneqq \frac{1}{2}[v^\top v+ \\ \sum_i (X^\top \mathring{y}_i - y_i)^\top R_i^{-1}(X^\top \mathring{y}_i - y_i)] - \mu^\top(u - Bv),\end{aligned} \tag{4.6}$$

where $\mu \in \mathbb{R}^3$ represents a costate variable $\Theta \in \mathfrak{so}^*(3)$ for system (4.1) via $\langle (\mu)_\times, \Gamma \rangle = \Theta(\Gamma)$ for all $\Gamma \in \mathfrak{so}(3)$. In the following the identification of $\Theta \in \mathfrak{so}^*(3)$ with $\mu_\times \in \mathfrak{so}(3)$ will be used without further reference. Since the pre-Hamiltonian (4.6) is quadratic in v, its minimum is given by the differential condition

$$\mathcal{D}_v \mathcal{H}^- \circ \gamma = 0, \ \forall \gamma \in \mathbb{R}^3. \tag{4.7}$$

Solving for v yields the optimal input $v^* = -B^\top \mu$. Substituting v^* in (4.6) yields the optimal Hamiltonian

$$\mathcal{H}(X,\mu,t) = \frac{1}{2}[-\mu^\top Q \mu + \sum_i (X^\top \mathring{y}_i - y_i)^\top R_i^{-1}(X^\top \mathring{y}_i - y_i)] - \mu^\top u. \tag{4.8}$$

Consider a value function depending on the state signal X and time t defined as

$$V(X,t) \coloneqq \min_{v|_{[0,\,t]}} J(t;\ X_0,\ v|_{[0,\,t]}), \tag{4.9}$$

where J is the cost (4.5) and the minimization is constrained by the system equations (4.1), (4.2) and (4.3). From (4.5) the initial time boundary condition is

$$V(X_0,0) = \frac{1}{2}\,\mathrm{trace}\left[(I - X_0)K_{X_0}(I - X_0)^\top\right]. \tag{4.10}$$

Performing the dynamic programming principle [5] using (4.5), (4.8) and (4.9) yields the Hamilton-Jacobi-Bellman equation

$$\mathcal{H}(X, \mathrm{TL}_X^*\, \nabla_1 V(X,t), t) - \frac{\partial V}{\partial t}(X,t) = 0. \tag{4.11}$$

Up to here the dynamic programming principle was utilized to address the optimal control part of the problem (by minimizing (4.5) over v). To complete the optimal filtering problem, the value function V is required to depend on the optimal state $X^*_{[0,t]}$. This can be posed as an optimization over the initial condition X_0 or equivalently as an optimization over the final condition $X(t)$ since the initial and final conditions are deterministically coupled by the optimal input $v^*|_{[0\,,\,t]}$. In other words, given the input v^* and any value of the trajectory $X^*_{[0,t]}$, one can integrate Equation (4.1) forward or backwards to obtain any other value of the trajectory $X^*_{[0,t]}$. Assuming that the value function is strictly convex, its minimum is characterized by the condition

$$\nabla_1 V(X,t)|_{X = X^*_{[0,t]}(t)} = 0. \tag{4.12}$$

Recall that the minimum-energy estimate $\hat{X}(t)$ is defined as the final value of the minimizing argument $X^*_{[0,t]}(t)$. Hence,

$$\nabla_1 V(X,t)|_{X=\hat{X}(t)} = 0. \tag{4.13}$$

Note that solving the HJB Equation (4.11) for $V(X,t)$ and then finding the solution to the final condition equation (4.13) characterizes the estimate $\hat{X}(t)$. However, this still requires an explicit solution to a potentially infinite dimensional optimization problem and must be repeated at every time t. To overcome this issue Mortensen's approach [31] is utilized to derive a recursive solution to this problem.

4.2 Filter Derivation Using Mortensen's Method

In this section goal is to obtain a dynamical equation for $\dot{\hat{X}}$ that will recursively update the minimum-energy filtering solution $\hat{X}(t)$. As in Mortensen's approach [31] this problem is tackled by deriving a total time derivative of the final condition (4.13), however by modifying the method with respect to the geometric structure of $\mathrm{SO}(3)$.

First rewrite the final condition (4.13) using the directional derivative (3.4) defined in Chapter 3. For all $\Gamma \in \mathfrak{so}(3)$

$$\langle \nabla_1 V(X,t), X\Gamma \rangle|_{X=\hat{X}(t)} = 0. \tag{4.14}$$

Define $G_\Gamma(X,t) := \langle \nabla_1 V(X,t), X\Gamma \rangle$. Therefore the final condition (4.14) yields

$$\{G_\Gamma(X,t)\}_{X=\hat{X}(t)} = 0. \tag{4.15}$$

The total time derivative of (4.15) is computed in order to obtain a dynamical equation for $\hat{X}$.

For all $\Gamma \in \mathfrak{so}(3)$

$$\frac{d}{dt}\{G_\Gamma(X,t)\}_{X=\hat{X}(t)} = 0. \tag{4.16}$$

Applying the chain rule to Equation (4.16) yields

$$\{\mathcal{D}_1 G_\Gamma(X,t) \circ \dot{\hat{X}}(t) + \frac{\partial G_\Gamma}{\partial t}(X,t)\}_{X=\hat{X}(t)} = 0. \tag{4.17}$$

Note that the first derivative is calculated in the tangent direction $\dot{\hat{X}}(t)$ since the final condition (4.15) is evaluated at $X = \hat{X}(t)$ first, and then the total time derivative is calculated.

Now it is clear that solving this equation for $\dot{\hat{X}}$ will yield a recursive update equation for the minimum energy estimate $\hat{X}(t)$. In order to solve this equation, one needs to calculate the derivatives of the function $G_\Gamma(X,t)$ first.

The second term in (4.17) equals $\langle \nabla_1 F(X,t), X\Gamma \rangle$ where

$$F(X,t) := \frac{\partial V}{\partial t}(X,t) = \mathcal{H}(X, \mathrm{TL}^*_X \nabla_1 V(X,t), t). \tag{4.18}$$

The last equality follows from (4.11). Denote $\mu_\times(X,t) \coloneqq \mathrm{TL}_X^* \nabla_1 V(X,t)$ and observe that

$$\begin{aligned} F(X,t) &= \mathcal{H}(X, \mu_\times(X,t), t), \\ G_\Gamma(X,t) &= \langle \mu_\times(X,t), \Gamma \rangle. \end{aligned} \tag{4.19}$$

The second identity in (4.19) follows from (3.5). Hence Equation (4.17) yields

$$\{ \langle \mathcal{D}_1 \mu_\times(X,t) \circ \dot{\hat{X}}(t), \Gamma \rangle + \langle \nabla_1 F(X,t), X\Gamma \rangle \}_{X=\hat{X}(t)} = 0. \tag{4.20}$$

The first term in (4.20) is calculated next. For all $\Psi \in \mathfrak{so}(3)$

$$\begin{aligned} \langle \mu_\times(X,t), \Psi \rangle &= \langle \mathrm{TL}_X^* \nabla_1 V(X,t), \Psi \rangle = \\ &\quad \langle \nabla_1 V(X,t), \mathrm{TL}_X \Psi \rangle = \mathcal{D}_1 V(X,t) \circ X\Psi. \end{aligned} \tag{4.21}$$

Therefore

$$\begin{aligned} \langle \mathcal{D}_1 \mu_\times(X,t) \circ X\Gamma, \Psi \rangle &= \mathcal{D}_1^2 V(X,t) \circ (X\Psi, X\Gamma) + \mathcal{D}_1 V(X,t) \circ \mathcal{D}_X(X\Psi) \circ X\Gamma \\ &= \langle \mathrm{Hess}_1 V(X,t) \circ X\Gamma, X\Psi \rangle + \langle \nabla_1 V(X,t), X \mathbb{P}_a(\Gamma\Psi) \rangle \\ &= \langle \mathrm{TL}_X^* \mathrm{Hess}_1 V(X,t) \circ X\Gamma, \Psi \rangle + \langle \mathbb{P}_a(\mathrm{TL}_X^* \nabla_1 V(X,t)\Gamma), \Psi \rangle, \end{aligned} \tag{4.22}$$

which yields

$$\mathcal{D}_1 \mu_\times(X,t) \circ X\Gamma = \mathrm{TL}_X^* \mathrm{Hess}_1 V(X,t) \circ X\Gamma + \mathbb{P}_a(\mathrm{TL}_X^* \nabla_1 V(X,t)\Gamma). \tag{4.23}$$

Given that $\{\nabla_1 V(X,t)\}_{X=\hat{X}(t)} = 0$ from the final condition (4.13), the second term in (4.23) is zero when evaluated at $X = \hat{X}(t)$.

In order to obtain an algebraic solution for the Hessian operator in (4.23), consider the matrix representation for $\mathcal{D}_1 \mu_\times(\hat{X},t) \circ \hat{X}\Gamma$ defined as follows.

$$\mathcal{D}_1 \mu_\times(\hat{X},t) \circ \hat{X}\Gamma =: K \,\mathrm{vex}(\Gamma), \tag{4.24}$$

where $K \in \mathbb{R}^{3\times 3}$ is a symmetric matrix. Note that K is defined to be symmetric since the Hessian is a symmetric operator.

Now consider the second term in (4.20). The identities (4.19) yield

$$\begin{aligned} \langle \nabla_1 F(X,t), X\Gamma \rangle &= \mathcal{D}_1 \mathcal{H}(X, \mu_\times(X,t), t) \circ X\Gamma \\ &\quad + \mathcal{D}_2 \mathcal{H}(X, \mu_\times(X,t), t) \circ \mathcal{D}_1 \mu_\times(X,t) \circ X\Gamma. \end{aligned} \tag{4.25}$$

Evaluate this equation at $X = \hat{X}(t)$.

$$\begin{aligned} \langle \nabla_1 F(X,t), X\Gamma \rangle|_{X=\hat{X}(t)} &= \langle \mathrm{TL}_X^* \nabla_1 \mathcal{H}(X, \mu_\times(X,t), t), \Gamma \rangle|_{X=\hat{X}(t)} \\ &\quad + \langle \nabla_2 \mathcal{H}(X, \mu_\times(X,t), t), \mathcal{D}_1 \mu_\times(X,t) \circ X\Gamma \rangle|_{X=\hat{X}(t)} \end{aligned} \tag{4.26}$$

Next, the derivatives of the optimal Hamiltonian H are calculated to be replaced

into (4.26). From (4.8),

$$\nabla_2 \mathcal{H}(X, \mu_\times(X,t), t) = -(u + Q\mu(X,t))_\times. \tag{4.27}$$

Also (4.8) yields that for all $\Gamma \in \mathfrak{so}(3)$

$$\begin{aligned}
&\langle \mathrm{TL}_X^* \nabla_1 \mathcal{H}(X, \mu_\times, t), \Gamma \rangle \\
&= \operatorname{trace}[\sum_i R_i^{-1}(X^\top \mathring{y}_i - y_i)(\Gamma^\top X^\top \mathring{y}_i)^\top] \\
&= -\operatorname{trace}[\sum_i \mathbb{P}_a(R_i^{-1}(X^\top \mathring{y}_i - y_i)\mathring{y}_i^\top X)\Gamma^\top] \\
&= -2\langle \sum_i \mathbb{P}_a(R_i^{-1}(X^\top \mathring{y}_i - y_i)\mathring{y}_i^\top X), \Gamma \rangle \\
&= -\langle \sum_i ((X^\top \mathring{y}_i) \times (R_i^{-1}(X^\top \mathring{y}_i - y_i))_\times, \Gamma \rangle
\end{aligned} \tag{4.28}$$

The last equality is due the identity (3.3). By evaluating at $X = \hat{X}(t)$ and by denoting $\hat{y}_i := \hat{X}^\top \mathring{y}_i$ one obtains

$$\mathrm{TL}^*_{\hat{X}(t)} \nabla_1 \mathcal{H}(\hat{X}(t), \mu_\times, t) = \sum_i ((R_i^{-1}(\hat{y}_i - y_i)) \times \hat{y}_i)_\times. \tag{4.29}$$

Replacing (4.27) and (4.29) back in Equation (4.26), using (4.24) and observing that $\mu_\times(\hat{X}, t)$ is zero from the final condition (4.13) yield

$$\begin{aligned}
\langle \nabla_1 F(X,t), X\Gamma \rangle|_{X=\hat{X}(t)} &= \langle \sum_i (R_i^{-1}(\hat{y}_i - y_i)) \times \hat{y}_i, \operatorname{vex}(\Gamma) \rangle - \langle K \operatorname{vex}(\Gamma), u \rangle \\
&= \langle \sum_i (R_i^{-1}(\hat{y}_i - y_i)) \times \hat{y}_i - Ku, \operatorname{vex}(\Gamma) \rangle.
\end{aligned} \tag{4.30}$$

Note that the last line follows from the fact that P is a symmetric matrix.

Recall Equation (4.20). Using (4.24) for the first term of (4.20) and replacing (4.30) for the second term yield

$$K \operatorname{vex}(\mathrm{TL}^*_{\hat{X}} \dot{\hat{X}}) = -\sum_i ((R_i^{-1}(\hat{y}_i - y_i)) \times \hat{y}_i) + Ku. \tag{4.31}$$

Now by rearranging the previous equation the $\dot{\hat{X}}$ equation is

$$\dot{\hat{X}} = \hat{X} \left(u - K^{-1} \sum_i (R_i^{-1}(\hat{y}_i - y_i)) \times \hat{y}_i \right)_\times, \tag{4.32}$$

where $\hat{y}_i = \hat{X}^\top \mathring{y}_i$ and $\hat{X}(0) = I$ is obtained by evaluating the final condition (4.13) at time 0 using the boundary condition (4.10) .

Note that Equation (4.32) is the *exact* form of a minimum-energy observer for system (4.1) where energy is measured by the cost (4.4). The observer contains the innovation term $K^{-1} \sum_i (R_i^{-1}(\hat{y}_i - y_i)) \times \hat{y}_i$ which is a weighted sum proportional to

the information contained in the error $\hat{y}_i - y_i$. The matrix K^{-1} acts as the gain for this innovation term.

To fully solve (4.32), the matrix P needs to be updated on-line. Therefore, in the following the goal is to find a differential equation that dynamically updates K. This is done, following the previous observer calculations, by computing the total time derivative $\frac{d}{dt}\langle K\gamma, \psi\rangle$.

Recall from (4.24) and (4.22) that for all $\gamma, \psi \in \mathbb{R}^3$

$$\begin{aligned}\langle K\gamma, \psi\rangle &= \langle \mathcal{D}_1\mu_\times(\hat{X}, t) \circ \hat{X}\Gamma, \Psi\rangle \\ &= \left\{\mathcal{D}_1^2 V(X,t) \circ (X\Gamma, X\Psi) + \mathcal{D}_1 V(X,t) \circ \mathcal{D}_X(X\Gamma) \circ X\Psi\right\}_{X=\hat{X}(t)},\end{aligned} \tag{4.33}$$

where $\Psi := \psi_\times$ and $\Gamma := \gamma_\times$. The total time derivative of (4.33) is calculated as

$$\begin{aligned}\frac{d}{dt}\langle K\gamma, \psi\rangle = \\ &\{\mathcal{D}_1^3 V(X,t) \circ (X\Gamma, X\Psi, \dot{\hat{X}}) + \mathcal{D}_1^2 V(X,t) \circ (\mathcal{D}_X(X\Gamma) \circ \dot{\hat{X}}, X\Psi) \\ &+ \mathcal{D}_1^2 V(X,t) \circ (X\Gamma, \mathcal{D}_X(X\Psi) \circ \dot{\hat{X}}) + \mathcal{D}_1^2 F(X,t) \circ (X\Gamma, X\Psi) \\ &+ \mathcal{D}_1^2 V(X,t) \circ (\mathcal{D}_X(X\Gamma) \circ X\Psi, \dot{\hat{X}}) + \mathcal{D}_1 V(X,t) \circ \mathcal{D}_X^2(X\Gamma) \circ (X\Psi, \dot{\hat{X}}) \\ &+ \mathcal{D}_1 V(X,t) \circ \mathcal{D}_X(X\Gamma) \circ \mathcal{D}_X(X\Psi) \circ \dot{\hat{X}} + \mathcal{D}_1 F(X,t) \circ \mathcal{D}_X(X\Gamma) \circ X\Psi\}_{X=\hat{X}(t)}.\end{aligned} \tag{4.34}$$

Note that in (4.34) the terms involving a first order derivative of V are zero from the final condition (4.13). Also the last and the fourth to last terms in (4.34) cancel each other from (4.20) and (4.22). We will neglect the first term in (4.34) since it is a third order term. The fourth term of (4.34) involves the second order derivative of $F(X,t)$ that is calculated next.

$$\begin{aligned}\mathcal{D}_1^2 F(X,t) \circ (X\Gamma, X\Psi) = \mathcal{D}_1^2\mathcal{H}(X, \mu_\times(X,t), t) \circ (X\Gamma, X\Psi) \\ &+ \mathcal{D}_1(\mathcal{D}_2\mathcal{H}(X, \mu_\times(X,t), t) \circ \mathcal{D}_1\mu_\times(X,t) \circ X\Gamma) \circ X\Psi \\ &+ \mathcal{D}_2(\mathcal{D}_1\mathcal{H}(X, \mu_\times(X,t), t) \circ X\Gamma) \circ \mathcal{D}_1\mu_\times(X,t) \circ X\Psi \\ &+ \mathcal{D}_2^2\mathcal{H}(X, \mu_\times(X,t), t)) \circ (\mathcal{D}_1\mu_\times(X,t) \circ X\Gamma, \mathcal{D}_1\mu_\times(X,t) \circ X\Psi) \\ &+ \mathcal{D}_2\mathcal{H}(X, \mu_\times(X,t), t) \circ \mathcal{D}_1^2\mu_\times(X,t) \circ (X\Gamma, X\Psi).\end{aligned} \tag{4.35}$$

Observe that from (4.8), the second and the third lines of (4.35) yield zero. To further simplify Equation (4.35), the terms $\mathcal{D}_1^2\mathcal{H}$, $\mathcal{D}_2^2\mathcal{H}$ and $\mathcal{D}_1^2\mu_\times$ are computed first. Recall from our previous calculations (4.28) that

$$\{\mathcal{D}_1\mathcal{H}(X, \mu_\times(X,t), t) \circ X\Gamma\}_{X=\hat{X}(t)} = -2\langle \sum_i X\mathbb{P}_a(R_i^{-1}(X^\top \mathring{y}_i - y_i)\mathring{y}_i^\top X), X\Gamma\rangle_{X=\hat{X}(t)}. \tag{4.36}$$

Therefore the second order derivative of $\mathcal{H}$ yields

$$\begin{aligned}
&\{\mathcal{D}_1^2\mathcal{H}(X,\mu_\times(X,t),t)\circ(X\Gamma,X\Psi)\}_{X=\hat{X}(t)} = \\
&-2\langle X\sum_i \mathbb{P}_a(\Psi\mathbb{P}_a(R_i^{-1}(\hat{y}_i-y_i)\hat{y}_i^\top)),X\Gamma\rangle|_{X=\hat{X}(t)} \\
&-2\langle X\sum_i \mathbb{P}_a(R_i^{-1}\Psi^\top\hat{y}_i\hat{y}_i^\top),X\Gamma\rangle|_{X=\hat{X}(t)} \\
&-2\langle X\sum_i \mathbb{P}_a(R_i^{-1}(\hat{y}_i-y_i)\hat{y}_i^\top\Psi),X\Gamma\rangle|_{X=\hat{X}(t)} = \\
&-2\langle X\sum_i \mathbb{P}_a(\Psi\mathbb{P}_s(R_i^{-1}(\hat{y}_i-y_i)\hat{y}_i^\top)),X\Gamma\rangle|_{X=\hat{X}(t)} \\
&-2\langle X\sum_i \mathbb{P}_a(R_i^{-1}\Psi^\top\hat{y}_i\hat{y}_i^\top),X\Gamma\rangle|_{X=\hat{X}(t)}.
\end{aligned} \tag{4.37}$$

Identities (3.7) and (3.8) yield the vector form of Equation (4.37). Denote $Z := \sum_i \mathbb{P}_s(R_i^{-1}(\hat{y}-y_i)\hat{y}_i^\top)$, hence

$$\begin{aligned}
&\mathcal{D}_1^2\mathcal{H}(\hat{X}(t),\mu_\times(\hat{X}(t),t),t)\circ(\hat{X}(t)\Gamma,\hat{X}(t)\Psi) = \\
&\qquad\langle-(\mathrm{trace}(Z)I-Z)\gamma,\psi\rangle + \langle(\hat{y}_i)_\times^\top R_i^{-1}(\hat{y}_i)_\times\gamma,\psi\rangle.
\end{aligned} \tag{4.38}$$

In order to compute $\mathcal{D}_2^2\mathcal{H}$, from (4.24) recall that $\mathcal{D}_1\mu_\times(\hat{X},t)\circ\hat{X}\Psi = K\psi$. Hence

$$\begin{aligned}
&\{\mathcal{D}_2^2\mathcal{H}(X,\mu_\times(X,t),t)\circ(\mathcal{D}_1\mu_\times(X,t)\circ X\Gamma,\mathcal{D}_1\mu_\times(X,t)\circ X\Psi)\}_{X=\hat{X}(t)} \\
&\qquad = -\langle QK\psi,K\gamma\rangle = -\langle KQK\gamma,\psi\rangle.
\end{aligned} \tag{4.39}$$

Now in order to compute the last term in (4.35) one needs to compute $\mathcal{D}_1^2\mu_\times(X,t)\circ(X\Gamma,X\Psi)$. Recall from (4.22) that for all $\Xi\in\mathfrak{so}(3)$

$$\langle\mathcal{D}_1\mu_\times(X,t)\circ X\Gamma,\Xi\rangle = \mathcal{D}_1^2V(X,t)\circ(X\Xi,X\Gamma)+\mathcal{D}_1V(X,t)\circ\mathcal{D}_X(X\Xi)\circ X\Gamma. \tag{4.40}$$

Therefore the following equation is obtained.

$$\begin{aligned}
&\langle\mathcal{D}_1^2\mu_\times(X,t)\circ(X\Gamma,X\Psi),\Xi\rangle = \\
&\quad\mathcal{D}_1^3V(X,t)\circ(X\Xi,X\Gamma,X\Psi)+\mathcal{D}_1^2V(X,t)\circ(X\mathbb{P}_a(\Psi\Xi),X\Gamma) \\
&\quad+\mathcal{D}_1^2V(X,t)\circ(X\mathbb{P}_a(\Gamma\Xi),X\Psi)+\mathcal{D}_1V(X,t)\circ\mathcal{D}_X^2(X\Xi)\circ(X\Gamma,X\Psi).
\end{aligned} \tag{4.41}$$

Here, the first term is a third order term and will be neglected. The last term is zero from the final condition (4.13) at $X=\hat{X}(t)$. The remaining two terms can be rewritten using (3.8), (4.22) and (4.24). We get for all $\xi := \mathrm{vex}(\Xi)$

$$\begin{aligned}
\langle\mathcal{D}_1^2\mu_\times(X,t)\circ(X\Gamma,X\Psi),\Xi\rangle|_{X=\hat{X}(t)} &= -\frac{1}{2}(\langle K\gamma,\xi\times\psi\rangle+\langle K\psi,\xi\times\gamma\rangle) = \\
&\frac{1}{2}\langle K\gamma\times\psi+K\psi\times\gamma,\xi\rangle.
\end{aligned} \tag{4.42}$$

The last line in (4.42) follows from the fact that for all $a, b, c \in \mathbb{R}^3$

$$\langle a, b \times c \rangle = \langle c, a \times b \rangle. \tag{4.43}$$

Recall Equation (4.35). Using equation (4.42) and (4.27) and the fact that $\mu_\times(\hat{X}, t)$ is zero from the final condition (4.13), the final term in (4.35) is

$$\begin{aligned} &\{\mathcal{D}_2\mathcal{H}(X, \mu_\times(X,t), t) \circ \mathcal{D}_1^2\mu_\times(X,t) \circ (X\Gamma, X\Psi)\}_{X=\hat{X}(t)} = \\ &\quad \frac{1}{2}\langle \psi \times K\gamma \rangle + \gamma \times K\psi, u\rangle = \frac{1}{2}\langle -u_\times K\gamma + Ku_\times\gamma, \psi\rangle = \langle \mathbb{P}_s(Ku_\times)\gamma, \psi\rangle. \end{aligned} \tag{4.44}$$

Going back to the derivative of K (4.34), the second and the third lines are computed similar to the last equation.

$$\begin{aligned} &\{\mathcal{D}_1^2 V(X,t) \circ (\mathcal{D}_X(X\Gamma) \circ \dot{\hat{X}}, X\Psi) + \mathcal{D}_1^2 V(X,t) \circ (X\Gamma, \mathcal{D}_X(X\Psi) \circ \dot{\hat{X}})\}_{X=\hat{X}(t)} = \\ &\quad \langle K\psi, \frac{1}{2}\operatorname{vex}(\mathrm{TL}_{\hat{X}}^* \dot{\hat{X}}) \times \gamma\rangle + \langle K\gamma, \frac{1}{2}\operatorname{vex}(\mathrm{TL}_{\hat{X}}^* \dot{\hat{X}}) \times \psi\rangle = \langle \mathbb{P}_s(K\,\mathrm{TL}_{\hat{X}}^* \dot{\hat{X}})\gamma, \psi\rangle. \end{aligned} \tag{4.45}$$

Finally, all the terms in Equation (4.34) are calculated. Replacing (4.44), (4.39) and (4.38) into Equation (4.35) followed by replacing (4.35) and (4.45) into Equation (4.34) and cancelling the directions γ and ψ yield the following Riccati equation.

$$\begin{aligned} \dot{K} = &-KQK + \mathbb{P}_s(K(2u - K^{-1}\sum_i (R_i^{-1}(\hat{y}_i - y_i)) \times \hat{y}_i)_\times) \\ &- \operatorname{trace}(\sum_i \mathbb{P}_s(R_i^{-1}(\hat{y} - y_i)\hat{y}_i^\top))I + \sum_i \mathbb{P}_s(R_i^{-1}(\hat{y} - y_i)\hat{y}_i^\top) + \sum_i (\hat{y}_i)_\times^\top R_i^{-1}(\hat{y}_i)_\times, \end{aligned} \tag{4.46}$$

where the initial condition $K(0) = \operatorname{trace}(K_{X_0})I - K_{X_0}$ is given by evaluating (4.33) using the boundary condition (4.10) at time 0. Note that K_{X_0} is known from the cost (4.4).

The Riccati equation (4.46) recursively updates the gain K of the minimum-energy observer (4.32). Therefore, the two interconnected equations (4.32) and (4.46) form a filter that recursively updates the estimate $\hat{X}(t)$ of the system trajectory $X(t)$ using the measurements $u(t)$ and $\{y_i(t)\}$. In the rest of this thesis, this filter is referred to as the geometric approximate minimum-energy (GAME) filter.

The approximation is due to neglecting the third order derivatives of the value function (4.9). One could go on with similar calculations to to obtain differential equations of the higher order derivatives of the value function. Later on in the Special Cases, Chapter 6, derivatives up to the order eight of the value function are derived for the case of rotations in a plane $\mathrm{SO}(2) \equiv S^1$ where the Hessian and all higher order derivatives of the value function are scalars.

4.3 The GAME Filter

In summary, the geometric approximate minimum-energy (GAME) filter proposed in Section 4.2 is given by

$$\dot{\hat{X}}(t) = \hat{X}\left(u - K^{-1}\sum_i (R_i^{-1}(\hat{y}_i - y_i)) \times \hat{y}_i\right)_\times, \tag{4.47a}$$

$$\begin{aligned}\dot{K} = &-KQK + \mathbb{P}_s(K(2u - K^{-1}\sum_i (R_i^{-1}(\hat{y}_i - y_i)) \times \hat{y}_i)_\times) \\ &- \operatorname{trace}(\sum_i \mathbb{P}_s(R_i^{-1}(\hat{y} - y_i)\hat{y}_i^\top))I + \sum_i \mathbb{P}_s(R_i^{-1}(\hat{y} - y_i)\hat{y}_i^\top) + \sum_i (\hat{y}_i)_\times^\top R_i^{-1}(\hat{y}_i)_\times,\end{aligned} \tag{4.47b}$$

where $\hat{X}(0) = I$, $K(0) = \operatorname{trace}(K_{X_0})I - K_{X_0}$ and $\hat{y}_i = \hat{X}^\top \mathring{y}_i$. The signals u and $\{y_i\}$ are measured from the models (4.2) and (4.3).

The filter (4.47) consists of two interconnected parts. Equation (4.47a) evolves on $\mathrm{SO}(3)$ and consists of a copy of system (4.1) plus an innovation term. The innovation term is a weighted difference between the (past) estimated signal and the noisy measured signal. Note that $(R_i^{-1}(\hat{y}_i - y_i)) \times \hat{y}_i$ encodes the axis of rotation required to take $R_i^{-1}(\hat{y}_i - y_i)$ to be collinear to $\hat{y}_i$ in Riemannian normal coordinates. The weighting K^{-1} is a scaling or gain applied to this tangent direction in the $\mathbb{R}^3$ representation of $\mathfrak{so}(3)$. The (inverse) weighting matrix K, dynamically generated by the Riccati equation (4.47b), depends on the past estimates and the past measurements.

In order to improve the numerical robustness of the filter (4.47), a gain matrix $P := K^{-1}$ is defined and Equation (4.47) is rewritten using $\dot{K} = -P\dot{P}P$. This will improve the numerics of the filter by leaving out all the matrix inverse operations.

$$\dot{\hat{X}}(t) = \hat{X}\left(u - P\sum_i (R_i^{-1}(\hat{y}_i - y_i)) \times \hat{y}_i\right)_\times, \tag{4.48a}$$

$$\begin{aligned}\dot{P} = &Q + \mathbb{P}_s(P(2u - P\sum_i (R_i^{-1}(\hat{y}_i - y_i)) \times \hat{y}_i)_\times) + \\ &P\left(\operatorname{trace}(\sum_i \mathbb{P}_s(R_i^{-1}(\hat{y} - y_i)\hat{y}_i^\top))I - \sum_i \mathbb{P}_s(R_i^{-1}(\hat{y} - y_i)\hat{y}_i^\top) - \sum_i (\hat{y}_i)_\times^\top R_i^{-1}(\hat{y}_i)_\times\right)P,\end{aligned} \tag{4.48b}$$

where $\hat{X}(0) = I$ and $P(0) = (\operatorname{trace}(K_{X_0})I - K_{X_0})^{-1}$.

Consider the system (4.1), the measurements equations (4.2) and (4.3) and the cost (4.4). Given some measurements $\{y_i|_{[0,\,t]}\}$ and $u|_{[0,\,t]}$, assume that unique solutions $\hat{X}(t)$ and $K(t)$ to (4.48a) and (4.48b) exist on the interval $[0\ ,\ t]$.

Theorem 1. *Assume that $V(X,t)$ from* (4.9) *is twice differentiable and that the Hessian of $V(X,t)$ (see* (4.23)*) is invertible. Denote by K the inverse of the matrix representation of the Hessian (see* (4.24)*). Then $\hat{X}(t)$ given from* (4.48a) *is a minimum-energy (optimal) estimate.*

Proof. From our previous calculations in Section 4.2 it is evident that Equation (4.48a) is derived only using the optimality conditions (4.8) and (4.13). □

Remark 1. *The observer* (4.48a) *is a gradient-like observer [22]. The innovation term in this equation is a gradient of the cost function* $f(\hat{X}, \{y_i\}) = \frac{1}{2}\sum_i \text{trace}(\hat{y}_i - y_i)R_i^{-1}(\hat{y}_i - y_i)^\top$ *with respect to* $\hat{X}$ *and the right invariant metric given by* $\langle \hat{X}A, \hat{X}B\rangle := \text{trace}[ASB^\top]$ *for all* $A, B \in \mathfrak{so}(3)$ *and* $X \in \text{SO}(3)$*, where* $S = \frac{1}{2}\text{trace}(P^{-1})I - P^{-1}$ *is a positive definite matrix given in terms of* P *in* (4.48b)*.*

Although (4.48a) yields the exact form of a minimum-energy observer (4.48a), one would need to obtain the true Hessian to be able to compute this minimum-energy filter. The next proposition states that K in Equation (4.48b) is an approximation to the dynamics of the (inverse) true Hessian operator.

Proposition 1. *Assuming that* $V(X,t)$ *is three times differentiable and that* $\text{Hess}_1 V(X,t)$ *is invertible,* $\dot{P}$ *in* (4.47b) *approximates the derivative of the inverse true Hessian of* $V(X,t)$ *to the order* $O(\nabla_1^3 V(X,t))$*.*

Proof. In Section 4.2, deriving Equation (4.48b) was derived by using the optimal equation (4.48a), the final value condition (4.13) and by neglecting the third order derivatives of the value function. Hence, the dynamics of the Hessian operator was approximated up to the second order derivative of the value function. . □

A similar approach to that proposed in Section 4.2 could be used to derive a higher order filter by differentiating the third order derivative terms of the value function. However, such a derivation would require tensor algebra. Note that due to the natural convexity of the value function at a minimum the odd derivatives of the value function are unlikely to contain much information and to obtain any significant improvement in the filter performance by including addition derivative approximations one would need to go to the fourth order term. Chapter 6 contains higher order derivatives of the value function for the case of rotations in a plane $\text{SO}(2) \equiv S^1$ where the Hessian and all higher order derivatives of the value function are scalars.

Chapter 5

Least Squares Analysis of the GAME Filter

This chapter contains a least squares analysis of the geometric approximate minimum-energy (GAME) filter proposed in Chapter 4. A mathematical expression of an upper bound on the (optimality) distance between the solution of the GAME filter and a minimum-energy solution is provided, although a minimum-energy filter is not expressed explicitly. This distance is quantifiable in simulations and is shown to be small in all the experiments considered, hence indicating that the GAME filter asymptotically acts like a minimum-energy filter. The term 'near-optimal' is sometimes used for filters with such performance characteristics [29, 42].

The remainder of the chapter is organized as follows. Section 5.1 includes a review of the equations of the attitude kinematics, measurements, the cost functional and the GAME filter proposed in Chapter 4. A least squares analysis of the GAME filter is provided in Section 5.2. In particular a detailed derivation of an upper bound (Gap) on the optimality performance of the GAME filter is provided. Section 5.3 contains an assumption on the positivity of the 'Gap' that leads to the main theorem of this chapter and some remarks on the results of this chapter. Finally, Section 5.4 provides a simulation study that further justifies the assumption made and the results.

5.1 A Review of the GAME Filter

Recall the attitude kinematics and measurements considered in Chapter 4

$$\boxed{\begin{cases} \dot{X}(t) &= X(t)\Omega_{\times}(t),\ X(0) = X_0, \\ u(t) &= \Omega(t) + Bv(t), \\ y_i(t) &= X(t)^{\top}\mathring{y}_i + D_i w_i(t),\ i = 1, \cdots, n\ , \end{cases}} \tag{5.1}$$

where X is a rotation matrix representing the attitude and Ω represents the angular velocity. The signals u and v denote the body-fixed frame measured angular velocity input and the input measurement error, respectively. The vectors $\mathring{y}_i$ are known reference vectors with y_i as their measurements and w_i as the measurement errors. The matrices B and D are known coefficients for the measurement errors with their

associated metrics $Q \coloneqq BB^\top$ and $R_i \coloneqq D_i D_i^\top$.

The cost functional considered in Chapter 4 was

$$\boxed{\begin{aligned} J_t(t; X_0, v|_{[0,\,t]}, \{w_i|_{[0,\,t]}\}) = \frac{1}{2}\int_0^t \left(v^\top v + \sum_i w_i^\top w_i \right) d\tau \\ + \frac{1}{2}\operatorname{trace}\left[(I - X_0) K_0^{-1} (I - X_0)^\top \right], \end{aligned}} \tag{5.2}$$

in which $K_0 \in \mathbb{R}^{3\times 3}$ is positive definite.

Recall the GAME filter given in Chapter 4

Attitude Observer	$\dot{\hat{X}} = \hat{X}(u - Pl)_\times, \quad \hat{X}(0) = I$ $l = 2\operatorname{vex}(\sum_i \mathbb{P}_a(\hat{y}_i(\hat{y}_i - y_i)^\top R_i^{-1}),\ \hat{y} \coloneqq \hat{X}^\top \mathring{y}$
Riccati Equation	$\dot{P} = Q + \mathbb{P}_s(P(2u - Pl)_\times) - PSP + PAP,\ P(0) = (\operatorname{trace}(K_0^{-1})I - K_0^{-1})^{-1},$ $S \coloneqq \sum_i (\hat{y}_i)_\times^\top R_i^{-1} (\hat{y}_i)_\times,$ $A \coloneqq \operatorname{trace}(C)I - C,\ C \coloneqq \sum_i \mathbb{P}_s(R_i^{-1}(\hat{y} - y_i)\hat{y}_i^\top).$

Table 5.1: GAME Filter

5.2 Optimality Gap of the GAME Filter

This section contains three lemmas that lead to the main result of this chapter (Theorem 2). Lemma 2 introduces the optimality distance $W(t)$ and contains the detailed derivation of $W(t)$. The positivity of $W(t)$ is considered in Lemma 3 and Assumption 1.

Before deriving the optimality Gap (distance) $W(t)$, let us introduce some auxiliary variables. Denote $K \coloneqq P^{-1}$. The time derivative of K is given by

$$\dot{K} = -KQK + \mathbb{P}_s(K(2u - Pl)_\times) + S - A, \tag{5.3}$$

where the initial condition $K(0) = \operatorname{trace}(K_0^{-1})I - K_0^{-1}$ and the variables l, S and A are given from Table 5.1. This easily follows from $\dot{K} = P^{-1}\dot{P}P^{-1}$. The following lemma is used later to rewrite the cost (5.2).

Lemma 1. *Denote* $G \coloneqq \frac{1}{2}\operatorname{trace}(K)I - K$*, then the following identities hold.*

$$\begin{aligned}
&\operatorname{trace}(G) = \frac{1}{2}\operatorname{trace}(K),\\
&K = \operatorname{trace}(G)I - G,\\
&\dot{G} = -\frac{1}{2}\operatorname{trace}(KQK)I + KQK + \mathbb{P}_s(G(2u - Pl)_\times) + \frac{1}{2}\operatorname{trace}(S)I - S - C.
\end{aligned} \tag{5.4}$$

Proof. Using the definition of G and using Table 5.1 the proof follows. □

The following lemma shows that the cost J_t (5.2) satisfies an equation that is comprised of a term depending on the difference between the current-time value of the state $X(t)$ and its estimated value $\hat{X}(t)$, as well as on an integral term which is an 'unavoidable optimal cost' and a remaining term $W(t)$ that is called the 'gap' of the GAME filter. This separation will help to show, later in Section 5.3, that an upper bound for the cost associated to the GAME filter is greater than an 'unavoidable optimal cost' by the value of $W(t)$, thus providing a bound on the GAME filter's distance to optimality.

Lemma 2. *The cost* (5.2) *satisfies the equation*

$$\begin{aligned}
J_t = {}& \frac{1}{2}\operatorname{trace}\left[(X(t) - \hat{X}(t))G(t)(X(t) - \hat{X}(t))^\top\right]\\
&- \frac{1}{2}\int_0^t \sum_i \left(\|v - 2B^\top \operatorname{vex}\mathbb{P}_a(\hat{X}^\top X G)\|^2 + \sum_i \|y_i - \hat{y}_i\|^2_{R_i^{-1}}\right) d\tau - W(t),
\end{aligned} \tag{5.5}$$

where,

$$\begin{aligned}
W(t) \coloneqq \int_0^t \sum_i \Bigg(&-2\|B^\top \operatorname{vex}\mathbb{P}_a(EG)\|^2 + \frac{1}{2}\|(\hat{X} - X)^\top \mathring{y}_i\|^2_{R_i^{-1}}\\
&+ \operatorname{trace}\left[(I - \mathbb{P}_s(E))\left(\frac{1}{2}\operatorname{trace}(KQK)I - KQK + \frac{1}{2}\operatorname{trace}(S)I - S\right)\right]\Bigg) d\tau,
\end{aligned} \tag{5.6}$$

and the term S is given in Table 5.1.

Proof. Consider the function

$$\mathcal{L} = \frac{1}{2}\operatorname{trace}\left[(X - \hat{X})G(X - \hat{X})^\top\right] = \operatorname{trace}\left[(I - \hat{X}^\top X)G\right]. \tag{5.7}$$

The time derivative of Equation (5.7) is given by

$$\dot{\mathcal{L}} = \operatorname{trace}\left[-(\dot{\hat{X}}^\top X)G - (\hat{X}^\top \dot{X})G + (I - \hat{X}^\top X)\dot{G}\right]. \tag{5.8}$$

Substituting from Equations (5.1) and (**??**) yields

$$\dot{\mathcal{L}} = \operatorname{trace}\left[-(u - Pl)_\times^\top \hat{X}^\top X G - \hat{X}^\top X(u - Bv)_\times G + (I - \hat{X}^\top X)\dot{G}\right]. \tag{5.9}$$

Denote the estimation error $\hat{X}^\top X$ by

$$E \coloneqq \hat{X}^\top X, \tag{5.10}$$

and recall the following identities. For all $A, F \in \mathbb{R}^{3\times 3}$

$$\begin{aligned} \operatorname{trace}(\mathbb{P}_a(A)F) &= \operatorname{trace}(\mathbb{P}_a(A)\mathbb{P}_a(F)) = \operatorname{trace}(A\mathbb{P}_a(F)), \\ \operatorname{trace}(\mathbb{P}_s(A)F) &= \operatorname{trace}(\mathbb{P}_s(A)\mathbb{P}_s(F)) = \operatorname{trace}(A\mathbb{P}_s(F)). \end{aligned} \tag{5.11}$$

These identities follow from the fact that a trace of a product between a skew-symmetric matrix and a symmetric matrix is zero. Using these identities and grouping the terms with u in Equation (5.9) yield

$$\begin{aligned} \dot{\mathcal{L}} = \operatorname{trace}\big[&-2\mathbb{P}_s(u_\times G)\mathbb{P}_s(E) - \mathbb{P}_a(E)\mathbb{P}_a(G(Pl)_\times) - \mathbb{P}_s(E)\mathbb{P}_s(G(Pl)_\times) \\ &+(Bv)_\times^\top \mathbb{P}_a(EG) + (I - \mathbb{P}_s(E))\dot{G}\Big]. \end{aligned} \tag{5.12}$$

Next rewrite the term with v in a vector form and add and subtract square terms in order to complete a square norm of v.

$$\begin{aligned} \dot{\mathcal{L}} = &+2v^\top B^\top \operatorname{vex}\mathbb{P}_a(EG) \pm \frac{1}{2}v^\top v \pm 2\operatorname{vex}\mathbb{P}_a^\top(EG)BB^\top \operatorname{vex}\mathbb{P}_a(EG) + \\ &\operatorname{trace}\big[-2\mathbb{P}_s(u_\times G)\mathbb{P}_s(E) - \mathbb{P}_a(E)\mathbb{P}_a(G(Pl)_\times) - \mathbb{P}_s(E)\mathbb{P}_s(G(Pl)_\times) + (I - \mathbb{P}_s(E))\dot{G}\big]. \end{aligned} \tag{5.13}$$

Completing the square yields

$$\begin{aligned} \dot{\mathcal{L}} = &-\frac{1}{2}\|v - 2B^\top \operatorname{vex}\mathbb{P}_a(EG)\|^2 + \frac{1}{2}\|v\|^2 + 2\|B^\top \operatorname{vex}\mathbb{P}_a(EG)\|^2 + \\ &\operatorname{trace}\big[-2\mathbb{P}_s(u_\times G)\mathbb{P}_s(E) - \mathbb{P}_a(E)\mathbb{P}_a(G(Pl)_\times) - \mathbb{P}_s(E)\mathbb{P}_s(G(Pl)_\times) + (I - \mathbb{P}_s(E))\dot{G}\big]. \end{aligned} \tag{5.14}$$

Replace $\dot{G}$ from (1).

$$\begin{aligned} \dot{\mathcal{L}} = &-\frac{1}{2}\|v - 2B^\top \operatorname{vex}\mathbb{P}_a(EG)\|^2 + \frac{1}{2}\|v\|^2 + 2\|B^\top \operatorname{vex}\mathbb{P}_a(EG)\|^2 + \\ &\operatorname{trace}\Big[-2\mathbb{P}_s(u_\times G)\mathbb{P}_s(E) - \mathbb{P}_a(E)\mathbb{P}_a(G(Pl)_\times) - \mathbb{P}_s(E)\mathbb{P}_s(G(Pl)_\times) + \\ &(I - \mathbb{P}_s(E))(-\frac{1}{2}\operatorname{trace}(KQK)I + KQK + \mathbb{P}_s(G(2u - Pl)_\times) + \frac{1}{2}\operatorname{trace}(S)I - S - C)\Big]. \end{aligned} \tag{5.15}$$

Note that the first two terms in the trace part of the previous equation cancel the third term that replaced $\dot{G}$ multiplied by $\mathbb{P}_s(E)$. The third term that replaced $\dot{G}$ multiplied by I yields zero under the trace operator. This is due the fact that for all F symmetric

and Γ skew-symmetric it holds that

$$\operatorname{trace}[\mathbb{P}_s(F\Gamma)] = \frac{1}{2}\operatorname{trace}[F\Gamma + \Gamma^\top F^\top] = \frac{1}{2}\operatorname{trace}[F\Gamma - \Gamma F] = 0. \tag{5.16}$$

Hence Equation (5.15) yields

$$\dot{\mathcal{L}} = -\frac{1}{2}\|v - 2B^\top \operatorname{vex}\mathbb{P}_a(EG)\|^2 + \frac{1}{2}\|v\|^2 + 2\|B^\top \operatorname{vex}\mathbb{P}_a(EG)\|^2 + \operatorname{trace}\Big[-$$
$$\mathbb{P}_s(E)\mathbb{P}_s(G(Pl)_\times) + (I - \mathbb{P}_s(E))(-\frac{1}{2}\operatorname{trace}(KQK)I + KQK + \frac{1}{2}\operatorname{trace}(S)I - S - C)\Big]. \tag{5.17}$$

Recall the following identity. For all $\gamma \in \mathbb{R}^3$ and all symmetric $F \in \mathbb{R}^{3\times 3}$

$$\mathbb{P}_a(F\gamma_\times) = \frac{1}{2}((\operatorname{trace}(F)I - F)\gamma)_\times. \tag{5.18}$$

Using this identity for the first term in the trace part of Equation (5.17) and recalling from (5.4) that $P^{-1} = K = \operatorname{trace}(G)I - G$ yield

$$\mathbb{P}_a(G(Pl)_\times) = \frac{1}{2}((\operatorname{trace}(G)I - G)Pl)_\times = \frac{1}{2}l_\times, \tag{5.19}$$

that from (**??**) is equal to

$$\mathbb{P}_a(G(Pl)_\times) = \sum_i \mathbb{P}_a(\hat{y}_i(\hat{y}_i - y_i)^\top R_i^{-1}) = -\sum_i \mathbb{P}_a(R_i^{-1}(\hat{y}_i - y_i)\hat{y}_i^\top). \tag{5.20}$$

Replace this identity and also the equivalence of C from Table 5.1 into Equation (5.17). Rearranging the order of these terms yields

$$\dot{\mathcal{L}} = -\frac{1}{2}\|v - 2B^\top \operatorname{vex}\mathbb{P}_a(EG)\|^2 + 2\|B^\top \operatorname{vex}\mathbb{P}_a(EG)\|^2 + \frac{1}{2}\|v\|^2$$
$$+ \operatorname{trace}\Bigg[\mathbb{P}_a(E)\sum_i \mathbb{P}_a(R_i^{-1}(\hat{y}_i - y_i)\hat{y}_i^\top) + \mathbb{P}_s(E)\sum_i \mathbb{P}_s(R_i^{-1}(\hat{y}_i - y_i)\hat{y}_i^\top) -$$
$$\sum_i \mathbb{P}_s(R_i^{-1}(\hat{y}_i - y_i)\hat{y}_i^\top) + (I - \mathbb{P}_s(E))(-\frac{1}{2}\operatorname{trace}(KQK)I + KQK + \frac{1}{2}\operatorname{trace}(S)I - S)\Bigg]. \tag{5.21}$$

Note that the third term in the trace is equal to $-\sum_i R_i^{-1}(\hat{y}_i - y_i)\hat{y}_i^\top$ as the symmetric projection is redundant under the trace operator. Recalling the definitions $E = \hat{X}^\top X$

and $\hat{y}_i = \hat{X}^\top \mathring{y}$, the first two terms of the trace can be rewritten in the following form.

$$\begin{aligned}
&\text{trace}[\mathbb{P}_a(E)\sum_i \mathbb{P}_a(R_i^{-1}(\hat{y}_i - y_i)\hat{y}_i^\top) + \mathbb{P}_s(E)\sum_i \mathbb{P}_s(R_i^{-1}(\hat{y}_i - y_i)\hat{y}_i^\top)] = \\
&\text{trace}[E\sum_i R_i^{-1}(\hat{y}_i - y_i)\hat{y}_i^\top] = \text{trace}[\hat{X}^\top X\sum_i R_i^{-1}(\hat{y}_i - y_i)\mathring{y}_i^\top \hat{X}] = \\
&\text{trace}[\sum_i R_i^{-1}(\hat{y}_i - y_i)\mathring{y}_i^\top X].
\end{aligned} \tag{5.22}$$

This expression substituted into (5.21) is grouped with the third term in the trace and the result is written in a vector inner product form. Also adding and subtracting the square norm of w_i yield

$$\begin{aligned}
\dot{\mathcal{L}} = &\frac{1}{2}\|v\|^2 - \frac{1}{2}\|v - 2B^\top \operatorname{vex}\mathbb{P}_a(EG)\|^2 + 2\|B^\top \operatorname{vex}\mathbb{P}_a(EG)\|^2 \\
&+ \sum_i \left(\pm\frac{1}{2}\|w_i\|^2 - (\hat{y}_i - X^\top \mathring{y}_i)^\top R_i^{-1}(\hat{y}_i - y_i)\right) \\
&+ \text{trace}\left[(I - \mathbb{P}_s(E))(-\frac{1}{2}\text{trace}(KQK)I + KQK + \frac{1}{2}\text{trace}(S)I - S)\right].
\end{aligned} \tag{5.23}$$

Rewrite this equation using the definitions $y = X^\top \mathring{y} + D_i w_i$ and $R_i = D_i D_i^\top$ to

$$\begin{aligned}
\dot{\mathcal{L}} = &\frac{1}{2}\|v\|^2 - \frac{1}{2}\|v - 2B^\top \operatorname{vex}\mathbb{P}_a(EG)\|^2 + 2\|B^\top \operatorname{vex}\mathbb{P}_a(EG)\|^2 + \frac{1}{2}\sum_i \|w_i\|^2 \\
&- \sum_i \left(\frac{1}{2}\|w_i\|^2 + (\hat{y}_i - X^\top \mathring{y}_i)^\top R_i^{-1}(\hat{y}_i - X^\top \mathring{y}_i) - (\hat{y}_i - X^\top \mathring{y}_i)^\top D_i^{-\top} w_i\right) \\
&+ \text{trace}\left[(I - \mathbb{P}_s(E))(-\frac{1}{2}\text{trace}(KQK)I + KQK + \frac{1}{2}\text{trace}(S)I - S)\right].
\end{aligned} \tag{5.24}$$

Completing the square in the second line of the previous equation yields

$$\begin{aligned}
\dot{\mathcal{L}} = &\frac{1}{2}\|v\|^2 - \frac{1}{2}\|v - 2B^\top \operatorname{vex}\mathbb{P}_a(EG)\|^2 + 2\|B^\top \operatorname{vex}\mathbb{P}_a(EG)\|^2 + \frac{1}{2}\sum_i \|w_i\|^2 \\
&- \frac{1}{2}\sum_i \left((y_i - \hat{y}_i)^\top R_i^{-1}(y_i - \hat{y}_i) + (\hat{y}_i - X^\top \mathring{y}_i)^\top R_i^{-1}(\hat{y}_i - X^\top \mathring{y}_i)\right) \\
&+ \text{trace}\left[(I - \mathbb{P}_s(E))(-\frac{1}{2}\text{trace}(KQK)I + KQK + \frac{1}{2}\text{trace}(S)I - S)\right].
\end{aligned} \tag{5.25}$$

Integrating $\dot{\mathcal{L}}$ to obtain $\mathcal{L}(t) - \mathcal{L}(0) = \int_0^t \dot{\mathcal{L}} d\tau$, and replacing $\hat{X}(0) = I$ results in

$$\begin{aligned}\frac{1}{2}\operatorname{trace}\left[(X(t)-\hat{X}(t))G(t)(X(t)-\hat{X}(t))^\top\right] &= \frac{1}{2}\operatorname{trace}\left[(X(0)-I)G(0)(X(0)-I)^\top\right] + \\ \int_0^t \Bigg(&\frac{1}{2}\|v\|^2 + \frac{1}{2}\sum_i \|w_i\|^2 - \frac{1}{2}\|v - 2B^\top \operatorname{vex}\mathbb{P}_a(EG)\|^2 + \\ &2\|B^\top \operatorname{vex}\mathbb{P}_a(EG)\|^2 - \frac{1}{2}\sum_i \left(\|y_i - \hat{y}_i\|^2_{R_i^{-1}} + \|\hat{y}_i - X^\top \mathring{y}_i\|^2_{R_i^{-1}}\right) + \\ &\operatorname{trace}\left[(I - \mathbb{P}_s(E))(-\frac{1}{2}\operatorname{trace}(KQK)I + KQK + \frac{1}{2}\operatorname{trace}(S)I - S)\right]\Bigg) d\tau.\end{aligned} \tag{5.26}$$

By definition and from Lemma 1, $G(0) = K_0^{-1}$ and hence the first three terms on the right hand side of the previous equation form the cost J_t (5.2). Therefore,

$$\begin{aligned}J_t = &\frac{1}{2}\operatorname{trace}\left[(X(t)-\hat{X}(t))G(t)(X(t)-\hat{X}(t))^\top\right] \\ &- \frac{1}{2}\int_0^t \sum_i \left(\|v - 2B^\top \operatorname{vex}\mathbb{P}_a(EG)\|^2 + \sum_i \|y_i - \hat{y}_i\|^2_{R_i^{-1}}\right) d\tau - W(t),\end{aligned} \tag{5.27}$$

where J_t is the cost (5.2) and

$$\begin{aligned}W(t) = \int_0^t \sum_i \Bigg(&-2\|B^\top \operatorname{vex}\mathbb{P}_a(EG)\|^2 + \frac{1}{2}\|(\hat{X}-X)^\top \mathring{y}_i\|^2_{R_i^{-1}} \\ &+ \operatorname{trace}\left[(I - \mathbb{P}_s(E))\left(\frac{1}{2}\operatorname{trace}(KQK)I - KQK + \frac{1}{2}\operatorname{trace}(S)I - S\right)\right]\Bigg) d\tau.\end{aligned} \tag{5.28}$$

This completes the proof. □

5.3 Near-Optimality of the GAME Filter

In Section 5.2 it was shown that the cost (5.2) satisfies an equation that involves an 'unavoidable optimal cost' and a 'gap' $W(t)$. One needs to prove that $W(t)$ is positive to be able to show that it acts as an upper bound (Gap) for the optimality performance of the GAME filter. The following lemma indicates that in fact, apart from an obvious negative squared norm in $W(t)$ (5.6), every other term in the mathematical expression for $W(t)$ has a positive value.

Lemma 3. *The trace part of the mathematical expression for $W(t)$ is nonnegative for all t.*

Proof. Note that $E = \hat{X}^\top X$ is a rotation matrix. The eigenvalues of a rotation matrix occur in one of the forms

- Three eigenvalues equal to 1 (the rotation E equals the identity matrix I in this case).
- One eigenvalue equals to 1 and the other two are -1 (rotation by 180 degrees).
- One eigenvalue equals to 1 but the rest are complex conjugates of the form $\cos(\theta) \pm i \sin(\theta)$ (rotation through an angle of θ).

Therefore, it is straightforward to see that the symmetric projection $\mathbb{P}_s(E)$ yields real eigenvalues less than or equal to 1. Thus the matrix $I - \mathbb{P}_s(E)$ has eigenvalues all nonnegative and hence is a positive semidefinite matrix.

Note that if $\text{trace}(A) \geq 0$ then the operator $\frac{1}{2}(A)I - A$ yields a positive semidefinite matrix. This can be shown by noting that $A \leq \frac{1}{3}\text{trace}(A)I$. Therefore the operator $\frac{1}{2}(A)I - A$ is greater than or equal to $\frac{1}{6}\text{trace}(A)I$ and hence is positive semidefinite.

Observe that $\text{trace}(KQK)$ also yields a nonnegative value. This is due to the fact that the matrix K is symmetric and the matrix $Q = BB^\top$ is positive definite and hence the term $\text{trace}(KQK)$ can be rewritten as a squared matrix norm.

$$\text{trace}(KQK) = \text{trace}[(B^\top K)^\top (B^\top K)] = \|B^\top K\|^2 \geq 0. \tag{5.29}$$

Therefore, according to what was shown in the previous paragraph, $\frac{1}{2}\text{trace}(KQK)I - KQK$ is positive semidefinite.

Similarly the term $\text{trace}(S) = \text{trace}(\sum_i (\hat{y}_i)_\times^\top R_i^{-1} (\hat{y}_i)_\times)$ is positive. This can be shown by recalling that $R_i = D_i D_i^\top$ is positive definite, $\hat{y}_i$ is a unit vector and hence

$$\text{trace}(\sum_i (\hat{y}_i)_\times^\top R_i^{-1} (\hat{y}_i)_\times) = \sum_i \|D_i (\hat{y}_i)_\times\|^2 \geq 0. \tag{5.30}$$

Hence similar to our previous argument the term $\text{trace}(S)I - S$ is positive semidefinite.

In summary, the two terms $I - \mathbb{P}_s(E)$ and $\frac{1}{2}\text{trace}(KQK)I - KQK + \frac{1}{2}\text{trace}(S)I - S$ are positive semidefinite and the proof is complete by recalling that a trace of a product between two positive semidefinite matrices is nonnegative. □

Up to here, the positivity of the trace part of the gap $W(t)$ was proven via Lemma 3. However, a proof of positivity of the overall gap $W(t)$ is not straightforward due to a negative squared norm that also exists in the expression for $W(t)$. Nevertheless, our intuition, which is the subject of the following assumption, is that the negative term in $W(t)$ will be dominated by the nonnegative terms and overall the gap $W(t)$ will be positive for all t. This intuition comes from the fact that the term $-2\|B^\top \text{vex}\,\mathbb{P}_a(EG)\|^2$ is second-order in the estimation error E and gets dominated by the other nonnegative terms if the estimation error is small enough. Note that the trace part of the mathematical expression for $W(t)$ has a component that is linear in E. Therefore, $W(t)$ stays positive if initially the filter is tuned in a way that the gap $W(t)$ is positive until the estimation error $E(t)$ converges to a small enough value.

Also note that if initially $W(t)$ is positive it is likely to stay positive since $W(t)$ is an accumulative integral term.

Assumption 1. *Assume that the gap $W(t)$ is positive for all t.*

A proof for Assumption 1 would require a result on filter error convergence, however, the proposition that $W(t)$ stays positive in all the situations is tested in the Monte-Carlo experiments Section 5.4.

Theorem 2. *Consider the system* (5.1) *and the cost* (5.2). *Given some measurements $\{y_i|_{[0,\,t]}\}$ and their associated inputs $u|_{[0,\,t]}$, assume that unique solutions $\hat{X}$ and $P(t)$ to 5.1 exist on $[0, t]$. Assuming further that Assumption 1 holds then the filter 5.1 yields a near-optimal estimate $\hat{X}(t)$ of the state $X(t)$ in the sense that for each time t there exists a hypothesized trajectory X_{ht} with the final value $X_{ht}(t) = \hat{X}(t)$ and $J_t \leq J_t^* + W(t)$, where J_t is the functional cost for X_{ht}, J_t^* denotes the minimum-energy value for the cost* (5.2) *and $W(t)$ is a bound on the optimality distance between the two trajectories X_{ht} and X_t^*, the latter denoting a minimum-energy trajectory corresponding to J_t^*.*

Proof. Lemma 2 states that

$$\begin{aligned}\frac{1}{2}\operatorname{trace}\left[(X(t)-\hat{X}(t))G(t)(X(t)-\hat{X}(t))^\top\right] &= J_t \\ -\frac{1}{2}\int_0^t \sum_i \left(\|v-2B^\top \operatorname{vex}\mathbb{P}_a(EG)\|^2 + \sum_i \|y_i-\hat{y}_i\|^2_{R_i^{-1}}\right) d\tau - W(t),\end{aligned} \tag{5.31}$$

Thus, the cost function J_t fulfils the inequality

$$J_t \geq \frac{1}{2}\int_0^t \sum_i \|y_i-\hat{y}_i\|^2_{R_i^{-1}} d\tau. \tag{5.32}$$

The right hand side of Equation (5.32) is independent of any specific choice of the unknown arguments of the cost (5.2), X_0, $v|_{[0,\,t]}$ and $\{w_i|_{[0,\,t]}\}$, and depends only on the measured data $\{y_i|_{[0,\,t]}\}$ and the filter estimates. Thus, the right hand side of Equation (5.32) is also a lower bound for the minimum J_t^* of the cost (5.2), i.e.

$$J_t^* \geq \frac{1}{2}\int_0^t \sum_i \|y_i-\hat{y}_i\|^2_{R_i^{-1}} d\tau. \tag{5.33}$$

Consider a hypothesis $X_{ht} : [0,\ t] \longrightarrow \mathrm{SO}(3)$ for the true trajectory of the system generated by

$$\dot{X}_{ht} = X_{ht}(u - 2Q\operatorname{vex}\mathbb{P}_a(\hat{X}^\top X_{ht} G))_\times, \tag{5.34}$$

with fixed *final* condition $X_{ht}(t) := \hat{X}(t)$ where $\hat{X}$ and G are solutions of the proposed filter 5.1 through (5.4). It is straightforward to show (by integrating in reverse time) that (5.34) has a unique initial state $X_{ht}(0)$ that produces the final condition $X_{ht}(t) =$

$\hat{X}(t)$. Define the signals $(w_i)_{ht} : [0,\ t] \longrightarrow \mathbb{R}^3$ by

$$(w_i)_{ht} := D_i^{-1}(y_i - \hat{y}_i), \tag{5.35}$$

and the signal $v_{ht} : [0,\ t] \longrightarrow \mathbb{R}^3$ by

$$v_{ht} := 2B^\top \operatorname{vex} \mathbb{P}_a(\hat{X}^\top X G) \tag{5.36}$$

Equations (5.34) and (5.35) show that $X_{ht}(0)$, $v_{ht}|_{[0,\ t]}$ and $\{(w_i)_{ht}|_{[0,\ t]}\}$ together with $u|_{[0,\ t]}$ and $\{y_i\}|_{[0,\ t]}$ satisfy the system equations (5.1).

Recalling Lemma 2 the functional cost J_t of X_{ht} is

$$J_t = \frac{1}{2}\int_0^t \sum_i \|y_i - \hat{y}_i\|^2_{R_i^{-1}} d\tau + W(t) \leq J_t^* + W(t). \tag{5.37}$$

This completes the proof. □

A key contribution of Theorem 2 lies in providing a bound $W(t)$ given by (5.6) for evaluating the performance of the filter. This bound is numerically quantifiable and is decreasing with the tracking error $\hat{X}^\top X$. Thus, once the initial transient of the filter is complete, and for moderate modeling error, it is to be expected that the filter will perform qualitatively as well as an optimal filter. This is further investigated in the following simulations.

5.4 Simulations

The following three cases are simulated with Monte-Carlo experiments with 100 repeats in each case. In all the cases, the GAME filter 5.1 is simulated using the identity matrix as both the initial rotation estimate and the initial gain. A sinusoidal input $\Omega = [0.2\sin(\frac{\pi}{3}t)\ \ -\cos(\frac{\pi}{3}t)\ \ 2\cos(\frac{\pi}{3}t)]$ drives the true trajectory X. We further assume that two orthogonal unit reference vectors are available.

Case 1

This case is a simulation setup with relatively low levels of initialization and measurement errors. The input measurement error v is a Gaussian zero mean random process with a unit standard deviation. The coefficient matrix B is chosen so that the signal Bv has a standard deviation of 3 degrees per 'second'. The system is initialized with a rotation of 47 degrees. We also consider Gaussian zero mean measurement noise signals w_i with unit standard deviations. The coefficient matrices D_i are chosen so that the signals $D_i w_i$ have standard deviations of 9 degrees. Although the filter does not have access to the noise signals v and w_i, it has access to the matrices $Q = BB^\top$ and $R_i = D_i D_i^\top$.

Case 2

This case is a simulation setup with relatively high levels of initialization and measurement errors. The coefficient matrix B is chosen so that the signal Bv has a standard deviation of 60 degrees per 'second'. The system is initialized with a rotation of

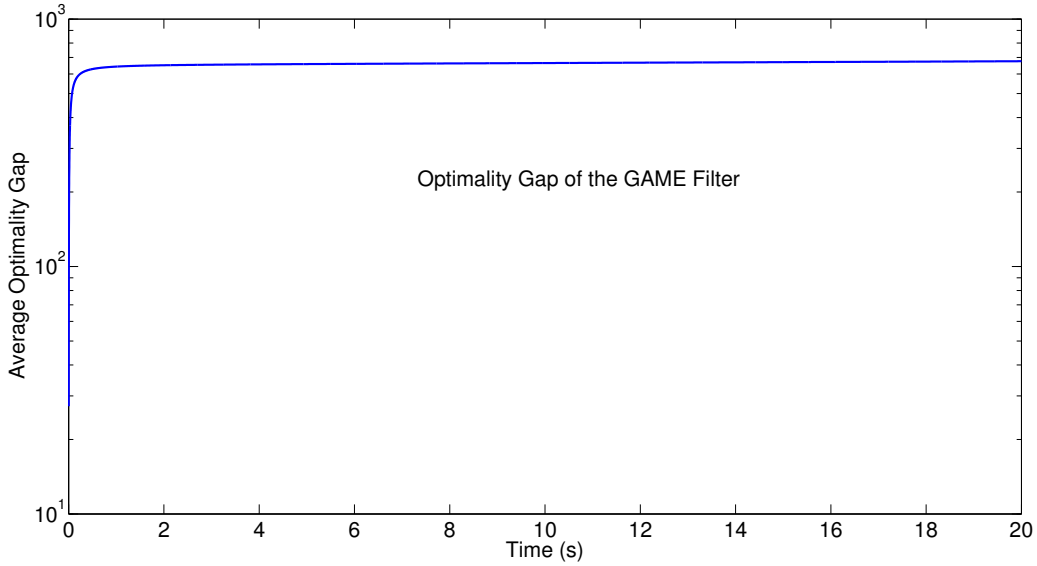

Figure 5.1: Case 1: The average of the bound on the optimality performance of the GAME filter ($W(t)$) over 100 repeats plotted against time.

120 degrees. Gaussian zero mean measurement noise signals w_i with unit standard deviations are considered for which the coefficient matrices D_i are chosen so that the signals $D_i w_i$ have standard deviations of 90 degrees. Figure 5.1 is the plot of $W(t)$ for the Case 1 experiment. As can be seen the average of $W(t)$ stays positive throughout the 100 experiments. Note that after a short transient period the average value of $W(t)$ reaches a plateau that indicates that once the Game filter converges it acts like a minimum-energy filter apart from the initially accumulated optimality error bound. This is more clear in Figure 5.2 where the average of the integrant of $W(t)$ throughout the 100 experiments is plotted against time. As can be seen in Figure 5.2 after a short transient period the average of the integrant of $W(t)$ converges to a very small value. This further supports the near-optimality claim of the proposed filter. Also note that the average of the integrant part of $W(t)$ is positive at all times which further supports Assumption 1. These conclusions are also valid for Figures 5.3 and 5.4. Note the larger errors considered in Case 2 have even increased the positivity margin of $W(t)$ that indicates that Assumption 1 is also valid for a large initial estimation error and a long convergence period. Note that in Figure 5.3, the average of the optimality gap $W(t)$ takes longer to converge than the time taken in Figure 5.1. This was expected due to the large errors considered in Case 2.

Figures 5.3 and 5.4 show that also in the higher noise Case 2 the optimality gap $W(t)$ stays positive. The only difference is that for this case the transient period is longer. However the integrant of the optimality cost will converge to a small value close to what was seen for Case 1.

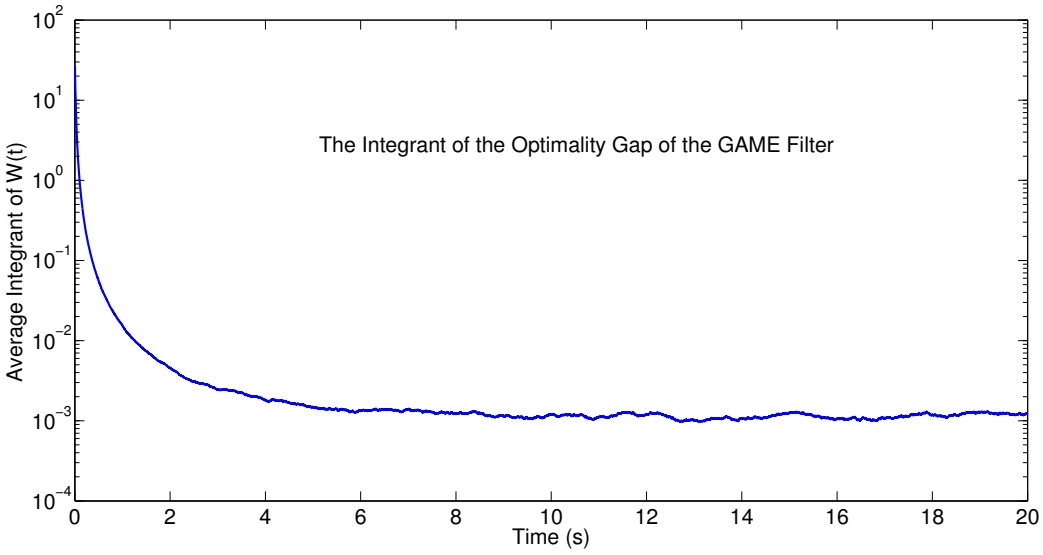

Figure 5.2: Case 1: The average of the integrant of $W(t)$ over 100 repeats plotted against time.

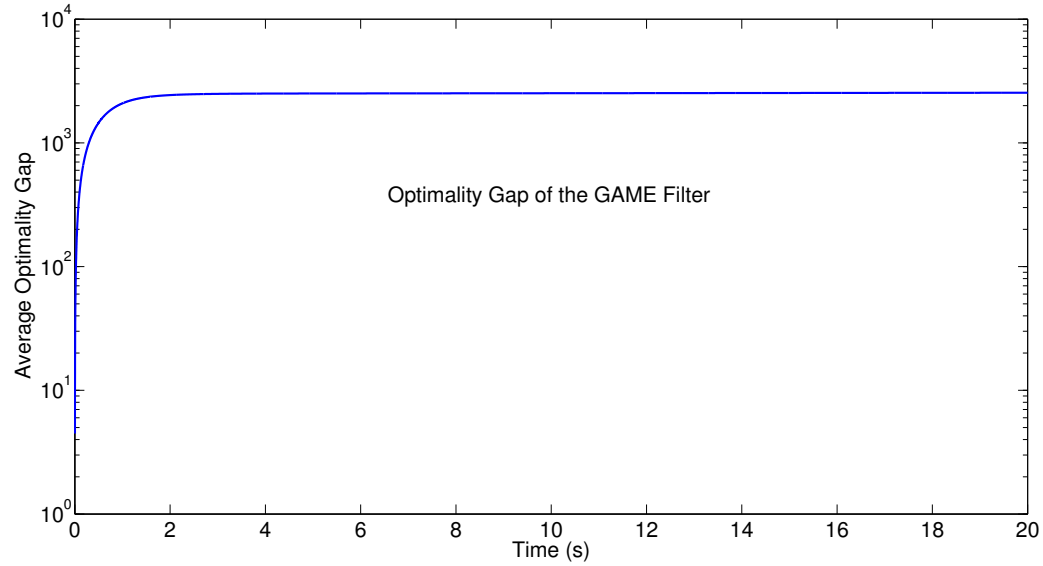

Figure 5.3: Case 2: The average of the bound on the optimality performance of the GAME filter ($W(t)$) over 100 repeats plotted against time.

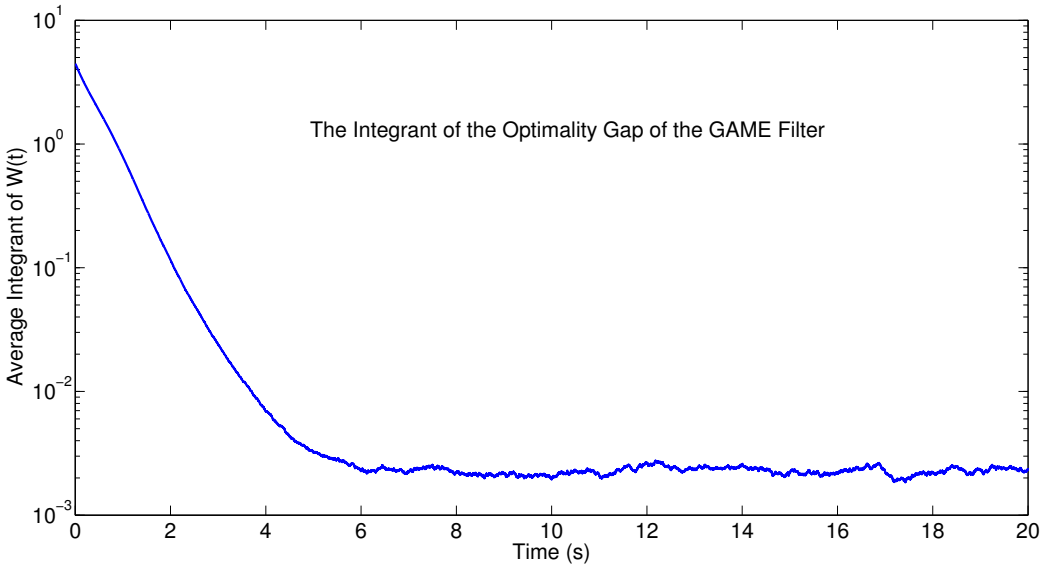

Figure 5.4: Case 2: The average of the integrant of $W(t)$ over 100 repeats plotted against time.

Chapter 6

Minimum-Energy Filtering on other Lie Groups

This chapter contains three special cases of the geometric approximate minimum-energy (GAME) filter developed in Chapter 4. Section 6.1 involves the case of estimating a rotation restricted to a single axis modelled on the two dimensional special orthogonal group $\mathrm{SO}(2)$. The kinematics on $\mathrm{SO}(2)$ is equivalent to the kinematics of an angle evolving on the unit circle S^1. Furthermore, the angular velocity measurements of the model are assumed to be contaminated with bias that is estimated and the overall filter is posed on $\mathrm{SO}(2) \times \mathbb{R}$. Next, this bias estimation result is generalized to three dimensional rotations and a generalized GAME filter is provided on $\mathrm{SO}(3) \times \mathbb{R}^3$. Lastly, minimum-energy filtering on the kinematics of pose (i.e. attitude and position) modeled on the special Euclidean group $\mathrm{SE}(3)$ is considered in Section 6.3.

6.1 Minimum-energy Filtering on the Unit Circle S^1

In this section, filtering on the kinematics of the special orthogonal group in two dimensions $\mathrm{SO}(2)$ is considered using angular velocity measurements with bias and vectorial measurements. The group $\mathrm{SO}(2)$ is an special case of the group $\mathrm{SO}(3)$ and filtering on $\mathrm{SO}(2)$ is a special case of the problem considered in Chapter 4. The system on $\mathrm{SO}(2)$ has many applications in robotics when rotations around a single axis are of interest. Example applications include determining the heading angle of a rigid-body moving in the 2D space and determining the rotation angle of a robotic joint with one degree of freedom. Other applications of the group $\mathrm{SO}(2)$ exist in communication radar systems where the angle of a rotating radar is sought or in power systems where the phase of an element of the grid is to be estimated. The system on $\mathrm{SO}(2)$ is also of interest since is often considered as a training ground for higher dimensional groups such as the group $\mathrm{SO}(3)$ and the group $\mathrm{SE}(3)$.

Consider a moving frame on the unit circle as shown in Figure 6.1. Let $\omega \in \mathbb{R}$ be the instantaneous angular velocity. The rotation X represents the angle *theta* and

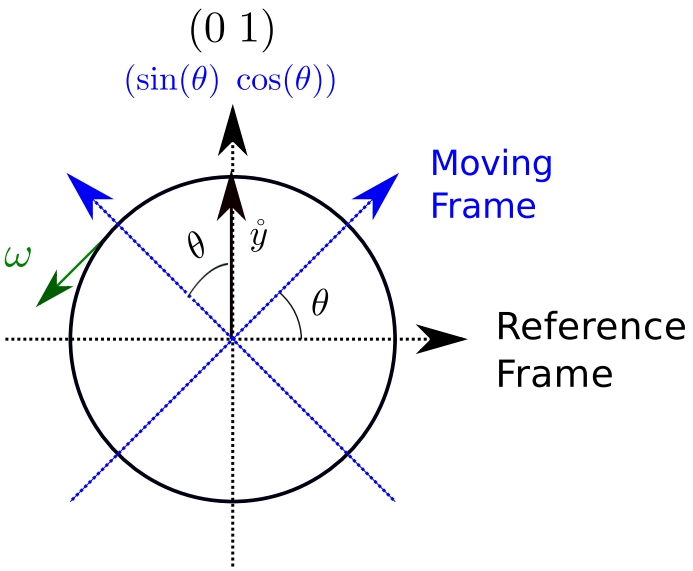

Figure 6.1: A rotating frame on the unit circle

satisfies the following kinematics equation

$$\dot{X} = X\omega_\times,\ X(0) = X_0, \tag{6.1}$$

where

$$X = \begin{bmatrix} \cos(\theta) & -\sin(\theta) \\ \sin(\theta) & \cos(\theta) \end{bmatrix} \in \mathrm{SO}(2). \tag{6.2}$$

The initial rotation X_0 is unknown. The cross notation $(\cdot)_\times : \mathbb{R} \longrightarrow \mathfrak{so}(2)$ is defined as

$$\omega_\times := \begin{bmatrix} 0 & -\omega \\ \omega & 0 \end{bmatrix}. \tag{6.3}$$

Conversely the notation $\mathrm{vex}(\cdot) : \mathfrak{so}(2) \longrightarrow \mathbb{R}$ extracts the scalar part, $\mathrm{vex}(\omega_\times) = \omega$.

Lemma 4. *The system* (6.1) *can be equivalently written in terms of the angle* θ *with kinematics*

$$\dot{\theta} = \omega,\ \theta(0) = \theta_0. \tag{6.4}$$

Proof. Note that from (6.1)

$$X^{-1}\dot{X} = \begin{bmatrix} 0 & -1 \\ 1 & 0 \end{bmatrix} \omega, \tag{6.5}$$

Also from (6.1) and (6.2)

$$X^{-1}\dot{X} = \begin{bmatrix} \cos(\theta) & \sin(\theta) \\ -\sin(\theta) & \cos(\theta) \end{bmatrix} \begin{bmatrix} -\sin(\theta) & -\cos(\theta) \\ \cos(\theta) & -\sin(\theta) \end{bmatrix} \dot{\theta} = \begin{bmatrix} 0 & -1 \\ 1 & 0 \end{bmatrix} \dot{\theta} \tag{6.6}$$

and the result (6.4) follows. □

The angular velocity ω is measured as

$$u = \omega + B_\omega v_\omega + b, \tag{6.7}$$

where $v_\omega \in \mathbb{R}$ is the measurement error signal and $B_\omega \in \mathbb{R}$ is a scaling known from the model. The signal $b \in \mathbb{R}$ is a constant or slowly time varying bias in the measurement $u \in \mathbb{R}$ that is modelled as

$$\dot{b} = B_b v_b,\ b(0) = b_0, \tag{6.8}$$

where b_0 is unknown, $v_b \in \mathbb{R}$ is an unknown rate of change of the bias b and $B_b \in \mathbb{R}$ is a scaling known from the model. Note that in measurement model (6.7) the measurement error v_ω and the bias b are modeled separately although a general deterministic measurement model is considered. This is due to the fact that the filter is going to be derived by minimizing a cost (6.12) in the size of the measurement error v_ω. The assumption behind this is that the measurement error should not, in general, be large. However, bias, in general, needs not to be small but rather slowly time-varying. Therefore, an independent bias model (6.8) is considered with v_b modeling a small unknown rate of change for b.

Assume a vector measurement obtained from

$$y = X^\top \mathring{y} + Dw, \tag{6.9}$$

where $\mathring{y} = (1\ ,\ 0)^\top$, $w \in \mathbb{R}^2$ is an unknown measurement error signal and $D \in \mathbb{R}^{2\times 2}$ is a full rank scaling matrix known from the model.

Remark 2. *Depending on the application one might have a different state measurement model such as*

$$y' = (WX)^\top \mathring{y}, \tag{6.10}$$

where $y' \in S^1$ is a vector measurement of the state X and $W \in \mathrm{SO}(2)$ represents the measurement error. In case the full angle measurement is available the following output map is suitable.

$$y'' = \theta + w', \tag{6.11}$$

where $y'' \in S^1$ is the measured state angle $\theta \in S^1$ and $w' \in S^1$ is the measurement error.

Consider the cost functional

$$\begin{aligned} J(t; X_0, b_0, v_\omega|_{[0\ ,\ t]}, v_b|_{[0\ ,\ t]}, w|_{[0\ ,\ t]}) = \\ \frac{\mathrm{trace}(I - X_0)}{K_1} + \frac{b_0^2}{2K_2} + \frac{1}{2}\int_0^t \left(v_\omega^2 + v_b^2 + \|w\|^2\right) d\tau, \end{aligned} \tag{6.12}$$

where $K_1, K_2 \in \mathbb{R}^+$ are given. Later on, these parameters will appear in the initial conditions of the proposed filter. If available, a priori information on the expected size of the initial state and the initial bias can be used to tune K_1 and K_2 relative to each other and the other unknowns in the cost function. The trace function is used

to measure the size of the initial state X_0 relative to the identity matrix $I \in \mathbb{R}^{2\times 2}$ (that is the identity element for the group $\mathrm{SO}(2)$).

Remark 3. *In case the measurement model* (6.11) *is used, the cost function* (6.12) *is modified to allow for measuring the measurement error w' as an angle.*

$$J'(t; X_0, b_0, v_\omega|_{[0\,,\,t]}, v_b|_{[0\,,\,t]}, w'|_{[0\,,\,t]}) = \frac{\mathrm{trace}(I - X_0)}{K_1} + \frac{b_0^2}{2K_2} + \int_0^t \left(\frac{1}{2}(v_\omega^2 + v_b^2) + 1 - \cos(w')\right) d\tau. \tag{6.13}$$

The following is the formal statement of the minimum-energy filtering problem for the system (6.1).

Problem 1. *Given the system* (6.1)*, the measurement models* (6.7), (6.9)*, the bias model* (6.8) *and the past measurements $u|_{[0\,,\,t]}$ and $y|_{[0\,,\,t]}$ find the state estimate $\hat{X}(t)$ for the current state $X(t)$ and the bias estimate $\hat{b}(t)$ for the current bias $b(t)$ such that the cost* (6.12) *is minimized over the unknowns X_0, b_0, $v_\omega|_{[0\,,\,t]}$, $v_b|_{[0\,,\,t]}$ and $w|_{[0\,,\,t]}$.*

Note that the cost (6.12) encodes the total energy associated with the unknowns X_0, b_0, $v_\omega|_{[0\,,\,t]}$, $v_b|_{[0\,,\,t]}$ and $w|_{[0\,,\,t]}$. In a sense, by minimizing (6.12) the goal is to find unknowns of minimum energy that together with the measurements $u|_{[0\,,\,t]}$ and $y|_{[0\,,\,t]}$ satisfy the model equations (6.1), (6.7), (6.8) and (6.9). Note that in general one might find infinitely many possible combinations of these unknowns that together with the measurements satisfy the model equations. However, by minimizing the cost (6.12) a set of minimizing unknowns is singled out that collectively has minimal energy. Substituting the minimizing unknowns and the measurements into equations (6.1), (6.7), (6.8) and (6.9) yields the minimum-energy state trajectory $X^*_{[0\,,\,t]}$ and the minimum-energy bias $b^*_{[0\,,\,t]}$. The subscript $[0\ ,\ t]$ indicates that the optimization takes place on the interval $[0\ ,\ t]$. The final values $X^*_{[0\,,\,t]}(t)$ and $b^*_{[0\,,\,t]}(t)$ are then assigned as the minimum-energy estimates at time t, $\hat{X}(t) := X^*_{[0\,,\,t]}(t)$ and $\hat{b}(t) := b^*_{[0\,,\,t]}(t)$. In the following, rather than resolving this infinite dimensional optimization problem at each time instance t, a recursive filter is derived that updates the estimates incorporating only the measurements at the current time t.

Problem 1 can be simplified by making the measurements constraint (6.9) explicit in the cost. Hence, substituting w in (6.12) from (6.9) yields the simplified cost

$$J(t; X_0, b_0, v_\omega|_{[0\,,\,t]}, v_b|_{[0\,,\,t]}) = \frac{\mathrm{trace}(I - X_0)}{K_1} + \frac{1}{2}\frac{b_0^2}{K_2} + \frac{1}{2}\int_0^t \left(v_\omega^2 + v_b^2 + \|y - X^\top \mathring{y}\|^2_{R^{-1}}\right) d\tau, \tag{6.14}$$

where $R := DD^\top$ is positive definite and

$$\|y - X^\top \mathring{y}\|^2_{R^{-1}} := (y - X^\top \mathring{y})^\top R^{-1} (y - X^\top \mathring{y}). \tag{6.15}$$

Now, similar to optimal control problems, the cost (6.14) is to be minimized over $v_\omega|_{[0\,,\,t]}, v_b|_{[0\,,\,t]}$. For now consider X_0 and b_0 as fixed but later to fully solve the

problem a further optimization over these two initial values are needed. In order to apply Hamilton Jacobi Bellman theory [5], define the following pre-Hamiltonian function,

$$\begin{aligned}\mathcal{H}^-(X, b, \mu_\omega, \mu_b, v_\omega, v_b, t) \coloneqq \\ \frac{1}{2}\left(v_\omega^2 + v_b^2 + \|y - X^\top \mathring{y}\|^2_{R^{-1}}\right) - \mu_\omega(u - b - B_\omega v_\omega) - \mu_b B_b v_b,\end{aligned} \tag{6.16}$$

where $\mu_\omega \in \mathbb{R}$ represents the costate variable $\Theta \in \mathfrak{so}^*(2)$ via $\langle (\mu_\omega)_\times, \Gamma\rangle = \Theta(\Gamma)$ for all $\Gamma \in \mathfrak{so}(2)$. This algebraic representation will be used in the following without further reference. The variable $\mu_b \in \mathbb{R}$ is the costate variable associated with the bias b. The optimal Hamiltonian $\mathcal{H}$ is obtained by minimizing the pre-Hamiltonian $\mathcal{H}^-$ over the signals v_ω and v_b that yields $v_\omega^* = -B_\omega \mu_\omega$ and $v_b^* = B_b \mu_b$.

$$\mathcal{H}(X, b, \mu_\omega, \mu_b, t) = \frac{1}{2}\left(-\mu_\omega^2 Q_\omega - \mu_b^2 Q_b + \|y - X^\top \mathring{y}\|^2_{R^{-1}}\right) - \mu_\omega(u - b), \tag{6.17}$$

where $Q_\omega \coloneqq B_\omega^2$ and $Q_b \coloneqq B_b^2$ are positive definite. Define the value function

$$V(X, b, t) \coloneqq \min_{v_\omega|_{[0\,,\,t]}, v_b|_{[0\,,\,t]}} J(t; X_0, b_0, v_\omega|_{[0\,,\,t]}, v_b|_{[0\,,\,t]}, w|_{[0\,,\,t]}), \tag{6.18}$$

where J is the cost (6.14) and the minimization is subject to the equations (6.1) and (6.8). The initial boundary condition for the value function (6.18) is obtained from (6.14)

$$V(X(0), b(0), 0) = \frac{\operatorname{trace}(I - X_0)}{K_1} + \frac{1}{2}\frac{b_0^2}{K_2}. \tag{6.19}$$

In the following, a Hamilton-Jacobi-Bellman equation [5] is considered that relates the optimal Hamiltonian (6.17) and the value function (6.18).

$$\mathcal{H}(X, b, \nabla_X V(X, b, t), \nabla_b V(X, b, t), t) - \nabla_t V(X, b, t) = 0. \tag{6.20}$$

Up to here only optimized over the signals $v_\omega|_{[0\,,\,t]}$ and $v_b|_{[0\,,\,t]}$ were considered. To complete the optimal filtering problem, one also needs to optimize V over the initial values X_0 and b_0. This is equivalent to further optimizations over $X(t)$ and $b(t)$ since (the minimizing) $X(t)$ and $b(t)$ are uniquely determined given the measurements $u|_{[0\,,\,t]}$, the equations (6.1), (6.7) and (6.8), the (minimizing) signals $v_\omega|_{[0\,,\,t]}$ and $v_b|_{[0\,,\,t]}$ and the (minimizing) initial values X_0 and b_0. Hence, similar to Mortensen's approach [31], the minimum-energy estimates $\hat{X}(t)$ and $\hat{b}(t)$ are characterized by the criticality conditions

$$\begin{aligned}\nabla_X V(X, b, t)|_{X=\hat{X}(t),\, b=\hat{b}(t)} = 0, \\ \nabla_b V(X, b, t)|_{X=\hat{X}(t),\, b=\hat{b}(t)} = 0.\end{aligned} \tag{6.21}$$

Solving Equations (6.21) is clearly a way to obtain the minimum-energy estimates $\hat{X}(t)$ and $\hat{b}(t)$, minimizing the cost (6.14) at every time t. However, in the following,

rather than solving this optimization problem for each time t, the goal is to find differential equations (filters) that dynamically update these estimates when new measurements are obtained as time evolves.

Consider the following definitions in order to rewrite (6.21) in terms of directional derivatives.

For all $\alpha, \gamma \in \mathbb{R}$

$$\begin{aligned} &\mathcal{D}_X V(X,b,t) \circ X\alpha_\times = \langle \nabla_X V(X,b,t), X\alpha_\times \rangle, \\ &\mathcal{D}_b V(X,b,t)\gamma = \langle \nabla_b V(X,b,t), \gamma \rangle, \end{aligned} \tag{6.22}$$

where the cross notation was defined in (6.3). The scalar inner product $\langle \cdot, \cdot \rangle : \mathbb{R} \times \mathbb{R} \longrightarrow \mathbb{R}$ is defined as

$$\langle \alpha, \gamma \rangle := \alpha\gamma, \tag{6.23}$$

and the left invariant inner product $\langle \cdot, \cdot \rangle : T\,\mathrm{SO}(2) \times T\,\mathrm{SO}(2) \longrightarrow \mathbb{R}$ is defined as

$$\langle X\alpha_\times, X\gamma_\times \rangle = \langle \alpha_\times, \gamma_\times \rangle := \mathrm{trace}(\frac{1}{2}\alpha_\times^\top \gamma_\times) = \langle \alpha, \gamma \rangle. \tag{6.24}$$

Similarly the following second order directional derivatives are defined.

$$\begin{aligned} &\mathcal{D}_X^2 V(X,b,t) \circ (X\alpha_\times, X\gamma_\times) = \langle \nabla_X^2 V(X,b,t) \circ X\alpha_\times, X\gamma_\times \rangle \\ &\qquad = \langle X\alpha_\times, \nabla_X^2 V(X,b,t) \circ X\gamma_\times \rangle, \\ &\mathcal{D}_b^2 V(X,b,t) \circ (\alpha, \gamma) = \langle \nabla_b^2 V(X,b,t) \circ \alpha, \gamma \rangle \\ &\qquad = \langle \alpha, \nabla_b^2 V(X,b,t) \circ \gamma \rangle, \\ &\mathcal{D}_b(\mathcal{D}_X V(X,b,t) \circ X\alpha_\times)\gamma = \mathcal{D}_X(\mathcal{D}_b V(X,b,t) \circ \alpha) \circ X\gamma_\times = \\ &\qquad \langle \nabla_b \nabla_X V(X,b,t) \circ \alpha, \gamma \rangle = \langle X\alpha_\times, \nabla_X \nabla_b V(X,b,t) \circ X\gamma_\times \rangle. \end{aligned} \tag{6.25}$$

Note that (6.25) shows that the second order derivatives are symmetric bi-linear mappings to $\mathbb{R}$, in the directions α and γ. Therefore, the following parametric representations are considered to serve as their values.

$$\begin{aligned} &\mathcal{D}_X^2 V(X,b,t) \circ (X\alpha_\times, X\gamma_\times) := P_1' \alpha\gamma, \\ &\mathcal{D}_b^2 V(X,b,t) \circ (\alpha, \gamma) := P_2' \alpha\gamma, \\ &\mathcal{D}_b(\mathcal{D}_X V(X,b,t) \circ X\alpha_\times)\gamma := P_{12}' \alpha\gamma, \\ &\mathcal{D}_X(\mathcal{D}_b V(X,b,t)\gamma) \circ X\alpha_\times := P_{12}' \alpha\gamma, \end{aligned} \tag{6.26}$$

where $P_1', P_2', P_{12}' \in \mathbb{R}$.

Now one can rewrite the final conditions (6.21) in terms of directional derivatives. For all $\alpha, \gamma \in \mathbb{R}$,

$$\begin{aligned} &\mathcal{D}_X V(X,b,t) \circ X\alpha_\times|_{X=\hat{X}(t),\, b=\hat{b}(t)} = 0, \\ &\mathcal{D}_b V(X,b,t)\gamma|_{X=\hat{X}(t),\, b=\hat{b}(t)} = 0. \end{aligned} \tag{6.27}$$

Condition (6.27) holds for every time t and therefore the total time derivative of (6.27) satisfies

$$\begin{aligned}\frac{d}{dt}\{\mathcal{D}_X V(X,b,t)\circ X\alpha_\times\}|_{X=\hat{X}(t),\, b=\hat{b}(t)} &= 0,\\ \frac{d}{dt}\{\mathcal{D}_b V(X,b,t)\gamma\}|_{X=\hat{X}(t),\, b=\hat{b}(t)} &= 0.\end{aligned} \tag{6.28}$$

Applying the chain rule and changing the order of the derivatives gives

$$\begin{aligned}\{\mathcal{D}_X^2 V(X,b,t)\circ(\dot{\hat{X}}, X\alpha_\times) + \mathcal{D}_X(\mathcal{D}_b V(X,b,t)\dot{\hat{b}})\circ X\alpha_\times +\\ \mathcal{D}_X(\nabla_t V(X,b,t))\circ X\alpha_\times\}|_{X=\hat{X}(t),\, b=\hat{b}(t)} = 0,\\ \{\mathcal{D}_b^2 V(X,b,t)\dot{\hat{b}}\gamma + \mathcal{D}_b(\mathcal{D}_X V(X,b,t)\circ\dot{\hat{X}})\gamma +\\ \mathcal{D}_b(\nabla_t V(X,b,t))\gamma\}|_{X=\hat{X}(t),\, b=\hat{b}(t)} = 0.\end{aligned} \tag{6.29}$$

Next, the derivatives $\mathcal{D}_X(\nabla_t V(X,b,t))\circ X\alpha_\times$ and $\mathcal{D}_b(\nabla_t V(X,b,t))\gamma$ are calculated by first replacing the time gradient $\nabla_t V(X,b,t)$ with $\mathcal{H}(X,b,\nabla_X V(X,b,t),\nabla_b V(X,b,t),t)$ using (6.53). First, using (6.17) and (6.22) yields

$$\begin{aligned}\mathcal{H}(X,b,\nabla_X V(X,b,t),\nabla_b V(X,b,t),t) = \frac{1}{2}\Big(-Q_\omega \mathcal{D}_X V(X,b,t)\circ\nabla_X V(X,b,t)\\ -Q_b\mathcal{D}_b V(X,b,t)\nabla_b V(X,b,t) + \|y - X^\top \mathring{y}\|^2_{R^{-1}}\Big) - \mathcal{D}_X V(X,b,t)\circ X(u-b)_\times.\end{aligned} \tag{6.30}$$

Therefore,

$$\begin{aligned}&\mathcal{D}_X(\mathcal{H}(X,b,\nabla_X V(X,b,t),\nabla_b V(X,b,t),t))\circ X\alpha_\times =\\ &\quad -Q_\omega\mathcal{D}_X^2 V(X,b,t)\circ(\nabla_X V(X,b,t), X\alpha_\times) - Q_b\mathcal{D}_b(\mathcal{D}_X V(X,b,t)\circ X\alpha_\times)\nabla_b V(X,b,t)\\ &\quad +2\alpha\,\mathrm{vex}\,\mathbb{P}_a(R^{-1}(y - X^\top\mathring{y})\mathring{y}^\top X) - \mathcal{D}_X^2 V(X,b,t)\circ(X(u-b)_\times, X\alpha_\times)\\ &\quad -\mathcal{D}_X V(X,b,t)\circ X\mathbb{P}_a(\alpha_\times(u-b)_\times),\\ &\mathcal{D}_b(\mathcal{H}(X,b,\nabla_X V(X,b,t),\nabla_b V(X,b,t),t))\gamma =\\ &\quad -Q_\omega\mathcal{D}_X(\mathcal{D}_b V(X,b,t)\gamma)\circ\nabla_X V(X,b,t) - Q_b\mathcal{D}_b^2 V(X,b,t)\nabla_b V(X,b,t)\gamma\\ &\quad -\mathcal{D}_X(\mathcal{D}_b V(X,b,t)\gamma)\circ X(u-b)_\times + \mathcal{D}_X V(X,b,t)\circ X\gamma_\times,\end{aligned} \tag{6.31}$$

where the anti-symmetric projection operator $\mathbb{P}_a(\cdot) : \mathbb{R}^{2\times 2} \longrightarrow \mathfrak{so}(2)$ for all $M \in \mathbb{R}^{2\times 2}$ is defined as

$$\mathbb{P}_a(M) \coloneqq \frac{1}{2}(M - M^\top). \tag{6.32}$$

Next, substitute (6.31) in (6.29). Note that the first order derivatives, that appear in (6.31), evaluated at $X = \hat{X}(t)$, $b = \hat{b}(t)$, yield zero. This is due to the final conditions (6.21) and (6.27). Replacing the second order derivatives from (6.26) and

canceling the arbitrary directions α and γ from both sides of (6.29) yields

$$\begin{aligned} &P_1 \operatorname{vex}(\hat{X}^\top \dot{\hat{X}}) + P_{12}\dot{\hat{b}} + 2\operatorname{vex}\mathbb{P}_a(R^{-1}(y-\hat{y})\hat{y}^\top) - P_1(u-\hat{b}) = 0, \\ &P_2\dot{\hat{b}} + P_{12}\operatorname{vex}(\hat{X}^\top \dot{\hat{X}}) - P_{12}(u-\hat{b}) = 0, \end{aligned} \tag{6.33}$$

where

$$\begin{aligned} \hat{y} &\coloneqq \hat{X}^\top \mathring{y}, \\ P_1 &\coloneqq P_1'|_{X=\hat{X}(t),\, b=\hat{b}(t)}, \\ P_2 &\coloneqq P_2'|_{X=\hat{X}(t),\, b=\hat{b}(t)}, \\ P_{12} &\coloneqq P_{12}'|_{X=\hat{X}(t),\, b=\hat{b}(t)}. \end{aligned} \tag{6.34}$$

Rearranging (6.33) yields the observer equations

$$\begin{aligned} \dot{\hat{X}} &= \hat{X}\left(u - \hat{b} - P_1^{-1}\left(l + P_{12}\dot{\hat{b}}\right)\right)_\times, \\ \dot{\hat{b}} &= -\frac{P_{12}}{P_2}\left(-u + \hat{b} + \operatorname{vex}(\hat{X}^\top \dot{\hat{X}})\right), \end{aligned} \tag{6.35}$$

where $l \coloneqq 2\operatorname{vex}\mathbb{P}_a(R^{-1}(y-\hat{y})\hat{y}^\top)$. The initial conditions $\hat{X}(0) = I$ and $\hat{b}(0) = 0$, are obtained using (6.19) and (6.27).

The proposed observers (6.35) yield the exact dynamical equations that will update the value of the minimum-energy estimates $\hat{X}(t)$ and $\hat{b}(t)$ (that are the solutions to Problem 1), for every time t. Note that the two observers (6.35) are interconnected and use the current measurements $u(t)$ and $y(t)$ to update their estimates. The measurements are weighted by dynamic gains P_1, P_2 and P_{12} that are related to the value function defined in (6.18) through (6.26).

In order to implement these observers one also needs dynamical equations that concurrently update the gains P_1, P_2 and P_{12}. This can be done using the definitions (6.26) and by calculating the total time derivatives

$$\begin{aligned} \dot{P}_1\alpha\gamma &= \frac{d}{dt}\{\mathcal{D}_X^2 V(X,b,t)\circ(X\alpha_\times, X\gamma_\times)\}_{X=\hat{X}(t),\, b=\hat{b}(t)}, \\ \dot{P}_2\alpha\gamma &= \frac{d}{dt}\{\mathcal{D}_b^2 V(X,b,t)\circ(\alpha,\gamma)\}_{X=\hat{X}(t),\, b=\hat{b}(t)}, \\ \dot{P}_{12}\alpha\gamma &= \frac{d}{dt}\{\mathcal{D}_b(\mathcal{D}_X V(X,b,t)\circ X\alpha_\times)\gamma\}_{X=\hat{X}(t),\, b=\hat{b}(t)}. \end{aligned} \tag{6.36}$$

The calculation details for (6.36) similarly follow from our observer derivations. It is worth noting that the right hand sides of (6.36) are going to depend on the third order derivatives of the value function. However, assuming that the third order derivatives of the value function are negligible, the following Riccati equations are obtained that

update the gains of the observers on-line.

$$\begin{aligned}\dot{P}_1 &= -Q_\omega P_1^2 - Q_b P_{12}^2 - \hat{y}^\top S R^{-1} S \hat{y} + (y-\hat{y})^\top R^{-1} \hat{y},\\ \dot{P}_2 &= -Q_b P_2^2 - Q_\omega P_{12}^2 + 2P_{12},\\ \dot{P}_{12} &= -Q_\omega P_{12} P_1 - Q_b P_2 P_1 + P_1,\end{aligned} \tag{6.37}$$

where

$$S \coloneqq \begin{bmatrix} 0 & -1 \\ 1 & 0 \end{bmatrix}. \tag{6.38}$$

The initial conditions $P_1(0) = K_1^{-1}$, $P_2(0) = K_2^{-1}$ and $P_{12}(0) = 0$ are obtained using (6.19) and (6.26).

Note that these Riccati equations (6.61b) provide a second-order approximation of the minimum-energy dynamics of the observer gains. However, as was suggested by simulations in previous work [41], the third order derivatives of the value function are going to be small and there is little advantage in increasing the dimension of the filter by considering the higher order derivatives of the value function. Therefore, the proposed filter's formulation is restricted to a second-order approximation of the minimum-energy filter.

Remark 4. *One can continue deriving dynamics of the higher order derivatives of the value function using our previous calculations. In fact, for a case that there is no bias in angular velocity measurements and where full state measurements* (6.11) *is used, it is straightforward to derive dynamics of the higher order derivatives of the value function up to arbitrary higher orders. Consider the following system.*

$$\begin{cases} \dot{\theta} = \omega,\ \theta(0) = \theta_0,\\ u = \omega + g\delta,\\ y'' = \theta + \epsilon, \end{cases} \tag{6.39}$$

where $\theta \in S^1$ is the state, the signal $\omega \in \mathbb{R}$ is the angular velocity input that is measured as $u \in \mathbb{R}$ with measurement error $\delta \in \mathbb{R}$ and a known scaling $g \in \mathbb{R}$. Full state measurement is given by $y'' \in S^1$ with measurement error $\epsilon \in S^1$. An eight-order approximate minimum-energy filter for this system is given in Table 6.1.

Observer	$\dot{\hat{\theta}} = u + P_1^{-1}\sin(y'' - \hat{\theta}),\ \hat{\theta}(0) = 0,$
Gains	$\dot{p}_1 = \cos(y'' - \hat{\theta}) - g^2 p_1^2 + p_2 p_1^{-1}\sin(y'' - \hat{\theta}),\ p_1(0) = K_1^{-1},$ $\dot{p}_2 = \sin(y'' - \hat{\theta}) - 3g^2 p_1 p_2 + p_3 p_1^{-1}\sin(y'' - \hat{\theta}),\ p_2(0) = 0,$ $\dot{p}_3 = -\cos(y'' - \hat{\theta}) - 4g^2 p_3 p_1 - 3g^2 p_2^2 + p_4 p_1^{-1}\sin(y'' - \hat{\theta}),\ p_3(0) = -K_1^{-1},$ $\dot{p}_4 = -\sin(y'' - \hat{\theta}) - 5g^2 p_4 p_1 - 10g^2 p_3 p_2 + p_5 p_1^{-1}\sin(y'' - \hat{\theta}),\ p_4(0) = 0,$ $\dot{p}_5 = \cos(y'' - \hat{\theta}) - 6g^2 p_5 p_1 - 10g^2 p_3^2 - 15g^2 p_2 p_4 + p_5 p_1^{-1}\sin(y'' - \hat{\theta}),\ p_5(0) = K_1^{-1},$ $\dot{p}_6 = \sin(y'' - \hat{\theta}) - 7g^2 p_6 p_1 - 21g^2 p_5 p_2 - 35g^2 p_4 p_3 + p_7 p_1^{-1}\sin(y'' - \hat{\theta}),\ p_6(0) = 0,$ $\dot{p}_7 = -\cos(y'' - \hat{\theta}) - 8g^2 p_7 p_1 - 28g^2 p_6 p_2 - 56g^2 p_5 p_3,\ p_7(0) = -K_1^{-1}.$

Table 6.1: The 8th-order approximate minimum-energy filter on S^1 using full state measurements.

In summary the following filter is proposed.

Observer	$\dot{\hat{X}} = \hat{X}\left(u - \hat{b} - \dfrac{P_2}{P_1 P_2 - P_{12}^2} l\right)_\times,\ \hat{X}(0) = I,$ $\dot{\hat{b}} = \dfrac{P_{12}}{P_1 P_2 - P_{12}^2} l,\ \hat{b}(0) = 0,$ $l \coloneqq 2\,\mathrm{vex}\,\mathbb{P}_a(R^{-1}(y - \hat{y})\hat{y}^\top),$
Gains	$\dot{P}_1 = -Q_\omega P_1^2 - Q_b P_{12}^2 - \hat{y}^\top S R^{-1} S \hat{y} + (y - \hat{y})^\top R^{-1}\hat{y},\ P_1(0) = K_1^{-1},$ $\dot{P}_2 = -Q_b P_2^2 - Q_\omega P_{12}^2 + 2P_{12},\ P_2(0) = K_2^{-1},$ $\dot{P}_{12} = -Q_\omega P_{12} P_1 - Q_b P_2 P_1 + P_1,\ P_{12}(0) = 0.$

Table 6.2: The approximate minimum-energy filter on $\mathrm{SO}(2) \times \mathbb{R}$.

Note that the equations (6.35) have been rearranged into a new form in which the kinematics of the state and the bias estimates are in cascade form. This form is more useful for implementing the filter by discretization.

Lemma 5. *If the measurement model* (6.11) *along with the cost* (6.13) *is considered instead*

of (6.9) *and* (6.12)*, the resulting filer equations are*

$$\begin{aligned}
\dot{\hat{\theta}} &= u - \hat{b} - \frac{P_2}{P_1P_2 - P_{12}^2}\sin(y'' - \hat{\theta}),\ \hat{\theta}(0) = 0,\\
\dot{\hat{b}} &= \frac{P_{12}}{P_1P_2 - P_{12}^2}\sin(y'' - \hat{\theta}),\ \hat{b}(0) = 0,\\
\dot{p}_1 &= -Q_\omega p_1^2 - Q_b p_{12}^2 + \cos(y'' - \hat{\theta}),\ p_1(0) = K_1^{-1},\\
\dot{p}_2 &= -Q_b p_2^2 - Q_\omega p_{12}^2 + 2p_{12},\ p_2(0) = K_2^{-1},\\
\dot{p}_{12} &= -Q_\omega p_{12}p_1 - Q_b p_2 p_1 + p_1,\ p_{12}(0) = 0.
\end{aligned} \tag{6.40}$$

Moreover, equations (6.40) *are equivalent to the proposed filter 6.2 if the matrices D and R are equal to the identity matrix.*

The proof of Lemma 5 involves an argument, similar to the proof of Lemma 4, to show the first equation in (6.40). Furthermore, all the calculations that involve the measurements y need to be done using y'' instead.

6.2 The GAME Filter with Bias Estimation

In Chapter 4, the attitude system considered did not include bias in the angular velocity measurements. Here, that result is generalized similar to Section 6.1 by adding bias to the angular velocity measurements. Recall the attitude kinematics given by

$$\dot{X}(t) = X(t)\Omega_\times(t),\ X(0) = X_0. \tag{6.41}$$

The matrix X is an $\mathrm{SO}(3)$-valued state signal with the unknown initial value X_0 and $\Omega \in \mathbb{R}^3$ represents the angular velocity of the moving body expressed in the body-fixed frame.

A rate-gyro sensor measures the angular velocity through the following equation

$$u(t) = \Omega(t) + B_\Omega v_\Omega(t) + b(t). \tag{6.42}$$

The signals $u \in \mathbb{R}^3$ and $v_\Omega \in \mathbb{R}^3$ denote the body-fixed frame measured angular velocity and the input measurement error, respectively. The coefficient matrix $B_\Omega \in \mathbb{R}^{3\times 3}$ allows for different weightings for the components of the unknown input measurement error v. We assume that B_Ω is full rank and hence that $Q_\Omega \coloneqq B_\Omega B_\Omega^\top$ is positive definite. The signal $b(t) \in \mathbb{R}^3$ is an unknown slowly time-varying bias signal generated from

$$\dot{b}(t) = B_b v_b(t), \quad b(0) = b_0, \tag{6.43}$$

where $B_b \in \mathbb{R}^{3\times 3}$ is a full rank weighting matrix known from the model with $Q_b \coloneqq B_b B_b^\top$ positive definite. The signal $v_b \in \mathbb{R}^3$ is a small unknown perturbation and $b_0 \in \mathbb{R}^3$ is an unknown initial bias.

Consider the vectors $\mathring{y}_i \in \mathbb{R}^3$ as known vector directions in the reference frame. Measuring these vectors in body-fixed frame provides partial information about the

attitude X. Typically, magnetometer, visual sensors, sun sensor and star tracker are deployed for this purpose. The following model yields the measurements of theses sensors.

$$y_i(t) = X(t)^\top \mathring{y}_i + D_i w_i(t),\ i = 1, \cdots, n \tag{6.44}$$

The measurements $y_i \in \mathbb{R}^3$ are measurements of the $\mathring{y}_i$ in the body-fixed frame and the signals $w_i \in \mathbb{R}^3$ are the unknown output measurement errors. The coefficient matrix $D_i \in \mathbb{R}^{3\times 3}$ allows for different weightings of the components of the output measurement error w_i. Again, assume that D_i is full rank and $R_i := D_i D_i^\top$ is positive definite.

Consider the cost

$$\begin{aligned} J(t;\ X_0,\ b_0,\ v_\Omega|_{[0,\,t]},\ v_b|_{[0,\,t]},\ \{w_i|_{[0,\,t]}\}) &= \frac{1}{2}\,\mathrm{trace}\left[(I - X_0)K_{X_0}^{-1}(I - X_0)^\top\right] + \\ &+ \frac{1}{2}b_0^\top K_{b_0}^{-1} b_0 + \frac{1}{2}\int_0^\top \left(v_\Omega^\top v_\Omega + v_b^\top v_b + \sum_i w_i^\top w_i\right) d\tau, \end{aligned} \tag{6.45}$$

in which $K_{X_0}, K_{b_0} \in \mathbb{R}^{3\times 3}$ are symmetric positive definite. The cost (6.45) can be thought of as a measure of the aggregate energy stored in the unknown initialization and measurement signals of (6.41), (6.42), (6.43) and (6.44).

Similar to the derivation presented in Section 6.1 the following filter is obtained.

Attitude Observer	$\dot{\hat{X}} = \hat{X}(u - \hat{b} - P_a l)_\times,\ \ X(0) = I,$, $l = \sum_i \hat{y}_i \times (R_i^{-1}(\hat{y}_i - y_i)),\ \hat{y}_i = \hat{X}^\top \mathring{y}_i,$
Bias Observer	$\dot{\hat{b}} = P_c^\top l,\ \hat{b}(0) = [0\ 0\ 0]^\top,$
Gains	$\dot{P}_a = Q_\Omega + 2\mathbb{P}_s(P_a(2(u - \hat{b}) - P_a l)_\times) + P_a(E - S)P_a - P_c^\top - P_c,\ P_a(0) = K_{X_0},$ $\dot{P}_c = -(u - \hat{b} - P_a l)_\times P_c + P_a(E - S)P_c - P_b,\ P_c(0) = 0_{3\times 3},$ $\dot{P}_b = Q_b + P_c(E - S)P_c,\ P_b(0) = K_{b_0},$ $S = \sum_i (\hat{y}_i)_\times^\top R_i^{-1}(\hat{y}_i)_\times,$ $E = \mathrm{trace}(C)I - C,\ C = \sum_i \mathbb{P}_s(R_i^{-1}(\hat{y}_i - y_i)\hat{y}_i^\top).$

Table 6.3: The GAME filter with bias estimation on $\mathrm{SO}(3) \times \mathbb{R}^3$

6.3 Minimum-energy Pose Filtering on the Special Euclidean Group SE(3)

The following is a model for the kinematics of the pose of a rigid body, and an associated vectorial measurement model, for which the problem of minimum-energy filtering is formulated here. Consider

$$\left\{\begin{array}{ll} \dot{X}(t) & = X(t)A(t),\ X(0) = X_0, \\ U(t) & = A(t) + (Bv(t))^{\curlywedge}, \\ y_i(t) & = X(t)^{-1}\mathring{y}_i + [D_i w_i(t)\ ,\ 1]^\top,\ i = 1, \cdots, n\ , \end{array}\right. \tag{6.46}$$

where X is an SE(3)-valued state signal representing the pose of a body-fixed frame, i.e. a frame attached to a moving rigid body, relative to a reference frame, i.e. a frame fixed at a reference point. We use the following matrix representation of pose that is commonly known as homogeneous coordinates. This model preserves the group structure of $\mathrm{SE}(3) \subseteq \mathbb{R}^{4\times 4}$ with the $GL(4)$ operation of matrix multiplication, i.e, $X_1 X_2 \in \mathrm{SE}(3)$, for all $X_1, X_2 \in \mathrm{SE}(3)$.

$$X = \left[\begin{array}{cc} R & p \\ 0 & 1 \end{array}\right].$$

Here the rotation R is an element of the rotation group $\mathrm{SO}(3) = \{R \in \mathbb{R}^{3\times 3} \,|\, R^\top R = I, \det(R) = 1\}$ where I is the 3 by 3 identity matrix and the translation p is an element of $\mathbb{R}^3$. The signal $A \in \mathfrak{se}(3) \subseteq \mathbb{R}^{4\times 4}$ represents the twist of the moving body expressed in the body-fixed frame and it comprises the angular velocity $\Omega_\times \in \mathfrak{so}(3)$ and the translational velocity $V \in \mathbb{R}^3$ of the moving body in the following matrix representation. Note that $\mathfrak{so}(3) = \{\Omega_\times \in \mathbb{R}^{3\times 3} \,|\, \Omega_\times = -\Omega_\times^\top\}$. Recall the cross notation $(\cdot)_\times : \mathbb{R}^3 \longrightarrow \mathfrak{so}(3)$ defined as

$$[w_1\ w_2\ w_3]_\times^\top := \left(\begin{array}{ccc} 0 & -w_1 & w_2 \\ w_1 & 0 & -w_3 \\ -w_2 & w_3 & 0 \end{array}\right), \text{ then } \quad A = \left[\begin{array}{cc} \Omega_\times & V \\ 0 & 0 \end{array}\right]. \tag{6.47}$$

Conversely, note that $\mathrm{vex}(\cdot) : \mathfrak{so}(3) \longrightarrow \mathbb{R}^3$ by $\mathrm{vex}(\Omega_\times) = \Omega$. The signals $U \in \mathfrak{se}(3)$ and $v \in \mathbb{R}^6$ denote the body-fixed frame measured velocity input and the input measurement error, respectively. The coefficient matrix $B \in \mathbb{R}^{6\times 6}$ allows for different weightings for the components of the unknown input measurement error v. We assume that B is full rank and hence that $Q := BB^\top$ is positive definite. The lift-up notation $(\cdot)^{\curlywedge} : \mathbb{R}^6 \longrightarrow \mathfrak{se}(3)$ is defined as

$$([z_1\ z_2]^\top)^{\curlywedge} := \left(\begin{array}{cc} (z_1)_\times & z_2 \\ 0 & 0 \end{array}\right) \tag{6.48}$$

where $z_1, z_2 \in \mathbb{R}^3$. Conversely the lift-down notation $(\cdot)^{\curlyvee} : \mathfrak{se}(3) \longrightarrow \mathbb{R}^6$ is defined as $(([z_1\ z_2]^\top)^{\curlywedge})^{\curlyvee} = [z_1\ z_2]^\top$.The vectors $\mathring{y}_i \in \mathbb{R}^4 = [\underline{\mathring{y}}_i\ ,\ 1]^\top$ where $\underline{\mathring{y}}_i \in \mathbb{R}^3$ are known

vector directions in the reference frame. The measurements $y_i \in \mathbb{R}^4 = [\underline{y}_i\ ,\ 1]^\top$ where $\underline{y}_i$ are measurements of the $\mathring{\underline{y}}_i$ in the body-fixed frame and the signals $w_i \in \mathbb{R}^3$ are the unknown output measurement errors. The coefficient matrix $D_i \in \mathbb{R}^{3\times 3}$ allows for different weightings of the components of the output measurement error w_i. Again assume that D_i is full rank and $M_i \coloneqq D_i D_i^\top$ is positive definite.

Consider the cost

$$J(t; X_0, v|_{[0,\,t]}, \{w_i|_{[0,\,t]}\}) = \frac{1}{2}\int_0^\top \left(\|Bv\|^2_{Q^{-1}} + \sum_i \|D_i w_i\|^2_{M_i^{-1}} \right) d\tau + \frac{1}{2}\|I - X_0\|^2_{K_0^{-1}}. \tag{6.49}$$

in which $K_0 \in \mathbb{R}^{3\times 3}$ is symmetric positive definite. The cost (6.49) can be thought of as a measure of the aggregate energy stored in the unknown signals of system (6.46).

This section concerns generalizing Mortensen's minimum-energy filtering [31] to the invariant pose kinematics (6.46). In other words, the minimum-energy state estimate at the current time t ($\hat{X}(t)$) is derived using the past measurements $y_i|_{[0\,,\,t]}$ and $U|_{[0\,,\,t]}$ such that the cost (6.49) is minimized. In principle this requires postulating a set of unknown signals $(X_0,\ v|_{[0,\,t]},\ \{w_i|_{[0,\,t]}\})$ that are compatible with the measurements $y_i|_{[0\,,\,t]}$ and $U|_{[0\,,\,t]}$ by fulfilling the system equations (6.46). One can easily find an estimate for the state at time t using the postulated unknowns by integrating the system (6.46). In general one might find infinitely many combinations of such unknown signals that lead to many different state estimates. However, minimizing (6.49) yields a triplet $(X_0^*,\ v^*|_{[0,\,t]},\ \{w_i^*|_{[0,\,t]}\})$ that contains minimum collective energy and yields an associated minimum-energy state trajectory $X^*_{[0,\,t]}$. The subscript $[0,\ t]$ indicates that the optimization takes place on the interval $[0,\ t]$. We pick the final optimal state $X^*_{[0,\,t]}(t)$ as our minimum-energy estimate at time t, $\hat{X}(t) \coloneqq X^*_{[0,\,t]}(t)$. In the following, rather than repeating this optimization process for every time interval $[0,\ t]$ Mortensen's approach is used to find an iterative dynamical equation that updates the minimum-energy estimate $\hat{X}(t)$ as its state value. More details are listed in Chapter 4.

Similar to optimal control theory [5], define a pre-Hamiltonian for this optimization problem. Note that although the optimization problem is carried out over the triplet $(X_0,\ v|_{[0,\,t]},\ \{w_i|_{[0,\,t]}\})$, one can skip optimizing over the $\{w_i|_{[0,\,t]}\}$ by replacing them using the measurements $y_i|_{[0\,,\,t]}$. Also for now assume that the initial state X_0 is fixed keeping in mind that later one, the solution needs to be optimized over X_0. Hence the problem becomes very similar to an optimal control problem where one needs to optimize the following Hamiltonian over v which can be seen as the control parameter.

$$\mathcal{H}^-(X, \mu\hat{}, v, t) \coloneqq \frac{1}{2}[v^\top v + \sum_i (X^\top \mathring{y}_i - y_i)^\top R_i^{-1}(X^\top \mathring{y}_i - y_i)] - \mu^\top(U\curlyvee - Bv), \tag{6.50}$$

where $\mu \in \mathbb{R}^6$ represents a costate variable $\Theta \in \mathfrak{se}^*(3)$ via $\langle \mu\hat{}, \Gamma \rangle = \Theta(\Gamma)$ for all

$\Gamma \in \mathfrak{se}(3)$. In the following the identification of $\Theta \in \mathfrak{se}^*(3)$ with $\hat{\mu} \in \mathfrak{se}(3)$ will be used without further reference. Minimizing the pre-Hamiltonian (6.50) over v yields the optimal Hamiltonian

$$\mathcal{H}(X, \hat{\mu}, t) = \frac{1}{2}[-\mu^\top Q \mu + \sum_i (X^\top \mathring{y}_i - y_i)^\top R_i^{-1} (X^\top \mathring{y}_i - y_i)] - \mu^\top \mathcal{U}. \tag{6.51}$$

In order to apply the Hamilton-Jacobi-Bellman principle [5] to this problem the following value function is defined

$$V(X, t) := \min_{v|_{[0,\,t]}} J(t; X_0, v|_{[0,\,t]}), \tag{6.52}$$

where J is the cost (6.49) and the minimization is constrained by the system equations (6.46). The Hamilton-Jacobi-Bellman equation is then

$$\mathcal{H}(X, \mathrm{TL}_X^* \nabla_1 V(X, t), t) - \frac{\partial V}{\partial t}(X, t) = 0. \tag{6.53}$$

From (6.49) the initial time boundary condition is

$$V(X_0, 0) = \frac{1}{2} \operatorname{trace} \left[(I - X_0)^\top K_0^{-1} (I - X_0) \right]. \tag{6.54}$$

Up to here, only the optimal control part of the problem has been addressed (by minimizing (6.49) over v) assuming that X_0 is fixed. To solve the original problem one needs to optimize V over X_0. This is equivalent to optimizating V over the final condition $X(t)$ since the initial and final conditions are deterministically coupled by the optimal input $v^*|_{[0\,,\,t]}$. Assuming that the value function is strictly convex, its minimum is characterized by the final condition

$$\nabla_1 V(X, t)|_{X=\hat{X}(t)} = 0. \tag{6.55}$$

Solving Equation (6.55) characterizes $\hat{X}(t)$ as the final value of the minimizing argument $X^*_{[0,t]}(t)$. However, this still requires an explicit solution to a potentially infinite dimensional nonlinear control problem and must be repeated at every time t. To overcome this issue Mortensen's approach [31] is utilized to derive a recursive solution to this problem.

Note that the final condition (6.55) characterizes the solution $\hat{X}(t)$ at the final time t. The final condition (6.55) is equivalent to

$$\langle \nabla_1 V(X, t), X\Gamma \rangle|_{X=\hat{X}(t)} = (\mathcal{D}_1 V(X, t) \circ X\Gamma)|_{X=\hat{X}(t)} = 0, \quad \text{for all } \Gamma \in \mathfrak{se}(3). \tag{6.56}$$

In order to get the dynamics of this solution, the total time derivative of the final condition (6.56) is calculated using the chain rule. Note that the nonlinear geometry

is maintained by using geometric differentiations.

$$\begin{aligned}\frac{d}{dt}(\mathcal{D}_1 V(X,t)\circ X\Gamma)|_{X=\hat{X}(t)} = \\ (\mathcal{D}_1^2 V(X,t)\circ(X\Gamma,\dot{\hat{X}}) + \mathcal{D}_1\frac{\partial V(X,t)}{\partial t}\circ X\Gamma)|_{X=\hat{X}(t)} = 0,\end{aligned} \tag{6.57}$$

The second order derivative of the value function is related to the Hessian of the value function as an operator acting on a tangent direction. A matrix $K \in \mathbb{R}^{6\times 6}$ representation is chosen to obtain a matrix formulation such that

$$\mathcal{D}_1^2 V(\hat{X},t)\circ(\hat{X}\Gamma,\dot{\hat{X}}) = \langle \mathrm{Hess}_1\, V(\hat{X},t)\circ\dot{\hat{X}},\hat{X}\Gamma\rangle := \langle \hat{X}\left[K(\dot{\hat{X}})^\vee\right]^\wedge,\hat{X}\Gamma\rangle \tag{6.58}$$

The term $\mathcal{D}_1\frac{\partial V(X,t)}{\partial t}\circ X\Gamma$ can be calculated after replacing the partial derivative from (6.53). Therefore, denoting $P := K^{-1}$ yields the following minimum-energy observer equation.

$$\dot{\hat{X}}(t) = \hat{X}\left(U - \left[P\left(\mathbb{P}\sum_i R_i^{-1}(y_i - \hat{X}^{-1}\mathring{y}_i)\mathring{y}_i^\top \hat{X}^{-\top}\right)^\vee\right]^\wedge\right), \tag{6.59}$$

where $\hat{X}(0) = I$ is calculated from (6.54) and (6.55) and $\mathbb{P} : \mathbb{R}^{4\times 4} \to \mathfrak{se}(3)$ denote the orthogonal projection with respect to the Euclidean inner product $\langle\cdot,\cdot\rangle$, i.e., for all $A \in \mathfrak{se}(3)$, $M \in \mathbb{R}^{4\times 4}$, one has $\langle A, M\rangle = \langle A, \mathbb{P}(M)\rangle = \langle \mathbb{P}(M), A\rangle$. One verifies that for all $M_1 \in \mathbb{R}^{3\times 3}, m_{2,3} \in \mathbb{R}^3, m_4 \in \mathbb{R}$,

$$\mathbb{P}\left(\begin{bmatrix} M_1 & m_2\\ m_3^\top & m_4\end{bmatrix}\right) = \begin{bmatrix}\mathbb{P}_a(M_1) & m_2\\ 0 & 0\end{bmatrix}.$$

Here, the symmetric projector $\mathbb{P}_s$ is defined by $\mathbb{P}_s(M) := 1/2(M + M^\top)$ for all $M \in \mathbb{R}^{n\times n}$ while the skew-symmetric projector $\mathbb{P}_a$ is defined by $\mathbb{P}_a(M) := 1/2(M - M^\top)$.

Equation (6.59) depends on the gain P and to implement the observer one needs to calculate the dynamics of the gain K and it's inverse P. According to the Mortensen's approach This is done by calculating the total time derivative of the following equation.

$$\langle \dot{K}\gamma,\omega\rangle = \frac{d}{dt}(\mathcal{D}_1^2 V(\hat{X},t)\circ(\hat{X}\Gamma,\hat{X}\Omega))^\vee, \quad \text{for all } \gamma,\omega \in \mathbb{R}^6, \tag{6.60}$$

where $\Gamma = \gamma^\wedge$ and $\Omega = \omega^\wedge$. Calculating the right hand side using the chain rule and then using the HJB equation (6.53), the final condition (6.56) and neglecting the third order derivatives of the value function yields a Riccati equation for the dynamics of P.

In summary the following filter is obtained.

$$\dot{\hat{X}}(t) = \hat{X}\left(U - (Pl)^\wedge\right), \tag{6.61a}$$

$$\dot{P} = Q + 2\mathbb{P}_{sym}(PU) - \mathbb{P}_{sym}(P(Pl)^\wedge) + PEP + PSP. \tag{6.61b}$$

where

$$l \coloneqq \left(\mathbb{P} \sum_i R_i^{-1} (y_i - \hat{X}^{-1} \mathring{y}_i) \mathring{y}_i^\top \hat{X}^{-\top} \right)^\vee, \tag{6.62a}$$

$$E \coloneqq \begin{pmatrix} \operatorname{trace}(\Delta) I - \Delta & \sum_i M_i^{-1} (\underline{\hat{y}}_i)_\times \\ -\sum_i (\underline{\hat{y}}_i)_\times M_i^{-1} & 0 \end{pmatrix}, \tag{6.62b}$$

$$\underline{\hat{y}}_i \coloneqq \hat{R}^\top (\mathring{y}_i - \hat{p}),\ \Delta \coloneqq \sum_i \mathbb{P}_s (M_i^{-1} (\underline{\hat{y}}_i - \underline{y}_i) \underline{\hat{y}}_i^\top), \tag{6.62c}$$

$$S \coloneqq \begin{pmatrix} \sum_i (\underline{\hat{y}}_i)_\times M_i^{-1} (\underline{\hat{y}}_i)_\times & -\sum_i (M_i^{-1} (\underline{\hat{y}}_i - \underline{y}_i))_\times \\ \sum_i (M_i^{-1} (\underline{\hat{y}}_i - \underline{y}_i))_\times & -\sum_i M_i^{-1} \end{pmatrix}. \tag{6.62d}$$

Here $\hat{X}(0) = I$ and $P(0) = \operatorname{diag}(\operatorname{trace}(K_0^{-1}) I - K_0^{-1}\ ,\ 0)$ are calculated using (6.54) and (6.55). The projection $\mathbb{P}_{sym} : \mathbb{S}^{6\times 6} \times \mathfrak{se}(3) \longrightarrow \mathbb{S}^{6\times 6}$ where $\mathbb{S}^{n\times n}$ is the space of symmetric matrices in $\mathbb{R}^{n\times n}$ is defined as follows. For $P = \begin{bmatrix} P_1 & P_2 \\ P_2^\top & P_3 \end{bmatrix}$ and $A = \begin{bmatrix} \Omega_\times & V \\ 0 & 0 \end{bmatrix}$ where $P_1, P_3 \in \mathbb{S}^{3\times 3}$, $P_2 \in \mathbb{R}^{3\times 3}$, $\Omega_\times \in \mathfrak{so}(3)$ and $V \in \mathbb{R}^3$ the symmetric projector yields

$$\mathbb{P}_{sym}(PA) \coloneqq \begin{bmatrix} \mathbb{P}_s(P_1 \Omega_\times) & \frac{1}{2}(P_2 \Omega_\times - \Omega_\times P_2) \\ \frac{1}{2}(P_2^\top \Omega_\times - \Omega_\times P_2^\top) & \mathbb{P}_s(P_3 \Omega_\times) \end{bmatrix}.$$

Chapter 7

Simulations

In this chapter a comprehensive simulation study is carried out to compare the performance of the proposed geometric approximate minimum-energy (GAME) filter on $\mathrm{SO}(3)$ against some of the important attitude filtering methods in the literature.

There are many highly-regarded attitude estimation methods in the literature although there are not many references to clear implementation blueprints for these methods. As a result there is a lack of comparative studies in the literature that can point out the relative advantages and disadvantages of these methods compared against each other. In fact, many of the advanced attitude filtering methods are still published showing their performance gain against the basic extended Kalman filter (EKF) that is an outdated attitude filter with well known convergence issues (cf. [13]). Therefore, to address these gaps, the following main contributions are provided in this chapter.

- A short literature review highlights some of the mainstream attitude filtering methods that are used in robotic applications. Some of these methods are already proven to be outperformed by other methods in cited references and therefore are not included in our simulation experiments. An account of some of the major attitude filtering methods is provided including all the filters considered in the simulation study. We don't intend to produce a full survey of all the numerous attitude estimation methods in the literature but rather to provide a reference guide for some of the mainstream attitude filtering methods and the ideas behind them. For a relatively recent summary of attitude estimation methods refer to the survey [18].

- Simple numerical unit quaternion implementation of attitude filters is explained. Moreover, algorithm summaries are provided for each of the attitude filters that are selected to be implemented in the simulation study.

- A comprehensive simulation study is provided that compares the selected major attitude filters against the proposed GAME filter. The main comparison study considers measurement errors and initialization errors that are normally expected in attitude filtering for inexpensive commercial unmanned aerial vehicles (UAVs). Moreover, a separate simulation study is provided considering the initialization errors and measurement errors that are expected in a satel-

lite attitude filtering problem as well as considering the tuning issues of the attitude filters.

The methods included in the comparison study of this chapter consist of the proposed GAME filter, the multiplicative extended Kalman filter (MEKF [24]), the right-invariant extended Kalman filter (RIEKF that is also known as the generalized multiplicative extended Kalman filter GMEKF [27]), the unscented quaternion estimator (USQUE [15]) as well as the nonlinear complimentary attitude observer [32] which is referred to as the constant gain observer (CGO).

The remainder of the chapter is organized as follows. In Section 7.1 a summary of some of the important attitude filtering methods are provided that also explains the choice of methods included in the simulation study. Section 7.2 is to explain the numerical implementation of filters considered in simulation study. In particular, the discretization details of each method are provided separately. In Section 7.3 a UAV simulation setup is considered for which the performance of the GAME filter is compared against the other attitude filters considered. Section 7.5 concludes this chapter.

7.1 Attitude Filtering Methods

This section includes a brief review of some the most important attitude filtering methods that are employed in aerial robotics. In particular, the main ideas behind some attitude filters are explained and a number of these methods are selected against which the performance of proposed GAME filter is evaluated in simulations.

There are numerously many attitude filtering methods employed for different applications that make it impossible to provide a comprehensive account of all the attitude filtering methods. The simulation study of this chapter does not include the methods that have been shown to be outperformed by other methods in the literature. Some of these methods are included in Table 7.1. The simulation study is restricted to recursive methods due to their limited computations as compared to the static attitude determination methods. Attitude determination methods are based on the Wahba's problem [40] and sometimes involve repeated optimization for each measurement received. Sequential methods based on attitude determination (cf. [37] and [14]) have also been proposed. These methods are based on minimizing a cost functional on the measurement errors only as opposed to the classical optimal filtering cost that depends on the measurements errors as well as the initialization errors. The simulation study mostly covers methods that are based on the classical optimal filtering cost functional. The focus of the simulations is to only consider methods that are based on nonsingular parameterizations of the attitude matrix. The only exception is the USQUE that only uses a singular parametrization to represent the error quaternion and hence is hoped not encounter singularities when the error is small. This chapter also not covers any methods that require normalization or projection of the filter estimates to convert them to the correct attitude space. The rationale is that these operations might affect the optimality of the filter in an unsystematic fashion

that might be difficult to track and evaluate.

As was pointed out by the 2007 survey on nonlinear attitude filters [18], the Multiplicative Extended Kalman filter (MEKF) is the method of choice in many spacecraft attitude filtering applications. Crassidis *et. al* [18] concluded that "Many nonlinear filtering methods have been applied to the problem of spacecraft attitude determination in the past 25 years. This paper has provided a survey of the methods that its authors consider to be most promising. It remains the case, however, that the extended Kalman filter, especially in the form known as the multiplicative extended Kalman filter, remains the method of choice for the great majority of applications.". Therefore, a unit quaternion MEKF is an obvious benchmark that is choosen for the proposed GAME filter.

The continuous-time MEKF [24] comprises the same observer equations (9.9a) and (9.9b) as the proposed GAME filter. However, in contrast to the GAME filter, in the Riccati equations of the MEKF a curvature correction term and a geometric second order derivate of the output function (denoted by E in (9.10)) are not present. The idea behind the MEKF is to consider the true attitude state as the product of a reference quaternion and an error quaternion that represents the difference between the reference and the true attitudes. The error quaternion is parameterized by a three dimensional representation of attitude and is estimated using an EKF. The MEKF estimates the true attitude by multiplying the estimated error quaternion (converted back to a unit quaternion) and the reference quaternion. In order to avoid the redundancy of having to estimate both the reference quaternion and the error quaternion, the reference quaternion is chosen in a way that the error quaternion is the identity quaternion. Therefore, the MEKF directly calculates the reference quaternion as a unit quaternion estimate of the true attitude by implicitly running an EKF in the vector space of its angular velocity input.

In the case of attitude filtering, the MEKF is in fact a special case of the left invariant extended Kalam filter IEKF [8, 10]. The invariant extended Kalman filter modifies the EKF equations by using an invariant output error rather than a linear error and also by updating the gain using an invariant state error instead of a linear state error. The right invariant EKF (RIEKF [27]) or generalized MEKF (GMEKF) is the most favored invariant EKF and therefore is included in our simulations. The gains of the RIEKF stabilize on a wide range of trajectories and are expected to result in better convergence properties of the filter than the MEKF. The RIEKF is based on the assumption that the state and the output errors are configured in the inertial frame rather than configured in the body-fixed frame.

The unscented quaternion estimator (USQUE [15]) is an attitude filter based on the unscented filter (UF [34]) that has proven to work well in many applications. The UF uses a carefully chosen set of sigma points to approximate the probability distribution as opposed to the EKF that uses a linearization of the nonlinear equations. In a straightforward implementation of the UF the updated quaternion mean would be obtained by an averaging process which would not maintain the unit norm condition of the unit quaternion representing the attitude. This maybe avoided by USQUE [15] where a three-component attitude error is used to derive an unscented filter and the

resulting estimated error is converted back to unit quaternions and multiplied with the previously estimated quaternion to produce the attitude estimate. The hope is that the singularities would not occur since a parameterization of attitude is only used for the quaternion error that is supposed to be small. The USQUE is shown to outperform the EKF in simulations with the cost of more computations and tuning needed. In a recent paper [38], it was shown in simulations that the USQUE has similar estimation error compared to the MEKF although with a faster convergence rate. Therefore, the USQUE is also included in the simulation study of this chapter. There is a large class of nonlinear observers designed for attitude estimation (cf. [32]) that are also attractive methods to consider, as they are proven to produce asymptotically convergent estimates. The observer proposed in [32] is a special case of the GAME or the MEKF filter that uses carefully tuned constant gains as opposed to a filter that automatically updates the matrix gains using Riccati equations. In a special case of our follow up simulations, a constant gain observer is also tested against the proposed GAME filter.

Attitude Filters	state	Ref.	Compared Against	Comments
GAME	$SO(3)$ (Unit Quaternions in Simulations)	Chap. 4, 7	MEKF, USQUE, Constant Gain Observer	The GAME filter is a 2nd-order approximation to a minimum-energy filter derived directly on $SO(3)$ that estimates the gyro bias fast and is more robust to different noise levels with minimal tuning.
MEKF	Unit Quaternions	[24]	USQUE, SR-QCKF [38]	The MEKF estimates a unit quaternion by implicitly running an EKF in the vector space of its angular velocity input.
RIEKF (GMEKF)	Unit Quaternions	[27]	MEKF	RIEKF is a right-invariant construction of the EKF, by considering measurement noise modeled in the inertial frame. RIEKF has better convergence properties than the MEKF.
USQUE	Unit Quaternions	[15]	MEKF, SR-QCKF [38], EKF [15], BAF [12]	A three-component attitude error is used to derive an unscented filter and the resulting estimated error is converted back to unit quaternions and multiplied with the previously estimated quaternion to produce the filter's estimate.
BAF	Unit Quaternions	[12]	USQUE [12]	The BAF achieves comparable performance to the USQUE, with the computational costs of particle filtering
SR-QCKF	Normalized Quaternions	[38]	USQUE, MEKF [38]	The USQUE requires more computation than the SR-QCKF but outperforms it in mean square Error.
AEKF	Normalized Quaternions	[25]	MEKF	AEKF is conceptually simpler than the MEKF, but with higher computational cost. The MEKF is also preferred as it avoids the embedding errors.
CGO	Unit Quaternions	[32]		A carefully tuned constant gain is used with the same observer equations as in the MEKF or the GAME filter. It is very robust and asymptotically convergent with minimal computational load but requires exact tuning.
EKF	Normalized Quaternions	[6]	USQUE [15]	The EKF in its standard form is outperformed by the USQUE. The AEKF and the MEKF build up on the EKF to improve the performance.

Table 7.1: GAME filter: Geometric Approximate Minimum-Energy Filter, MEKF: Multiplicative Extended Kalman Filter,RIEKF: Right-Invariant Extended Kalman Filter, GMEKF: Generalized Multiplicative Extended Kalman Filter, SR-QCKF: Square-Root Quaternion Kalman Filter, USQUE: Unscented Quaternion Kalman Filter, BAF:Bootstrap Attitude Filter, AEKF:Additive Extended Kalman Filter, CGO: Constant Gain Observer, EKF:Extended Kalman Filter.

7.2 Numerical Implementation

The unit quaternion representation of a rotation is employed in this chapter for numerical implementation of the algorithms considered. Using unit quaternions rather than rotation matrices in numerical analysis yields more efficient and more robust numerical implementations due to the vector form of quaternions. Moreover, unit quaternions do not have the singularity issue that is associated with many other rotation representations. However, a unit quaternion is not a unique representation of a rotation. Nevertheless, since our filter derivation is done using rotation matrices non-uniqueness is not an issue for the proposed GAME filter.

A brief overview of unit quaternions and the algebra associated to them is provided in Appendix 9. In particular, a unit quaternion version of the attitude kinematics and the GAME filter are derived.

In order to numerically study and compare the filters in this chapter, discrete-time derivations of these continues-time filters are required. Discretization is also required for practical onboard implementations due to the discrete-time nature of the readings obtained from the attitude and angular velocity sensors. This is not a trivial task in attitude filtering (and similar problems) as the Lie group configuration of the underlying state space has to be preserved under any numerical calculation. Proper treatments of the numerical implementation issue include deriving a discrete version of the proposed GAME filter and the other competing methods or using Lie group variational (symplectic) integrators [2] to discretize the continuous-time differential state equations. Nevertheless, this thesis is to serve as a proof of concept of the advantage of minimum-energy filtering done directly on Lie groups of $\mathrm{SO}(3)$ and $\mathrm{SE}(3)$ as a systematic way of deriving approximate geometric filters. Therefore, the simulation study is restricted to the use of a simple Lie group Euler method where the time step is small enough, hence simulating a continuous time situation. The choice of simple numerical implementation along with a small time step serves well to the purpose of keeping the comparison simple without providing any numerical advantage to any of the competing attitude filtering methods.

The numerical integration of (9.4) is approximated by assuming that the simulation time step dt is small enough. Then, one can assume that Ω remains constant in every period of time $[kdt,\ (k+1)dt]$ for all $k \in \mathbb{N}$. Let us denote this value by Ω_k. Then the exact integration of (9.4) yields

$$q_{k+1} = \frac{1}{2}\exp(dtA(\Omega_k))q. \tag{7.1}$$

For the GAME filter, the numerical implementation of the quaternion equation (9.9a) is similar to Equation (7.1). The bias observer (9.9b) as well as the Riccati equations (9.9d) and (9.9e) can be implemented with a simple Euler method.

Note that when the measurements $\{y_i\}$ are received at a different frequency than the angular velocity measurements the continuous-discrete form of the EKF is usually employed for the numerical implementation of the MEKF [24]. However, observation with a different frequency are not considered in the following simulations and

hence the continuous-discrete implementation is not used.

Detailed implementations of the attitude kinematics and measurements as well as the methods compared in this chapter are given in the following tables.

Kinematics	$q(k+1) = \frac{1}{2}\exp(dtA(\Omega(k)))q(k)$, $q(0) = q_0$, $A(\Omega(k)) = \begin{bmatrix} 0 & -\Omega(k)^\top \\ \Omega(k) & -\Omega(k)_\times \end{bmatrix}$
Gyro Measurements	$u(k) = \Omega(k) + b(k) + B_\Omega v_\Omega(k)$, $Q_\Omega = B_\Omega B_\Omega'$
Bias Model	$b(k+1) = b(k) + dt[B_b v_b(k)]$, $Q_b = B_v B_v'$
Vector Measurements	$y_i(k) = \mathbf{p}^\dagger(q(k)^{-1} \otimes \mathbf{p}(\mathring{y}_i) \otimes q(k)) + D_i w_i(k)$, $R_i = D_i D_i'$, $\mathbf{p}(\mathring{y}_i) = \begin{bmatrix} 0 \\ \mathring{y}_i \end{bmatrix}$, $\mathbf{p}^\dagger(\mathbf{p}(\mathring{y}_i)) = \mathring{y}_i$

Table 7.2: Discrete Attitude Kinematics and Measurements

Attitude Observer	$\hat{q}(k+1) = \frac{1}{2}\exp(dtA[u(k) - \hat{b}(k) + P_a(k)l(k)])\hat{q}(k)$, $l(k) = \sum_i \hat{y}_i(k) \times (R_i^{-1}(\hat{y}_i(k) - y_i(k)))$, $\hat{y}_i(k) = \mathbf{p}^{\dagger}(\hat{q}(k)^{-1} \otimes \mathbf{p}(\mathring{y}_i) \otimes \hat{q}(k))$, $\hat{q}(0) = [1\ 0\ 0\ 0]^{\top}$
Bias Observer	$\hat{b}(k+1) = \hat{b}(k) + dt[P_c(k)^{\top} l(k)]$, $\hat{b}(0) = [0\ 0\ 0]^{\top}$,
Riccati Gains	$P_a(k+1) = P_a(k) + dt[Q_\Omega + 2\mathbb{P}_s[P_a(k)(u(k) - \hat{b}(k) - \frac{1}{2}P_a(k)l(k))_\times - P_c(k)] + P_a(k)(E(k) - S(k))P_a(k)]$, $P_c(k+1) = P_c(k) + dt[-(u(k) - \hat{b}(k) - \frac{1}{2}P_a(k)l(k))_\times P_c(k) + P_a(k)(E(k) - S(k))P_c(k) - P_b(k)]$, $P_b(k+1) = P_b(k) + dt[Q_b + P_c(k)(E(k) - S(k))P_c(k)]$, $S(k) = \sum_i (\hat{y}_i(k))_\times^{\top} R_i^{-1} (\hat{y}_i(k))_\times$, $E(k) = \text{trace}(C(k))I - C(k)$, $C(k) = \sum_i \mathbb{P}_s(R_i^{-1}(\hat{y}_i(k) - y_i(k))\hat{y}(k)_i^{\top})$,

Table 7.3: GAME Filter

Attitude Observer	$\hat{q}(k+1) = \frac{1}{2}\exp(dtA[u(k) - \hat{b}(k) + P_a(k)l(k)])\hat{q}(k)$, $l(k) = \sum_i \hat{y}_i(k) \times (R_i^{-1}(\hat{y}_i(k) - y_i(k)))$, $\hat{y}_i(k) = \mathbf{p}^{\dagger}(\hat{q}(k)^{-1} \otimes \mathbf{p}(\mathring{y}_i) \otimes \hat{q}(k))$, $\hat{q}(0) = [1\ 0\ 0\ 0]^{\top}$
Bias Observer	$\hat{b}(k+1) = \hat{b}(k) + dt[P_c(k)^{\top} l(k)]$, $\hat{b}(0) = [0\ 0\ 0]^{\top}$,
Riccati Gains	$P_a(k+1) = P_a(k) + dt[Q_\Omega + 2\mathbb{P}_s[P_a(k)(u(k) - \hat{b}(k))_\times - P_c(k)] - P_a(k)S(k)P_a(k)]$, $P_c(k+1) = P_c(k) + dt[-(u(k) - \hat{b}(k))_\times P_c(k) - P_a(k)S(k)P_c(k) - P_b(k)]$, $P_b(k+1) = P_b(k) + dt[Q_b - P_c(k)S(k)P_c(k)]$, $S(k) = \sum_i (\hat{y}_i(k))_\times^{\top} R_i^{-1} (\hat{y}_i(k))_\times$,

Table 7.4: MEKF

Attitude Observer	$\hat{q}(k+1) = \frac{1}{2}\exp(dtA[u(k) - \hat{b}(k) + P_a(k)l(k)])\hat{q}(k)$, $l(k) = \sum_i \mathring{y}_i \times (R_i^{-1}(\mathring{y}_i - \hat{y}_i(k)))$, $\hat{y}_i(k) = \mathbf{p}^{\dagger}(\hat{q}(k) \otimes \mathbf{p}(y_i(k)) \otimes \hat{q}^{-1}(k))$, $\hat{q}(0) = [1\ 0\ 0\ 0]^{\top}$
Bias Observer	$\hat{b}(k+1) = \hat{b}(k) + dt[\hat{q}(k)^{-1} \otimes \mathbf{p}(P_c(k)^{\top} l(k)) \otimes \hat{q}(k)]$, $\hat{b}(0) = [0\ 0\ 0]^{\top}$,
Riccati Gains	$P_a(k+1) = P_a(k) + dt[Q_\Omega - 2\mathbb{P}_s[P_c(k)] - P_a(k)S(k)P_a(k)]$, $P_c(k+1) = P_c(k) + dt[-P_c(k)\hat{q}(k) \otimes \mathbf{p}((u(k) - \hat{b}(k))_\times) \otimes \hat{q}^{-1}(k) - P_a(k)S(k)P_c(k) - P_b(k)]$, $P_b(k+1) = P_b(k) + dt[2\mathbb{P}_s(\hat{q}(k) \otimes \mathbf{p}((u(k) - \hat{b}(k))_\times) \otimes \hat{q}^{-1}(k)P_b(k) + Q_b - P_c(k)S(k)P_c(k)]$, $S(k) = \sum_i (\mathring{y}_i(k))_\times^{\top} R_i^{-1} (\mathring{y}_i(k))_\times$,

Table 7.5: RIEKF (GMEKF)

Note that the formulation provided here for the RIEKF is different to the one given in the reference [27] in two aspects. First, the state error in [27] is modeled two times larger, giving the filter formulation a factor of 2 higher gain. Although this results in a faster transient response, also causes the asymptotic response of the RIEKF to be two times more noisy. In order to be consistent in our comparison this factor difference has been removed from the RIEKF. We have included a simulation instance that shows this effect in the original formulation of the RIEKF (see Figure 7.6). Secondly, there seems to be a factor of $\frac{1}{2}$ inconsistency in the A matrix calculation of the RIEKF [27] that leads to occasional singularities in the simulation results of the RIEKF. This has also been corrected in our simulations. For further details, see the proof in Section 9.12 of the Appendix. Also note that, the RIEKF is derived based on considering the state and the output errors in the inertial frame that is different to our formulation that models errors in the body-fixed frame. Nevertheless, the RIEKF is claimed to have better convergence properties than the MEKF and is even named the generalized MEKF (see [27]) and hence is compared against the rest of the filters in our simulations with errors generated in the body-fixed frame as is the case for the MEKF.

Initial Conditions	$\hat{q}(0) = \hat{q}_0,\ \hat{b}(0) = \hat{b}_0,\ P(0) = P_0 \in \mathbb{R}^{6\times 6},$ $\hat{x}^+(0) = [\mathbf{0}^\top\ \hat{b}(0)^\top]^\top,$
Tuning	$a = 1,\ f = 4,\ \lambda = 1,$
Discrete Q_k	$Q_k = \frac{dt}{2}\begin{bmatrix} Q_\Omega - \frac{dt^2}{6}Q_b & 0_{3\times 3} \\ 0_{3\times 3} & Q_b \end{bmatrix},$
Sigma Points	$\sigma_k \leftarrow 2n$ columns from $\pm\sqrt{(n+\lambda)[P_k^+ + Q_k]},$ $\mathcal{X}_k(0) = \hat{x}_k^+,\ \mathcal{X}_k(i) = \sigma_k(i) + \hat{x}_k^+,$
Error Quaternions	$\delta q_{4_k}^+(i) = \frac{-a\|\mathcal{X}_k^{\delta p}(i)\|^2 + f\sqrt{f^2+(1-a^2)\|\mathcal{X}_k^{\delta p}(i)\|^2}}{f^2+\|\mathcal{X}_k^{\delta p}(i)\|^2},$ $\delta\varrho_k^+(i) = f^{-1}[a + \delta q_{4_k}^+(i)]\mathcal{X}_k^{\delta p}(i),$ $\delta q_k^+(i) = [\delta q_{4_k}^+(i)\ \delta\varrho_k^{+^\top}(i)]^\top,\ i = 1, 2\cdots, 12$
Sigma Quaternions	$\hat{q}_k^+(0) = \hat{q}_k^+,$ $\hat{q}_k^+(i) = \delta q_k^+(i) \otimes \hat{q}_k^+$
Propagation	$\hat{q}_{k+1}^-(i) = \frac{1}{2}\exp(dtA[u(k) - \mathcal{X}_k^{\hat{b}}(i)])\hat{q}_k^+(i), i = 0, 1, \cdots, 12,$ $\delta q_{k+1}^-(i) = \hat{q}_{k+1}^-(i) \otimes (\hat{q}_{k+1}^-(0))^{-1},\ \delta q_{k+1}^-(0) = [1\ 0\ 0\ 0]^\top$ $[\delta q_{4_{k+1}}^-(i)\ \delta\varrho_{k+1}^{-^\top}(i)]^\top = \delta q_{k+1}^-(i)$ $\mathcal{X}_{k+1}^{\delta p}(i) = f\frac{\delta\varrho_{k+1}^-(i)}{a+\delta q_{4_{k+1}}^-(i)},\ \mathcal{X}_{k+1}^{\delta p}(0) = \mathbf{0},$ $\mathcal{X}_{k+1}^{\hat{b}}(i) = \mathcal{X}_k^{\hat{b}}(i),$
Prediction	$\hat{x}_{k+1}^- = \frac{1}{n+\lambda}\left\{\lambda\mathcal{X}_{k+1}(0) + \frac{1}{2}\sum_{i=1}^{2n}\mathcal{X}_{k+1}(i)\right\},$ $P_{k+1}^- = \frac{1}{n+\lambda}\left\{\lambda[\mathcal{X}_{k+1}(0) - \hat{x}_{k+1}^-][\mathcal{X}_{k+1}(0) - \hat{x}_{k+1}^-]^\top\right.$ $\left.+\frac{1}{2}\sum_{i=1}^{2n}[\mathcal{X}_{k+1}(i) - \hat{x}_{k+1}^-][\mathcal{X}_{k+1}(i) - \hat{x}_{k+1}^-]^\top\right\} + Q_k$
Mean Observations	$\gamma_{k+1}(i) = \begin{bmatrix} \mathbf{p}^\dagger(\hat{q}_{k+1}^-(i)^{-1} \otimes \mathbf{p}(\mathring{y}_1) \otimes \hat{q}_{k+1}^-(i)) \\ \mathbf{p}^\dagger(\hat{q}_{k+1}^-(i)^{-1} \otimes \mathbf{p}(\mathring{y}_2) \otimes \hat{q}_{k+1}^-(i)) \\ \vdots \end{bmatrix}$ $\hat{y}_{k+1}^- = \frac{1}{n+\lambda}\left\{\lambda\gamma_{k+1}(0) + \frac{1}{2}\sum_{i=1}^{2n}\gamma_{k+1}(i)\right\}$
Covariance Update	$P_{k+1}^{yy} = \frac{1}{n+\lambda}\left\{\lambda[\gamma_{k+1}(0) - \hat{y}_{k+1}^-][\gamma_{k+1}(0) - \hat{y}_{k+1}^-]^\top\right.$ $\left.+\frac{1}{2}\sum_{i=1}^{2n}[\gamma_{k+1}(i) - \hat{y}_{k+1}^-][\gamma_{k+1}(i) - \hat{y}_{k+1}^-]^\top\right\},$ $P_{k+1}^{\nu\nu} = P_{k+1}^{yy} + R_{k+1},$ $P_{k+1}^{xy} = \frac{1}{n+\lambda}\left\{\lambda[\mathcal{X}_{k+1}(0) - \hat{x}_{k+1}^-][\gamma_{k+1}(0) - \hat{y}_{k+1}^-]^\top\right.$ $\left.+\frac{1}{2}\sum_{i=1}^{2n}[\mathcal{X}_{k+1}(i) - \hat{x}_{k+1}^-][\gamma_{k+1}(i) - \hat{y}_{k+1}^-]^\top\right\}$
Update	$\hat{x}_{k+1}^+ = \hat{x}_{k+1}^- + P_{k+1}^{xy}(P_{k+1}^{\nu\nu})^{-1}(y_{k+1} - \hat{y}_{k+1}),$ $P_{k+1}^+ = P_{k+1}^- - P_{k+1}^{xy}(P_{k+1}^{\nu\nu})^{-\top}P_{k+1}^{xy}$
Quaternion Update	$\hat{x}_{k+1}^+ = [\delta p^\top\ \hat{b}^{+^\top}]^\top$ $\delta q_{4_{k+1}}^+ = \frac{-a\|\delta p\|^2 + f\sqrt{f^2+(1-a^2)\|\delta p\|^2}}{f^2+\|\delta p\|^2},$ $\delta\varrho_{k+1}^+ = f^{-1}[a + \delta q_{4_{k+1}}^+]\delta p,$ $\delta q_{k+1}^+ = [\delta q_{4_{k+1}}^+\ \delta\varrho_{k+1}^{+^\top}]^\top,$ $\hat{q}_{k+1}^+ = \delta q_{k+1}^+ \otimes \hat{q}_{k+1}^-$

Table 7.6: USQUE

Attitude Observer	$\hat{q}(k+1) = \frac{1}{2}\exp(dtA[u(k) - \hat{b}(k) + k_P l(k)])\hat{q}(k)$, $l(k) = \sum_i y_i(k) \times \hat{y}_i(k)$, $\hat{y}_i(k) = \mathbf{p}^{\dagger}(\hat{q}(k)^{-1} \otimes \mathbf{p}(\mathring{y}_i) \otimes \hat{q}(k))$, $\hat{q}(0) = [1\ 0\ 0\ 0]^{\top}$
Bias Observer	$\hat{b}(k+1) = \hat{b}(k) - dt[k_I l(k)]$, $\hat{b}(0) = [0\ 0\ 0]^{\top}$

Table 7.7: CGO

7.3 Methodology

In this section, multiple simulated experiments are presented that compare the filtering methods considered in Section 7.2.

7.3.1 Case 1: Measurement Errors Expected from Low-Cost UAV Sensors

The first experiment is simulating attitude filtering of a low cost unmanned aerial vehicle (UAV) system for which the measurement errors are relatively large. It is also assumed that the rotation and the bias initialization errors are large, as is the case when using low cost MEMS gyros such as the popular InvenSense MPU-3000 family. The simulation parameters are summarized in Table 7.8. The GAME filter 7.3 is compared against the MEKF 7.4, the RIEKF 7.5, the USQUE 7.6 and the CGO 7.7 that are explained in detail in Section 7.2.

Simulated attitude kinematics and measurements (see Table 7.2) are considered with the following parameters that are also summarized in Table 7.8. A sinusoidal input $\Omega = [\sin(\frac{2\pi}{15}t)\ \ -\sin(\frac{2\pi}{18}t + \pi/20)\ \ \cos(\frac{2\pi}{17}t)]$ drives the true trajectory q. The input measurement errors v and v_b are Gaussian zero mean random processes with unit standard deviation. The coefficient matrix B is chosen so that the signal Bv has a standard deviation of 25 degrees per 'second'. The bias variation is adjusted by B_b such that $B_b v_b$ has a standard deviation of 0.1 degrees per 'second' squared. The system is initialized with a unit quaternion representing a rotation with standard deviation of $std_{q_0} = 60$ degrees and an initial bias with standard deviation of $std_{b_0} =$ 20 degrees per 'second'. We assume that two orthogonal unit reference vectors are available. We also consider Gaussian zero mean measurement noise signals w_i with unit standard deviations. The coefficient matrices D_i are chosen so that the signals $D_i w_i$ have standard deviations of 30 degrees. Although the two filters do not have access to the noise signals v_Ω, v_b and w_i themselves, they have access to the matrices $Q_\Omega = BB^{\top}$, $Q_b = B_b B_b^{\top}$ and $R_i = D_i D_i^{\top}$. The filters are simulated using zero

initial bias estimates and using the identity unit quaternion as their initial quaternion estimate.

The following filter initializations are considered that are also summarized in Table 7.9. The initial quaternion and bias gain matrices of the USQUE are chosen according to the variance of the system's initial quaternion in radians $P_a(0) = std_{q_0}^2 I_{3\times3}$ and the variance of the system's initial bias in radians per 'seconds' $P_b(0) = std_{b_0}^2 I_{3\times3}$. The initial quaternion and bias gain matrices of the GAME filter, the MEKF and the RIEKF are chosen according to the inverse variance of the system's initial quaternion in radians $P_a(0) = \frac{1}{std_{q_0}^2} I_{3\times3}$ and the inverse variance of the system's initial bias in radians per 'seconds' $P_b(0) = \frac{1}{std_{b_0}^2} I_{3\times3}$ as these filters are in the information form. The coupling initial gain is considered as the zero matrix $P_c(0) = 0_{3\times3}$ for all the filters. The CGO is initialized with $k_p = 1$ and $k_I = 0.3$ as in [32].

Time Step	0.001 (s)
Simulation Time	50 (s)
Angle of Rotation Initialization Error	$\mathcal{N} \sim (0, 60^2)^\circ$
Bias Initialization Error	$\mathcal{N} \sim (0, 20^2)\frac{^\circ}{s}$
Reference Directions	$\mathring{y}_1 = [1\ 0\ 0]$, $\mathring{y}_2 = [0\ 1\ 0]$
Input signal	$\Omega = [\sin(\frac{2\pi}{15}t)\ \ -\sin(\frac{2\pi}{18}t + \pi/20)\ \ \cos(\frac{2\pi}{17}t)]\frac{rad}{s}$
Input error $B_\Omega v_\Omega$	$\mathcal{N} \sim (0, 25^2)\frac{^\circ}{s}$
Bias Variation $B_b v_b$	$\mathcal{N} \sim (0, 0.1^2)\frac{^\circ}{s^2}$
Measurement error $D_i w_i$	$\mathcal{N} \sim (0, 30^2)^\circ$

Table 7.8: Simulation Parameters for the UAV Situation Case 1

USQUE	$P_a(0) = std_{q_0}^2 I_{3\times3}$, $P_b(0) = std_{b_0}^2 I_{3\times3}$, $P_c(0) = 0_{3\times3}$
GAME, MEKF, RIEKF	$P_a(0) = \frac{1}{std_{q_0}^2} I_{3\times3}$, $P_b(0) = \frac{1}{std_{b_0}^2} I_{3\times3}$, $P_c(0) = 0_{3\times3}$
CGO	$k_p = 1$, $k_I = 0.3$

Table 7.9: Initial Filter Gain Matrices for the UAV Situation Case 1

7.3.2 Case 2: Measurement Errors Expected in a Satellite

In this experiment much smaller measurement error signals are considered as is the case for a satellite attitude filtering problem. The simulation parameters are according to the reference [14] and are described in Table 7.10. Note that the angular velocity input of the attitude kinematics is also considered with a much smaller frequency as the movement of a satellite is restricted to an earth orbit.

The initial gains of the filters are chosen according to Table 7.11. Note that these values are not exactly according to the statistics of the initialization errors of the system, as was the case in our previous experiment. This is to avoid singularities that are due to the fact that the numerical values of some the parameters of the simulation are too small and close to the computational limits of the MATLAB programming platform.

Time Step	0.001 (s)
Simulation Time	50 (s)
Angle of Rotation Initialization Error	$\mathcal{N} \sim (0, 60^2)^\circ$
Bias Initialization Error	$\mathcal{N} \sim (0, 20^2)\frac{^\circ}{s}$
Reference Directions	$\mathring{y}_1 = [1\ 0\ 0]$, $\mathring{y}_2 = [0\ 1\ 0]$
Input signal	$\Omega = \sin(\frac{2\pi}{150}t)[1\ \ -1\ \ 1]\frac{^\circ}{s}$
Input error $B_\Omega v_\Omega$	$\mathcal{N} \sim (0, 0.31623^2)\frac{\mu\ rad}{s}$
Bias Variation $B_b v_b$	$\mathcal{N} \sim (0, 0.031623^2)\frac{n\ rad}{s}$
Measurement error $D_i w_i$	$\mathcal{N} \sim (0, 1^2)^\circ$

Table 7.10: Simulation parameters for a satellite situation

USQUE	$P_a(0) = std_{q_0}^2 I_{3\times3},\ P_b(0) = std_{b_0}^2 I_{3\times3},\ P_c(0) = 0_{3\times3}$
GAME, MEKF, RIEKF	$P_a(0) = \frac{10^{-1}}{std_{q_0}^2} I_{3\times3},\ P_b(0) = \frac{10^{-9}}{std_{b_0}^2} I_{3\times3},\ P_c(0) = 0_{3\times3}$
CGO	$k_p = 10,\ k_I = 2$

Table 7.11: Initial Filter Gain Matrices for the Satellite Case 2

7.4 Results

Figures 7.1 and 7.3 show the performance of the GAME filter compared against the MEKF, the RIEKF, the USQUE and the CGO in the Case 1 experiment. We have performed a Monte-Carlo simulation and the RMS of the estimation errors of the two filters are demonstrated for 100 repeats.

Figures 7.1 and the zoomed version 7.2 indicate that the RMS of the rotation angle estimation error of the proposed GAME filter rapidly converges towards zero in the transient and also maintains the lowest error compared to the rest of the filters in the asymptotic response. Figure 7.3 shows that the GAME filter also has the lowest asymptotic bias estimation error compared to the bias estimation error of all the other filters.

Note that the initial pick in the angle error of the filters, GAME, MEKF and RIEKF is associated to the period that the bias estimates of these filters are not accurate enough yet. The adaptive nature of these filters is allowing a higher uncertainty in the angle estimates until a reasonable bias estimate is obtained which is then used to achieve an accurate asymptotic angle estimate. The bias error of these filters in Figure 7.3 is showing the peaking phenomenon that is also seen in a high-gain observer. This is not the case for the USQUE which has the fastest angle estimation but the slowest bias estimation. This is due to the fact that the USQUE is setting a high gain for its angle observer and a low gain for its bias observer that leads to the amplified noise on the angle estimation error of the USQUE in Figure 7.1. The CGO on the other hand is not an adaptive filter but it has an asymptotically convergent estimation error that is a priori adjusted through the gains k_p and k_I.

Also note that the RIEKF is in fact outperforming the MEKF as was noted in [27] too. It is interesting that the CGO has the second lowest estimation error with the lowest computational cost. Of course the downside of the CGO is that it needs exact tuning depending on the information about the true attitude trajectory that might not always be available a priori. The USQUE has the fastest angle convergence to a relatively low error. However, the noisy asymptotic performance (which might be due to lack of complicated tuning in our experiments), very slow bias estimation and the heavy computational cost of the USQUE compared to the other filters considered makes USQUE not desirable for the UAV application considered. This argument is further investigated in the following experiment.

7.4.1 Gain Scaling

One can choose different gain scalings for a particular filter. A higher scaled gain can result in faster convergence of a filter with the disadvantage of increasing the asymptotic estimation error. Depending on the application, one has to trade-off between the transient and the asymptotic performance of a filter. The following two examples are demonstrations of this trade-off seen in the results above.

As was apparent in Figures 7.1 and 7.3, the USQUE is inherently using a higher angle gain than the other filters. In fact, zooming into the asymptotic angle estima-

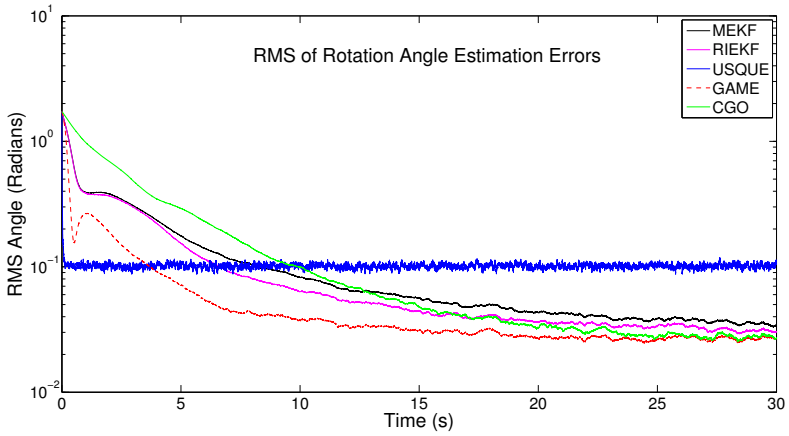

Figure 7.1: Case 1: The RMS of the estimation error in angle of rotations for a UAV simulation setup. Note that the angle axis is in logarithmic scale.

tion error graph of the USQUE, it is apparent that the estimation error is approximately 30 times lager than the estimation error of the other filters (See Figure 7.4). Next, this hypothesis is put to experiment comparing the USQUE with a version of the GAME filter that has a factor of 30 multiplying its gain P_a. As can be seen in Figure 7.4 the estimation errors of the two filters are now almost identical, confirming that the USQUE algorithm is rendering an undesirable scaling in its angle gain P_a that, although it results in a very fast angle estimation also results in a noisy asymptotic estimation error. We have tried to account for this effect in the USQUE algorithm by means of simple tuning. However, due to the involved nature of this algorithm 7.6 it is unclear how to provide a fix. On the other hand note that the bias estimation of the GAME filter is still much faster than that of the USQUE indicating the advantage of the GAME filter over the USQUE even in this case.

As was mentioned in Section 7.2, the original formulation of the RIEKF [27] has an inconsistency as well as a factor of 2 in the system model different to the model considered in the GAME filter and the MEKF. As a result, the original RIEKF has a larger gain than the considered RIEKF 7.5. This is investigated in the following simulation comparing the two formulations of the RIEKF. As can be seen in Figure 7.6, the original RIEKF has a faster decaying convergence error. However the asymptotic error of the original RIEKF is approximately two times more noisy than that of the considered RIEKF 7.5, confirming the gain difference of the two filters.

7.4.2 Case 2

Figures 7.7 and 7.8 show the performance of the GAME filter compared against the MEKF, the RIEKF, the USQUE and the CGO in the Case 2 experiment. Note that the figures shown are due to a single repeat of an experiment that is typical to the results seen in more repeats. In this case the small frequency of the angular velocity input leads to a slow dynamics of the angle trajectory. Due to this slow dynamics

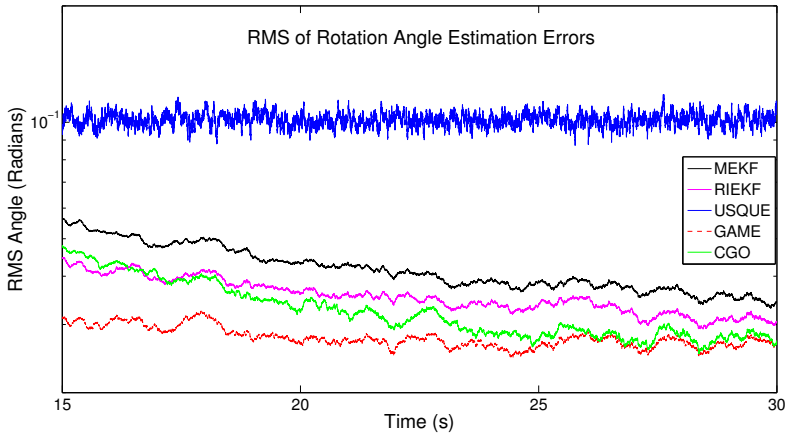

Figure 7.2: Case 1: The RMS of the estimation error in angle of rotations for a UAV simulation setup. Zoomed on the asymptotic error of the GAME filter, the MEKF and the RIEKF. Note that the angle axis is in logarithmic scale.

and also due to the small measurement errors considered, the estimation errors of all the filters converge towards zero rapidly. The GAME filter outperforms the rest of the filters in achieving the lowest asymptotic estimation error. The USQUE converges very fast although its asymptotic estimation error is noisy as was the case in the UAV experiment.

7.5 Conclusions

In conclusion, the geometric approximate minimum-energy (GAME) filter proves to be a very robust filter both in situations with large measurement errors and fast attitude dynamics, such as the case of a low cost UAV, and also in a situation with small measurement errors and slow attitude dynamics such as in the case of a satellite. In fact in both cases, it was shown in the previous section that the GAME filter outperforms the state-of-the-art attitude filters such as the multiplicative extended Kalman filter MEKF, the right-invariant extended Kalman filter RIEKF, the unscented quaternion estimator USQUE and the constant gain observer CGO.

The USQUE proves to be very fast in angle estimation but on the other hand very slow in estimating the gyro bias. The asymptotic angle estimation error of the USQUE is very noisy due the high gain of the angle error. Also the computational cost of the USQUE proves to be much higher than the other filters considered.

The CGO yields desirable low estimation errors with minimal computational cost. However, the gains of the CGO need to be tuned a priori. Also there is a trade-off between the speed of convergence and the asymptotic performance of the CGO that needs to be tuned using the constant gains. This could be a complicated process for the CGO whereas the GAME filter automatically performs this trade-off for each situation.

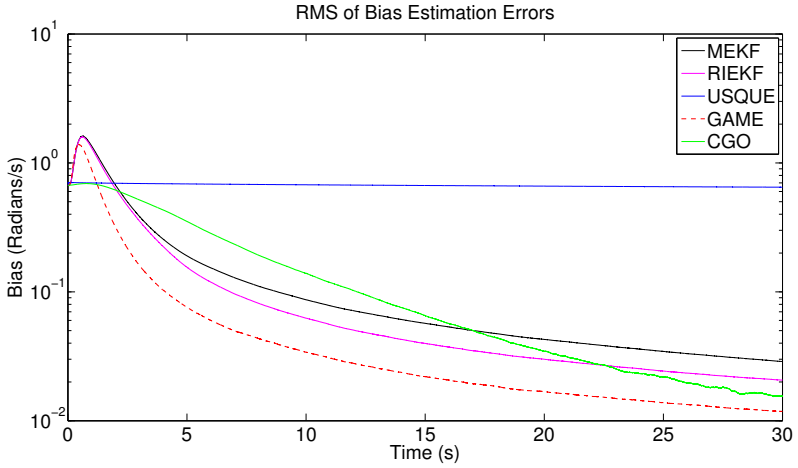

Figure 7.3: Case 1: The RMS of the bias estimation error for a UAV simulation setup. Note that the bias axis is in logarithmic scale.

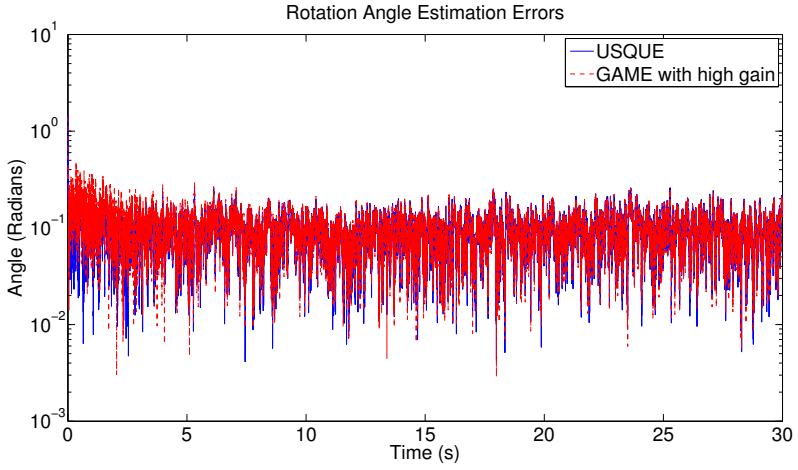

Figure 7.4: Case 1: The USQUE is compared against the GAME filter when the angle gain of the GAME P_a is multiplied by 30. Note that the angle axis is in logarithmic scale.

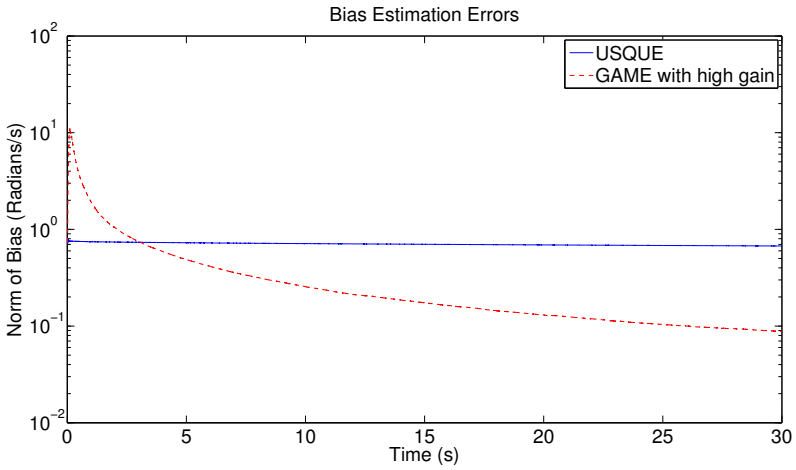

Figure 7.5: Case 1: The USQUE is compared against the GAME filter when the angle gain of the GAME P_a is multiplied by 30. Note that the bias axis is in logarithmic scale.

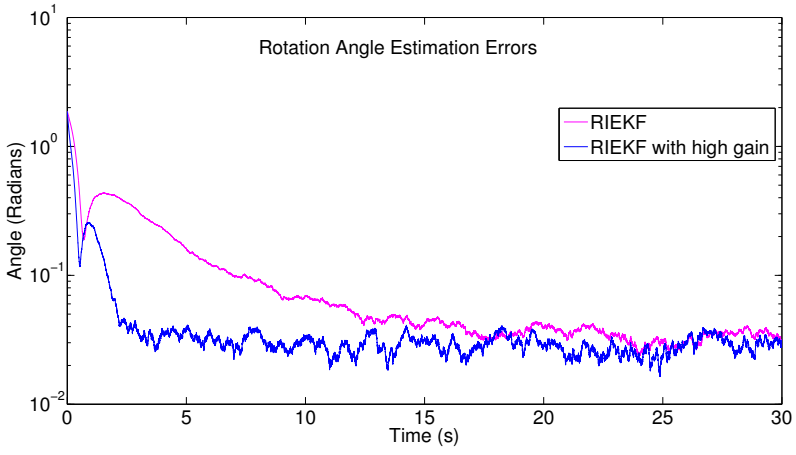

Figure 7.6: Case 1: The gain difference between the RIEKF in [27] and the RIEKF 7.5. Note that the angle axis is in logarithmic scale.

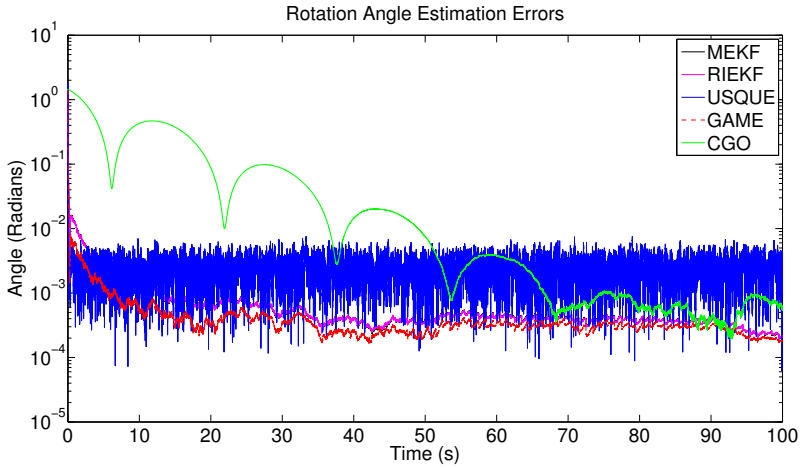

Figure 7.7: Case 2: The estimation error in angle of rotations for a satellite simulation setup. Note that the angle axis is in logarithmic scale.

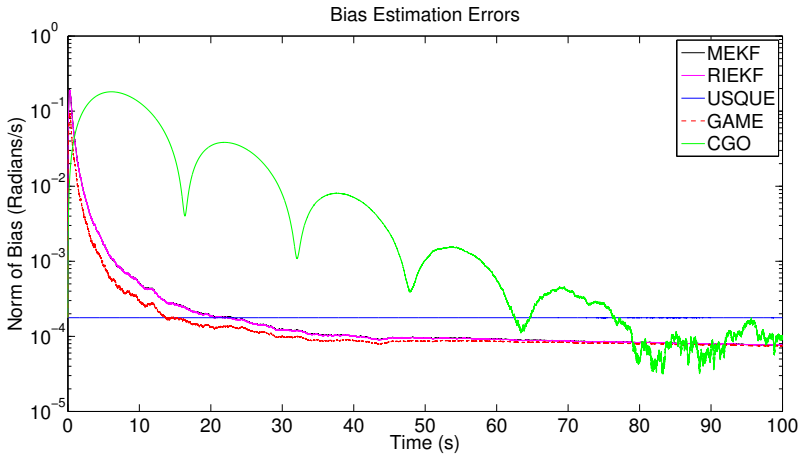

Figure 7.8: Case 2: The bias estimation error for a satellite simulation setup. Note that the bias axis is in logarithmic scale.

Chapter 8

Conclusion

In this thesis the problem of attitude filtering was considered on the Lie group $\mathrm{SO}(3)$. A nonlinear deterministic minimum-energy filtering approach was adapted to the Lie group $\mathrm{SO}(3)$ to derive a geometric approximate minimum-energy (GAME) attitude filter. This approach taken allowed systematic and complete derivation of the GAME on $\mathrm{SO}(3)$ in contrast to many of the competing attitude filtering methods that are based on un-systematic modifications to the well-known extended Kalman filter (EKF) or the unscented Kalman filters.

In simulations, the proposed GAME filter was shown to outperform state-of-the-art attitude filters such as the multiplicative extended Kalman filter (MEKF), the right-invariant extended Kalman filter (RIEKF), the unscented quaternion estimator (USQUE) and the constant gain nonlinear observer (CGO). Discretized unit quaternion versions of all the considered filters were provided and simulated in the simulations Chapter 7. There are certainly many more attitude filters in the literature that either have been shown to be outperformed by the aforementioned methods or are based on different design strategies. Some of these methods are reviewed in the simulations Chapter.

The superior performance of the proposed GAME filter in simulations was further supported with a least squares analysis in Chapter 5. It was shown that the distance to optimality of the GAME filter is numerically quantified by an upper bound on the difference between the cost that the GAME filter attains in comparison with a minimum-energy cost 5. The upper bound is decreasing in the estimation error and is shown to be small in simulations.

Furthermore, the method taken proved to be helpful for deriving minimum-energy filtering based methods on other Lie groups in Chapter 6. In particular, problems such as attitude filtering around one axis modelled on the unit circle S^1 and the special orthogonal group $\mathrm{SO}(2)$, attitude and gyro bias filtering $\mathrm{SO}(2) \times \mathbb{R}$ and $\mathrm{SO}(3) \times \mathbb{R}^3$ and pose filtering on the special Euclidean group $\mathrm{SE}(3)$ were tackled in Chapter 6.

8.1 Future Work

Possible future directions of this research include but are not restricted to

- Minimum-energy filtering on general Lie groups.
- Considering both the kinematic and the dynamic models on Lie groups.
- Attitude filtering using only one reference direction. As was observed in the simulation studies of this work, the GAME filter needs to have access to at least two vector direction in order to yield desirable low estimation errors. It would be interesting to investigate this phenomenon using convergence and observability analysis of the problem.
- Stability analysis of the proposed GAME filters using Lyapunov type approaches.
- Facilitating practical onboard implementation by providing discrete versions of the proposed filters along with using variational numerical integration methods that preserve the geometric properties of these filters.

Appendix

9.1 Unit Quaternion Representation

In this section the unit quaternion representation of rotations is introduced. Using unit quaternions in numerical analysis yields more efficient and more robust numerical implementations due to the vector form of quaternions.

A unit quaternion belongs to the set

$$\mathbb{Q} = \left\{ q = \begin{pmatrix} s \in \mathbb{R} \\ v \in \mathbb{R}^3 \end{pmatrix} \in \mathbb{R}^4 : \|q\| = 1 \right\}. \tag{9.1}$$

The set $\mathbb{Q}$ is a group under the operation

$$q_1 \otimes q_2 = \begin{pmatrix} s_1 s_2 - v_1^\top v_2 \\ s_1 v_2 + s_2 v_1 + v_1 \times v_2 \end{pmatrix}, \tag{9.2}$$

with identity element $\mathbf{1} = (1,\ 0,\ 0,\ 0)^\top$ and inverse $q^{-1} = (s,\ -v)^\top$. The quaternion $q = (s,\ v)^\top$ is given by a rotation $X \in \mathrm{SO}(3)$ through

$$X = I_3 + 2sv_\times + 2v_\times^2. \tag{9.3}$$

The attitude kinematics $\dot{X} = X\Omega_\times$, in the unit quaternions form is

$$\dot{q} = \frac{1}{2} A(\Omega) q, \tag{9.4}$$

where $\Omega \in \mathbb{R}^3$ and for $\gamma \in \mathbb{R}^3$

$$A(\gamma) \coloneqq \begin{bmatrix} 0 & -\gamma^\top \\ \gamma & -\gamma_\times \end{bmatrix}. \tag{9.5}$$

Note that the vectorial measurements $\{y_i\}$, that are given from $y_i = X^\top \mathring{y}_i + D_i w_i$, are equivalently given from the following model with the unit quaternion q representation of X.

$$y_i = q^{-1} \otimes \mathbf{p}(\mathring{y}_i) \otimes q + D_i w_i, \tag{9.6}$$

where for all $\gamma \in \mathbb{R}^3$

$$\mathbf{p}(\gamma) = \begin{bmatrix} 0 \\ \gamma \end{bmatrix}, \tag{9.7}$$

and conversely

$$\mathbf{p}^{\dagger}(\mathbf{p}(\gamma)) = \gamma. \tag{9.8}$$

9.2 The GAME Filter in Unit Quaternions

The notation introduced in the previous section can now be employed to provide a unit quaternion formulation of the proposed GAME filter. Note that quaternions are known to have a non-uniqueness issue in representing the rotations. However, this issue does not apply to the GAME filter that is primarily derived using rotations in SO(3). The following equations provide a unit quaternion representation of the GAME filter.

$$\dot{\hat{q}} = \frac{1}{2} A \left(u - \hat{b} - P_a l \right) \hat{q}, \tag{9.9a}$$

where $\hat{b}$ is the estimate of the bias b given from

$$\dot{\hat{b}} = P_c^{\top} l, \tag{9.9b}$$

where the innovation term l is defined as

$$l \coloneqq \sum_i (R_i^{-1}(\hat{y}_i - y_i)) \times \hat{y}_i. \tag{9.9c}$$

The gains P_a and P_c are updated from the following equations.

$$\begin{aligned} \dot{P}_a &= Q_\Omega + 2\mathbb{P}_s(P_a(2(u - \hat{b}) - P_a l)_\times) + P_a(E - S)P_a - P_c^{\top} - P_c, \\ \dot{P}_c &= -(u - \hat{b} - P_a l)_\times P_c + P_a(E - S)P_c - P_b, \end{aligned} \tag{9.9d}$$

where the gain P_b is given from

$$\dot{P}_b = Q_b + P_c(E - S)P_c. \tag{9.9e}$$

The initial conditions are given from $\hat{b}(0) = 0$, $\hat{q}(0) = \mathbf{1}$ and $P_a(0) = (\text{trace}(K_{X_0})I - K_{X_0})^{-1}$ where K_{X_0} is a known variable from the cost function. The vector $\hat{y} = \hat{q}^{-1} \otimes \mathbf{p}(\mathring{y}_i) \otimes \hat{q}$ is given similar to (9.6) and the operator $\mathbb{P}_s$ is a symmetric projector defined in (3.1). Note that the signals E and S are defined as

$$S \coloneqq \sum_i (\hat{y}_i)_\times^{\top} R_i^{-1} (\hat{y}_i)_\times, \; E \coloneqq \text{trace}(C) I - C, \; C \coloneqq \sum_i \mathbb{P}_s(R_i^{-1}(\hat{y} - y_i)\hat{y}_i^{\top}). \tag{9.10}$$

Recall that the matrices $Q_\Omega \coloneqq BB^{\top}$, $Q_b \coloneqq B_b B_b^{\top}$ and $R_i \coloneqq D_i D_i^{\top}$ are known from the measurement models.

9.3 The RIEKF

The RIEKF formulation considers the quaternion system model

$$\begin{cases} \dot{q} = \frac{1}{2} q \otimes \Omega, \\ u = \Omega - 2q^{-1} \otimes (B_\Omega v_\Omega) \otimes q + b, \\ \dot{b} = q^{-1} \otimes (B_B v_b) \otimes q, \\ y_i = q^{-1} \otimes (\mathring{y}_i + D_i w_i) \otimes q. \end{cases} \tag{9.11}$$

Note that the state and the out errors are modelled in the inertial frame which is different to the conventional modelling of errors in the body-fixed frame. The RIEKF then is

$$\begin{cases} \dot{\hat{q}} = \frac{1}{2} \hat{q} \otimes (u - \hat{b} + 2\hat{q}^{-1} \otimes (\sum_i K_q(\mathring{y}_i - \hat{y}_i) \otimes \hat{q}), \\ \hat{y}_i = \hat{q} \otimes (y_i) \otimes \hat{q}^{-1}, \\ \dot{\hat{b}} = \hat{q}^{-1} \otimes (\sum_i K_b(\mathring{y}_i - \hat{y}_i) \otimes \hat{q}. \end{cases} \tag{9.12}$$

Consider the errors

$$\begin{cases} \tilde{q} = \hat{q} \otimes q^{-1}, \\ \tilde{b} = q \otimes (\hat{b} - b) \otimes q^{-1}. \end{cases} \tag{9.13}$$

The error system is given by

$$\begin{cases} \dot{\tilde{q}} = -\frac{1}{2}\tilde{q} \otimes (\tilde{b}) + (\sum_i K_q(\mathring{y}_i - \hat{y}_i) \otimes \hat{q}) \otimes \tilde{q} - \tilde{q} \otimes (B_\Omega v_\Omega), \\ \dot{\tilde{b}} = +2(B_\Omega v_\Omega) \times \tilde{b} + \tilde{q}^{-1} \otimes (\sum_i K_b(\mathring{y}_i - \hat{y}_i) \otimes \tilde{q} - B_B v_b + (\tilde{q}^{-1} \otimes (\tilde{u}) \otimes \tilde{q}) \times \tilde{b}, \\ \tilde{u} = \hat{q}^{-1} \otimes (u - \hat{b}) \otimes \hat{q}. \end{cases} \tag{9.14}$$

Next, linearize the error system using $\tilde{q} \longrightarrow [1, \frac{1}{2}\delta\tilde{q}]^\top$ and $\tilde{b} \longrightarrow \delta\tilde{b}$, and neglect the quadratic terms in noise and infinitesimal state error similar to [27].

$$\begin{pmatrix} \dot{\delta\tilde{q}} \\ \dot{\delta\tilde{b}} \end{pmatrix} = (A - KC) \begin{pmatrix} \delta\tilde{q} \\ \delta\tilde{b} \end{pmatrix} - \begin{pmatrix} B_\Omega v_\Omega + (\sum_i K_q D_i w_i) \\ B_b v_b + (\sum_i K_b D_i w_i) \end{pmatrix}, \tag{9.15}$$

where

$$A = \begin{pmatrix} 0 & -I \\ 0 & \tilde{u}_\times \end{pmatrix}, \; C = (2(\mathring{y}_i)_\times \;\; 0), K = -[K_q, K_b]^\top. \tag{9.16}$$

Then similar to the EKF the full filter is realized using

$$\begin{cases} K = PC^\top R^{-1}, \\ \dot{P} = AP + PA^\top + Q - PC^\top R^{-1} CP, \\ Q = \mathrm{diag}(Q_\omega, \; Q_b). \end{cases} \tag{9.17}$$

Note that in [27] there is typo in the matrix A with an extra factor of $\frac{1}{2}$ multiplying the identity matrix I.

If the state noise is considered without a factor of two, according to our usual

setup in this thesis such that

$$\begin{cases} \dot{q} = \frac{1}{2} q \otimes \Omega, \\ u = \Omega - q^{-1} \otimes (B_\Omega v_\Omega) \otimes q + b, \\ \dot{b} = q^{-1} \otimes (B_B v_b) \otimes q, \\ y_i = q^{-1} \otimes (\mathring{y}_i + D_i w_i) \otimes q, \end{cases} \tag{9.18}$$

then the matrix C of the RIEKF is modified to

$$C = \left((\mathring{y}_i)_\times \;\; 0 \right), \tag{9.19}$$

that is the version used in the simulations Chapter 7.

Bibliography

1. A. H. Jazwinski, 1970. *Stochastic processes and filtering theory*. Academic Press. ISBN 0123815509. (cited on page 19)

2. A. Iserles; H.Z. Munthe-Kaas; S.P. Nørsett; and A. Zanna, 2001. Lie-group methods. *Acta numerica*, 9 (2001), 215–365. (cited on page 74)

3. Abraham, R. and Marsden, J.E. and Raiu, T.S., 1988. *Manifolds, tensor analysis, and applications*, vol. 75. Springer. (cited on page 15)

4. Aguiar, A. and Hespanha, J., 2006. Minimum-energy state estimation for systems with perspective outputs. *IEEE Transactions on Automatic Control*, 51, 2 (2006), 226–241. (cited on page 19)

5. Athans, M. and Falb, P., 1966. *Optimal control: an introduction to the theory and its applications*. McGraw-Hill. ISBN 0070024138. (cited on pages 25, 28, 55, 64, and 65)

6. B. D. O. Anderson and J. Moore, 1979. *Optimal filtering*. Prentice Hall. (cited on pages 17 and 73)

7. B. F. La Scala; R. R. Bitmead; and M. R. James, 1995. Conditions for stability of the Extended Kalman Filter and their application to the frequency tracking problem. *Mathematics of Control, Signals, and Systems (MCSS)*, 8, 1 (March 1995), 1–26. (cited on page 18)

8. Bonnabel, S., 2007. Left-invariant extended Kalman filter and attitude estimation. In *Proceedings of the IEEE Conference on Decision and Control*, 1027–1032. (cited on pages 17 and 71)

9. Bonnabel, S.; Martin, P.; and Rouchon, P., 2009. Non-linear symmetry-preserving observers on Lie groups. *IEEE Transactions on Automatic Control*, 54, 7 (2009), 1709–1713. (cited on page 20)

10. Bonnabel, S. and Martin, P. and Salaun, E., 2009. Invariant Extended Kalman Filter: theory and application to a velocity-aided attitude estimation problem. In *Proceedings of the 48th IEEE Conference on Decision and Control*, 1297–1304. (cited on pages 17 and 71)

11. Chaturvedi, N.A. and Sanyal, A.K. and McClamroch, N.H., 2011. Rigid-body attitude control. *Control Systems, IEEE*, 31, 3 (2011), 30–51. (cited on page 15)

12. Cheng, Y. and Crassidis, J., 2004. Particle filtering for sequential spacecraft attitude estimation. In *AIAA Guidance, Navigation, and Control Conference and Exhibit*, 16–19. (cited on pages 18 and 73)

13. Choukroun, D.; Bar-Itzhack, I.; and Oshman, Y., 2006. A novel quaternion Kalman filter. *IEEE Transactions on Aerospace and Electronic Systems*, 42, 1 (2006), 174–190. (cited on pages 17 and 69)

14. Crassidis, J.; Alonso, R.; and Junkins, J., 2000. Optimal attitude and position determination from line-of-sight measurements. *Journal of Astronautical Sciences*, 48, 2 (2000), 391–408. (cited on pages 70 and 82)

15. Crassidis, J. and Markley, F., 2003. Unscented filtering for spacecraft attitude estimation. *Journal of Guidance Control and Dynamics*, 26, 4 (2003), 536–542. (cited on pages 18, 70, 71, and 73)

16. E. D. Sontag, 1998. *Mathematical control theory: deterministic finite dimensional systems*. Springer. (cited on page 19)

17. J. C. Willems, 2004. Deterministic least squares filtering. *Journal of Econometrics*, 118, 1-2 (2004), 341–373. (cited on page 19)

18. J. L. Crassidis; F. L. Markley; and Y. Cheng, 2007. Survey of nonlinear attitude estimation methods. *Journal of Guidance Control and Dynamics*, 30 (2007), 12–28. (cited on pages 17, 20, 69, and 71)

19. J. Thienel and R. M. Sanner, 2003. A coupled nonlinear spacecraft attitude controller and observer with an unknown constant gyro bias and gyro noise. *IEEE Transactions on Automatic Control*, 48, 11 (2003), 2011–2015. (cited on page 20)

20. J. Vasconcelos; R. Cunha; C. Silvestre; and P. Oliveira, 2007. Landmark based nonlinear observer for rigid body attitude and position estimation. In *Proceedings of the 46th IEEE Conference on Decision and Control*, 1033–1038. (cited on page 20)

21. Krener, A., 2004. The convergence of the minimum energy estimator. In *Lecture Notes in Control and Information Sciences* (Ed. W. Kang), 187–208. Springer. (cited on page 19)

22. Lageman, C.; Trumpf, J.; and Mahony, R., 2010. Gradient-like observers for invariant dynamics on a Lie group. *IEEE Transactions on Automatic Control*, 55, 2 (2010), 367–377. (cited on pages 20 and 36)

23. Marcus, S. I., 1984. Algebraic and geometric methods in nonlinear filtering. *SIAM Journal on Control and Optimization*, 22, 6 (1984), 817–844. (cited on page 17)

24. Markley, F., 2003. Attitude error representations for Kalman filtering. *Journal of guidance, control, and dynamics*, 26, 2 (2003), 311–317. (cited on pages 17, 70, 71, 73, and 74)

25. Markley, F., 2004. Multiplicative vs. additive filtering for spacecraft attitude determination. *Dynamics and Control of Systems and Structures in Space*, (2004). (cited on page 73)

26. Markley, F L; Berman, N; and Shaked, U, 1993. H (sub infinity)-type filter for spacecraft attitude estimation. In *AAS/GSFC International Symposium on Space Flight Dynamics, Greenbelt, MD*. (cited on page 20)

27. Martin, P.; Salaün, E.; et al., 2010. Generalized multiplicative extended kalman filter for aided attitude and heading reference system. In *Proceedings of 2010 AIAA Guidance, Navigation, and Control Conference*. (cited on pages 17, 70, 71, 73, 78, 83, 84, 87, and 93)

28. O. B. Hijab, 1980. *Minimum energy estimation*. Ph.D. thesis, University of California, Berkeley. (cited on page 19)

29. P. Coote; J. Trumpf; R. Mahony; and J. C. Willems, 2009. Near-optimal deterministic filtering on the unit circle. In *Prooceedings of the 48th IEEE Conference on Decision and Control*, 5490–5495. (cited on pages 19, 21, and 37)

30. R. E. Kalman, 1960. A new approach to linear filtering and prediction problems. *Journal of Basic Engineering, Transactions of the ASME*, 82, 1 (1960), 35–45. (cited on page 16)

31. R. E. Mortensen, 1968. Maximum-likelihood recursive nonlinear filtering. *Journal of Optimization Theory and Applications*, 2, 6 (1968), 386–394. (cited on pages 19, 25, 29, 55, 64, and 65)

32. R. Mahony; T. Hamel; and J. -M. Pflimlin, 2008. Nonlinear complementary filters on the special orthogonal group. *IEEE Transactions on Automatic Control*, 53, 5 (2008), 1203–1218. (cited on pages 20, 70, 72, 73, and 81)

33. S. Bonnabel; P. Martin; and P. Rouchon, 2008. Symmetry-preserving observers. *IEEE Transactions on Automatic Control*, 53, 11 (2008), 2514–2526. (cited on page 20)

34. S. J. Julier and J. K. Uhlmann, 2002. Reduced sigma point filters for the propagation of means and covariances through nonlinear transformations. In *Proceedings of the American Control Conference*, vol. 2, 887–892. (cited on pages 18 and 71)

35. S. Salcudean, 1991. A globally convergent angular velocity observer for rigid body motion. *IEEE Transactions on Automatic Control*, 36, 12 (1991), 1493–1497. (cited on page 20)

36. Sanyal, A., 2006. Optimal Attitude Estimation and Filtering Without Using Local Coordinates Part I: Uncontrolled and Deterministic Attitude Dynamics. In *American Control Conference*. (cited on page 19)

37. Sanyal, A.; Lee, T.; Leok, M.; and McClamroch, N., 2008. Global optimal attitude estimation using uncertainty ellipsoids. *Systems & Control Letters*, 57, 3 (2008), 236–245. (cited on pages 19 and 70)

38. Tang, X.; Liu, Z.; and Zhang, J., 2012. Square-root quaternion cubature kalman filtering for spacecraft attitude estimation. *Acta Astronautica*, 76 (2012), 84–94. (cited on pages 18, 72, and 73)

39. U. Helmke and J. B. Moore, 1994. *Optimization and dynamical systems*. Springer-Verlag. (cited on page 15)

40. Wahba, G., 1965. A least squares estimate of satellite attitude. *Siam Review*, 7, 3 (1965), 409–409. (cited on pages 19 and 70)

41. Zamani, M.; Trumpf, J.; and Mahony, R., 2011. Minimum-energy filtering on the unit circle. In *Proceedings of the Australian Control Conference (AUCC)*, 236–241. (cited on page 59)

42. Zamani, M.; Trumpf, J.; and R. Mahony, 2011. Near-Optimal deterministic filtering on the rotation group. *IEEE Transactions on Automatic Control*, 56, 6 (2011), 1411–1414. (cited on pages 19, 21, and 37)